Title
Improving Nitrogen Management in California Rice Systems: A Synergy Between Remote Sensing Technology and Fundamental Agronomy

Author
Rehman, Telha

Publication Date
2022

Peer reviewed|Thesis/dissertation

Improving Nitrogen Management in California Rice Systems: A Synergy Between Remote Sensing Technology and Fundamental Agronomy

By

TELHA HAFEEZ REHMAN
DISSERTATION

Submitted in partial satisfaction of the requirements for the degree of

DOCTOR OF PHILOSOPHY

in

Horticulture and Agronomy

in the

OFFICE OF GRADUATE STUDIES

of the

UNIVERSITY OF CALIFORNIA

DAVIS

Approved:

Bruce A. Linquist, Chair

Patrick H. Brown

Mark E. Lundy

Committee in Charge

2022

In the Name of God, the Most Gracious, the Most Merciful

With Peace and Blessing upon His final Prophet and Messenger, Muhammad, and his Family

Dedicated to my Parents

ACKNOWLEDGEMENTS

I am grateful to

Bruce Linquist, for giving me the opportunity to take on this challenge, and then setting me up to succeed through your steadfast support, commitment, guidance, and mentorship. Thank you for being an excellent Ph.D. advisor. It truly has been a pleasure to learn from you.

The California Rice Research Board, the National Science Foundation, the William G. Golden, Jr. and Kathleen H. Golden International Agriculture Fellowship, the Jastro-Shields Graduate Research Awards, the UC Davis Horticulture & Agronomy Graduate Fellowships, and the Dr. D. Marlin Brandon Rice Research Fellowship for supporting my research and education.

Cesar "Kapitan" Abrenilla, for being my guardian angel these past six years. Your companionship and witty sense of humor is what made it possible to get through the most difficult of days underneath the sun. Thank you for always being there for me and thank you for being a dear friend.

Mark Lundy and Patrick H. Brown for serving on my Dissertation and Qualifying Exam Committees. A special thanks to Mark for sharing so much of your time and knowledge with me over these past few years. Your help was indispensable to the formation of this dissertation. I would also like to thank Matthew Gilbert, Yufang Jin, and Andrew Walker for serving on my Qualifying Exam

Committee. A special thanks to Matthew for also serving as my Academic Advisor and for always taking the time out to watch the last five overs with me.

Past and present members of the Agroecosystems Lab for all your assistance over the years. Thank you for all your help. I could not have done it without you all.

Lisa Brown, for making life as a graduate student more manageable in a world where not many things do. Thank you for always taking the time to reply to the millions of emails that you receive with a sweet, kind, and gentle response. It certainly takes a special person to do that.

The many devoted teachers I have had throughout my academic career. I would not be here if it wasn’t for you. Thank you for your contributions to my intellectual growth.

ACKNOWLEDGEMENTS

I am grateful to

My late mother, Nisar Fatima Rehman, for sacrificing everything to give me the opportunity to succeed. I will always be indebted to you, my dear Mama Jaan. I love you and I miss you, and I hope that someday I can be as good of a parent as you were.

My father, Hafeez-ur-Rehman, for teaching me what it means to work hard and to support one's family. Thank you for everything that you do for us. I hope that someday I can be as good of a father as you are.

My wife, Zahra, for being my support system. Thank you for leaving your world to come live in mine. Also, thank you for letting me be an absentee husband/father these past two years and raising our beautiful daughter all by yourself. I am so blessed to have you in my life, and I look forward to us finally being a family.

My brother, Dr. Haroon Rehman, for being my role model. Thank you for always protecting me when I needed to be protected, yet challenging me when I needed to be challenged. I am so proud of the hard work and dedication you put forth in achieving your goals. Thank you for setting an excellent example for me.

My parents-in-law, Uncle Taimur and Aunty Saadia, for all your love, support, encouragement, and prayers. Thank you for all that you have done for Zahra and I. Thank you for trusting me to take care of your daughter.

My sister-in-law, Raisa, for always being there for me. Thank you for all the times you stepped in for me over the years. I could not have done this without your help.

My beautiful daughter, Maira, for allowing me to experience a love that I did not know existed. Your birth will always be the most cherished moment of my life. Thank you for making life worth living.

My nephews, Hashim and Kabeer, for being the purest sources of joy and happiness in my life. There are no words to describe how much I love you two. Thank you for always brightening my day.

The pioneers of my family, Babaji Imam Bakhsh and Babaji Kalu Khan, for leaving everything behind and coming to a new world to create a brighter future for your descendants. Thank you for your sacrifice and thank you for giving me this opportunity.

All my friends, especially Ali, Amir, Jabbar, Adeel, and all members of the NFFL, for always being there for me like true brothers. Thank you for helping me maintain a sense of normalcy throughout my time in grad school.

Finally, and above all, I am grateful to God.

ABSTRACT

Improving nitrogen (N) management is critical to maximizing the productivity and sustainability of our agroecosystems. Improving N management requires an understanding of crop N status and yield potential early enough in the growing season when changes to N management can influence yields. However, given the lack of tools currently available to accurately assess crop N status, farmers continuously face the challenge of determining whether their crops require additional N fertilizer. The recent emergence of remote sensing technology has provided a promising alternative that can provide farmers the information they need in an accurate and timely manner. Several studies have demonstrated the potential of remote sensing technology to accurately assess the health and vigor of vegetation at the landscape scale, however few have explored how this technology can be utilized to inform sustainable crop management at the farm scale. This knowledge gap is what inspired this research and led us to investigate how remote sensing technology can be utilized to improve in-season N management in California rice systems.

In California, where more than 200,000 ha of flooded rice (*Oryza sativa*) is cultivated annually, the recommended N management strategy is for farmers to apply the average seasonal N fertilizer requirement prior to flooding and planting as aqua-ammonia injected into the soil. On-farm studies have reported that N fertilizer applied in this manner is efficiently utilized by the crop as it remains protected from denitrification and ammonia volatilization losses until the crop needs it. At panicle initiation (PI), it is recommended to assess crop N status to determine if additional N fertilizer inputs are required as top-dress. The current tools available to assess rice N status include the SPAD chlorophyll meter and Leaf Color Chart, but these tools are not often

used as they are time consuming and subjective. Thus, most top-dress N applications take place without evaluating crop N status; possibly resulting in inefficiencies due to over application.

Our goal was to improve N management in California rice systems by developing a sensor-based decision support tool that could guide California rice farmers in their mid-season top-dress N management. This was pursued through N response trials that were established over a 4-yr. period across fourteen on-farm locations throughout the Sacramento Valley rice growing region of California. At PI, Normalized Difference Vegetation Index (NDVI) was measured using both a proximal crop sensor and a multispectral aerial sensor, and Normalized Difference Red-Edge Index (NDRE) was measured only using an aerial sensor. After NDVI and NDRE measurements, biomass was sampled destructively and then top-dress N fertilizer was applied. At maturity, rice plants were harvested to quantify grain yield.

In the first chapter, our objective was to determine which N status parameter is best assessed by NDVI at PI and how accurately NDVI at PI can predict grain yield. The N status parameters quantified in this study were aboveground biomass, plant N concentration, and total N uptake. Quadratic linear regression models were developed to describe the relationship between each N status parameter and NDVI, and a simple linear regression model was developed to describe the relationship between grain yield and NDVI. Our results showed that PI N status was best assessed by NDVI when quantified as total N uptake and that NDVI at PI was positively correlated with grain yield. However, our results also showed that NDVI saturated once crop N uptake exceeded a certain threshold, suggesting alternative indices that do not saturate may provide a basis for a better assessment.

In the second chapter, our objective was to compare the sensitivity of aerially sensed NDVI and NDRE to proximally sensed NDVI for assessing rice crop status when quantified as

PI N uptake and grain yield. In order to make direct comparisons across the three indices, the raw values from each index were normalized by calculating the Sufficiency-Index (SI). Quadratic-plateau linear regression models were developed to describe the relationship between each SI and PI N uptake and linear mixed effects models were developed to describe the relationship between each SI and grain yield. Our results showed that aerial NDRE SI and proximal NDVI SI were similarly sensitive at assessing PI N uptake and grain yield, whereas aerial NDVI SI was poorly sensitive. The difference in sensitivity among the three indices was attributed to the relative amount of saturation of each index. Our finding that both the aerial NDRE SI and proximal NDVI SI measured PI rice crop status effectively provides a unique advantage for end-users as it allows them the flexibility to choose the sensor most suitable for their goals.

In the final chapter, our objective was to develop a NDVI Response-Index capable of predicting the grain yield response to top-dress N fertilizer applied at PI. The NDVI Response-Index was developed by comparing the NDVI of each field treatment to the NDVI of a N non-limiting plot. At PI, top-dress N fertilizer was applied to every plot, and at maturity grain yield was quantified. A linear mixed effects model was developed to describe the relationship between NDVI Response-Index and grain yield with and without top-dress N. An economic analysis was performed to determine the magnitude of grain yield response required for top-dress N applications to be economically feasible. Based on our results, we found that top-dress N applications become profitable once NDVI Response-Index exceeds 1.07 by PI. The NDVI Response-Index presented here provides a useful tool for farmers to make precise mid-season top-dress N decisions which can result in positive outcomes for both crop productivity and environmental sustainability.

LIST OF TABLES

CHAPTER ONE

CHAPTER TWO

CHAPTER THREE

LIST OF FIGURES

CHAPTER ONE

CHAPTER TWO

CHAPTER THREE

TABLE OF CONTENTS

INTRODUCTION

Nitrogen (N) is an essential element for plant growth and an adequate supply of N is fundamental to maximizing rice (*Oryza sativa* L.) grain yield and quality (**De Datta, 1981**). However, despite being the most studied nutrient worldwide, N use efficiency in global rice production is estimated to be less than 50% (**Ladha et al., 2016**). Annually, approximately 8 Tg of N fertilizer is applied to agricultural soils worldwide to produce rice, suggesting that approximately 4 Tg of N is lost to the environment (**Ladha et al., 2020)**. This disparity between N fertilizer inputs and outputs negatively impacts the environment in many ways. For example, excessive N fertilization combined with improper water management causes nitrate to leach through the soil profile and pollute underlying aquifers; resulting in a variety of diseases when consumed by humans and animals (**Di and Cameron, 2002; Fan and Steinberg, 1996; Fowler et al., 2013**). Agriculture becomes a driver of global climate change through the significant amounts of greenhouse gases (e.g. NOx and N2O) that are emitted from fields where N fertilizer levels in the soil exceed crop N requirements (**Almaraz et al., 2018; Pittelkow et al., 2014a; Tubiello et al., 2013**). Elevated N inputs from agricultural tailwater convert downstream marine ecosystems into hypoxic dead zones due to eutrophication and the proliferation of harmful algal blooms (**Conley et al., 2009; Howarth et al., 2011**). Given the intensification of global agriculture required to feed the growing world population, these negative impacts on the biosphere will likely worsen unless new practices are developed and adopted that allow farmers to more efficiently utilize N fertilizer.

In California (CA), where more than 200,000 ha of flooded rice is cultivated annually, the recommended practice is to apply the average seasonal N fertilizer requirement (typically 150 to 200 kg N ha^{-1}) before flooding and planting (**Linquist et al., 2009; Williams et al.,**

2010). Aqua ammonia (NH_4OH) is the primary preplant N fertilizer used and it is injected 7 to 10 cm deep in the soil, after which the fields are flooded and remain so continuously until harvest, thus keeping the N fertilizer protected from denitrification and ammonia volatilization losses until the crop needs it (**Broadbent and Mikkelsen, 1968; Chuong et al., 2020**). **Linquist et al. (2009)** reported from 14 on-farm studies that N applied in this manner led to an average fertilizer N recovery in the crop of 53%. Similarly, in dry-seeded systems in the mid-southern USA and Australia, it is also recommended to apply the total N requirement early in the season, prior to the establishment of permanent flood (**Dunn et al., 2014, 2016; Norman et al., 2021; Troldahl, 2018**). In both these systems, it is recommended to assess the crop at panicle initiation (PI) to determine whether the crop requires additional N fertilizer inputs to achieve maximum yields (**Pittelkow et al., 2014b; Williams, 2010**).

Panicle initiation is considered a critical stage for in-season N management, as it marks the physiological shift from vegetative to reproductive plant growth (**Counce et al., 2000**), and N applications later than PI are less efficiently utilized for grain yield (**DeDatta, 1981; Linquist and Sengxua, 2003**). For short duration rice varieties such as M-206, which is the predominant variety in CA, PI occurs approximately 45 to 50 days after sowing and is visually determined by a dark green ring just below the initiating panicle, occurring 5 to 7 days before panicle differentiation (PD) (when the panicle becomes visible) (**De Datta, 1981**). Furthermore, most, if not all, of the pre-plant N fertilizer has been taken up by this stage in both water-seeded (**LaHue et al., 2016)** and dry-seeded systems **(Norman et al., 2021)**. Because preplant N fertilizer has been taken up by this stage, further N uptake between PI and harvest relies on late season soil indigenous N supply (INS) and any top-dress fertilizer that may have been applied. If required, in CA typical PI top-dress rates range from 22 to 45 kg N ha^{-1} (**Williams, 2010**) with the average application being around 34 kg N ha^{-1} (**Hartley and van Kessel, 2003**). While the N rate applied at this stage is relatively low, it is still an important adjustment in a year where yield potential may be higher than average. Importantly, by PI, the yield components of tiller and panicle number have been determined, so major deficiencies due to initially low N rates would be too late to correct by this stage (**DeDatta, 1981; Dunn et al., 2016**).

Some methods are available to assess midseason plant N status but have not been widely adopted by CA rice farmers due to their limitations. Plant tissue analysis provides the most direct measure; however, this technique is also time consuming and lab results are often received past the time when fertilizer decisions need to be made (**Daugherty et al., 2000**). Alternative technologies are available to expedite in-field N status assessment, such as the Leaf Color Chart (LCC) and the Soil Plant Analysis Development (SPAD) chlorophyll meter (**Balasubramanian et al., 1999; Peng et al., 1996**). The LCC estimates N content based on leaf greenness, while the SPAD chlorophyll meter measures the difference in transmittance between red and near infrared light passing through the leaf to estimate chlorophyll content (**Alam et al., 2005; Uddling et al., 2007**). Previous research has demonstrated the ability of these technologies to assess rice N status and promote sustainable N management (**Islam et al., 2007; Singh et al., 2007; Yang et al., 2003**). However, both the LCC and SPAD chlorophyll meter are inefficient as they only assess a single leaf at a time, thus requiring considerable time and effort to accurately assess N status of an entire field (**Daugherty et al., 2000; Saberioon et al., 2004; Xue et al., 2004**). Given the limitations of the SPAD meter and the LCC, assessing crop N status in an accurate and timely manner remains a challenge in these systems, thus most top-dress N applications take place without evaluating crop N status; possibly resulting in inefficiencies due to over application.

The recent development of remote sensing techniques has provided a promising alternative to accurately assess crop N status and better manage N resources. Remote sensing of crops is based on the collection of canopy reflectance spectra at specific wavelengths in the electromagnetic spectrum, usually corresponding to regions where the plant canopy experiences strong absorption or reflectance of incoming radiation (**Xue and Su, 2017)**. The most common method of assessing crop status using remote sensing is to place the proportion of observed reflectance at different wavelengths into a vegetative index, which is a mathematical combination of wavelengths related to specific biophysical characteristics of the plant (**Hatfield et al., 2019**). Among the most commonly measured indices in agricultural remote sensing applications is the Normalized Difference Vegetation Index (NDVI), as it has been shown to be sensitive to photosynthetic compounds, making it a useful index to measure the productivity of vegetation in a defined area (**Huang et al., 2021; Tucker, 1979; Tucker et al., 1985**). Within the past decade, the rapid development of new sensors with higher spatial and spectral sensing abilities, as well as new platforms that can carry such sensors and easily maneuver over the object space have led to a significant broadening of remote sensing applications in many fields including agriculture (**Toth and Jóźków, 2016**). As such, some of the current applications of remotely sensed data in agriculture include biomass estimation, assessing crop nutritional status, detecting plant stress, identifying disease incidence, scouting fields for weeds, and predicting potential yield among others.

Remote sensing data can be collected using several different platforms including proximal handheld sensors or aerial sensors which can be mounted to airplanes, satellites, or unmanned aircraft vehicles (UAV; sensor mounted to an UAV is referred to as an unmanned aircraft system, UAS) (**Toth and Jóźków, 2016)**. Over the past two decades, most of the research in agricultural remote sensing has focused on the use of proximal sensors, especially those that utilize an active light source (**Saberioon et al., 2014).** However, with the recent development of compact aerial sensors that can be easily mounted to an UAV, an increasing number of studies have shifted toward utilizing UAS based platforms (**Colomina and Molina, 2014**). Relative to proximal and UAS based remote sensing, airplane and satellite based measurements are less frequently used in agricultural applications due to the high complexity and costs of operating an airplane, and insufficient spatial and temporal resolution often experienced with satellite imagery (**Zheng et al., 2018**). However, despite more convenient than airplane and satellite based remote sensing, both proximal and UAS based remote sensing also come with their own unique advantages and disadvantages.

Among proximal sensors, one of the most often used in agricultural research is the GreenSeeker (GS) HandHeld (Trimble Inc., Sunnyvale, CA, USA), which is an active canopy sensor, thus allowing it to collect reflectance data at any time during the day regardless of ambient light conditions or cloud cover (**Saberioon et al., 2014)**. The GreenSeeker measures canopy reflectance at specific bands in the red (670 nm) and near infrared (780 nm) spectral regions and then automatically displays the NDVI. Among previously published studies that tested the ability of GS NDVI ($NDVI_{GS}$) to assess crop N status in rice, **Yao et al. (2014)** and reported strong correlations between $NDVI_{GS}$ and aboveground biomass and total N uptake measured at the PI stage. However, a key disadvantage of the GS, as was noted by the study mentioned above, as well as many others, is that the GS can only measure $NDVI_{GS}$ which has been shown to lose its sensitivity (i.e. saturate) once crop biomass exceeds a certain threshold (**Huang et al., 2021**).

When collecting canopy reflectance data aerially, a passive multispectral sensor (in most cases) is mounted to an UAV and flown in a grid-style pattern over the field or experimental area; thus, facilitating the assessment of larger areas more efficiently and potentially identifying the spatial variability that is often present within a field (**Delavarpour et al., 2021; Fu et al., 2021; Tsouros et al., 2019**). A multispectral sensor that is frequently used in agricultural applications is the MicaSense Red-Edge M (MicaSense, Inc., Seattle, WA, USA) which is a passive sensor and collects canopy reflectance across five spectral bands (blue, green, red, red edge, and near infrared) (**Esposito et al., 2021**). The additional bands included in multispectral sensors such as the MicaSense sensor and others provide an important advantage over proximal sensors like the GS as they permit the calculation of a wide range of vegetative indices, including red edge based indices, among which the Normalized Difference Red Edge Index (NDRE) is the most commonly used (**Dunn et al., 2016).** The NDRE is based on the same calculation as the NDVI but incorporates a red edge band in place of red, which allows the NDRE to be more resistant to the saturation problem inherent with NDVI (**Dunn et al., 2016; Li et al, 2014).** However, aerial based remote sensing also has its own limitations, among which some include the narrow timeframe around solar noon during which data must be collected, the prohibitive costs of UAS platforms which can be far more expensive than proximal sensors, and the concern that UAS platform can often experience technical issues mid-air, such as loss of power or an engine breakdown (**Hardin and Jensen, 2011; Zhang and Kovacs, 2012**). Among the studies that used aerial sensors to assess N status in rice, **Dunn et al., 2016** reported strong correlations between NDVI and NDRE and total N uptake at PI but noted that the NDRE was less saturated than the NDVI. Similarly, **Wang et al. (2021)** reported stronger correlations between NDRE and red edge chlorophyll index and N-index (ratio of N concentration between fertilized and non-fertilized plants), for measurements collected between 30 to 55 days after transplanting relative to the NDVI. Although, **Zheng et al. (2019**) did not measure NDVI in their study, among the six indices evaluated in their study, they reported the highest accuracy between NDRE and red edge chlorophyll index when estimating total leaf N uptake and plant N uptake across the tillering, jointing, and heading stages.

While NDVI or NDRE measurements are useful to assess the N status of a crop, a single measurement does not indicate the likelihood of a crop to respond to additional N. To address this issue, an N-enriched area, which is non-limiting with respect to N, can be used (**Colaço and Bramley, 2018; Hussain et al., 2000**). If the crop outside the N-enriched area has a lower NDVI than the N-enriched area, it is inferred that the crop may respond to additional N inputs (**Raun et al., 2002; Tubaña et al., 2012)**. **Mullen et al. (2003)** developed an NDVI Response-Index (RI_{NDVI}) by dividing the NDVI from the N-enriched area by the NDVI from an adjacent area in the field. The RI_{NDVI} values will usually be > 1.0 with higher numbers indicating increased potential for N responsiveness. The N-enriched area and RI_{NDVI} have been used in many different applications across a wide range of crops and have been shown to be a robust indicator of crop responsiveness to N **(Arnall et al., 2009; Cao et al., 2016; Lofton et al., 2012; Lu et al., 2020; Tubaña et al., 2008).**

In situations where N fertilizer may be split throughout the season, previous studies have used a N fertilization optimization algorithm (NFOA) to determine N needs throughout the season (**Lukina et al., 2001; Raun et al., 2002; 2005)**. This approach also uses a N-enriched area, but the basic estimation of N needs is based on a mass balance calculation of the optimal N rate required for an expected yield **(Colaço and Bramley, 2018**). Several studies have demonstrated that this approach improves nitrogen use efficiency in rice relative to standard farmer practice by producing similar grain yields with less N fertilizer (**Ali et al., 2014; Bijay-Singh et al., 2015; Xue et al., 2014; Xue and Yang, 2008; Yao et al., 2012**). While this approach has a strong theoretical basis, it is based on several assumptions (e.g. seasonal N_{UP}, grain yield potential, and N use efficiency) that vary considerably across fields and over time. Such an approach is also not easy to employ by a farmer who may not have access to such information.

The overarching objective of this research was to improve mid-season N management in CA rice systems by using remote sensing technology in synergy with fundamental agronomy. The goal being to develop a remote sensing-based decision support tool that could aid CA rice farmers in their mid-season top-dress N management. Such a tool could help CA rice farmers inform sustainable top-dress N management, resulting in positive outcomes for crop productivity and environmental health. This objective was pursued through N response trials established over a 4-yr. period across fourteen on-farm locations throughout the Sacramento Valley rice growing region of CA.

LITERATURE CITED

Alam, M.M., Ladha, J.K., Khan, S.R., Foyjunnessa, Harun-ur-Rashid, Khan, A.H., and R.J. Buresh. 2005. Leaf color chart for managing nitrogen fertilizer in lowland rice in Bangladesh. Agron. J. 97:949-959.

Ali, A.M., Thind, H.S., Singh, V., and B., Singh. 2014. A framework for refining nitrogen management in dry direct-seeded rice using GreenSeeker optical sensor. Comput. Electron. Agric. 110:114-120.

Almaraz, M., Bai, E., Wang, C., Trousdell, J., Conley, S., Faloona, I., and B.Z. Houlton. 2018. Agriculture is a major source of NO_x pollution in California. Sci. Adv. 4:8.

Arnall, D.B., Tubaña, B.S., Holtz, S.L., Girma, K., and W.R. Raun. 2009. Relationship between nitrogen use efficiency and response index in winter wheat. J. Plant Nutr. 32:502-515.

Balasubramanian, V., Morales, A.C., Cruz, R.T., and S. Abdulrachman. 1999. On-farm adaptation of knowledge-intensive nitrogen management technologies for rice systems. Nutr Cycl Agroecosys. 53:59-69.

Bijay-Singh, Varinderpal-Singh, Purba, J., Sharma, R.K., Jat, M.L., Yadvinder-Singh, Thind, H.S., Gupta, R.K., Chaudhary, O.P., Chandna, P., Khurana, H.S., Kumar, A., Jagmohan-Singh, Uppal, H.S., Uppal, R.K., Vashistha, M., and R. Gupta. 2015. Site-specific fertilizer nitrogen management in irrigated transplanted rice (*Oryza sativa*) using and optical sensor. Precis. Agric. 16:455-475.

Broadbent, F.E. and D.S. Mikkelsen. 1968. Influence of placement on uptake of tagged nitrogen by rice. Agron. J. 60:674-677.

Cao, Q., Miao, Y., Shen, J., Yu, W., Yuan, F., Cheng, S., Huang, S., Wang, H., Yang, W., and F. Liu. 2016. Improving in-season estimation of rice yield potential and responsiveness to topdressing nitrogen application with Crop Circle active crop canopy sensor. Precis. Agric. 17:136-154.

Chuong, T., Plant, R.E., and B.A. Linquist. 2020. Fertilizer source and placement influence ammonia volatilization losses from water-seeded rice systems. Soil Sci. Soc. Am. J. 84:784-797.

Colaço, A.F. and R.G. Bramley. 2018. Do crop sensors promote improved nitrogen management in grain crops?. Field Crop. Res. 218:126-140.

Colomina, I. and P. Molina. 2014. Unmanned aerial systems for photogrammetry and remote sensing: A review. ISPRS J Photogramm. 92:79-97.

Conley D.J., Paerl, H.W., Howarth, W.R., Boesch, D.F., Seitzinger, S.P., Haven, K.E., Lancelot, C., and G.E. Likens. 2009. Controlling eutrophication: Nitrogen and phosphorus. Science. 323:1014-1015.

Counce, P.A., Keisling, T.C., and A.J. Mitchell. 2000. A uniform, objective, and adaptive system for expressing rice development. Crop Sci. 40:436-443.

Daughtry, C.S.T., Walthall, C.L., Kim, M. S., Brown de Colstoun, E., and J.E. McMurtrey III. 2000. Estimating corn leaf chlorophyll concentration from leaf and canopy reflectance. Remote Sens. Environ. 74:229-239.

DeDatta, S.K. Principles and practices of rice production. 1981. John Wiley & Sons. Singapore.

Delavarpour, N., Koparan, C., Nowatzki, J., Bajwa, S., and X. Sun. 2021. A technical study on UAV characteristics for precision agriculture applications and associated practical challenges. Remote Sens. 13:1204.

Di, H.J. and K.C. Cameron. 2002. Nitrate leaching in temperate agroecosystems: sources, factors, and mitigating strategies. Nutr. Cycl. Agroecosys. 46:237-256.

Dunn, B.W., Dunn, T.S., and H.G. Beecher. 2014. Nitrogen timing and rate effects on. Growth and grain yield of delayed permanent-water rice in south-eastern Australia. Crop Pasture Sci. 65: 878-887.

Dunn B.W., Dunn, T.S., and B.A. Orchard. 2016. Nitrogen rate and timing effects on growth and yield of drill-sown rice. 2016. Crop Pasture Sci. 67: 1149-1157.

Esposito, M., Crimaldi, M., Cirillo, V., Sarghini, F., and A. Maggio, A. 2021. Drone and sensor technology for sustainable weed management: A review. Chem. Biol. Technol. Agric. 8:1-11.

Fan, A.M. and V.E. Steinberg 1996. Health implications of nitrate and nitrite in drinking water: An update of methemoglobinemia occurrence and reproductive and developmental toxicity. Regul. Toxicol. Pharm. 23:35-43.

Fowler, D., Coyle, M., Skiba, U., Sutton, M.A., Cape, J.N., Reis, S., Sheppard, L.J., Jenkins, A., Grizzetti, B., Galloway, J.N. and P. Vitousek. 2013. The global nitrogen cycle in the twenty-first century. Philos. T. Roy. Soc. B. 368:20130164.

Fu, Y., Yang, G., Song, X., Li, Z., Xu, X., Feng, H., and C. Zhao. 2021. Improved estimation of winter wheat aboveground biomass using multiscale textures extracted from UAV-based digital images and hyperspectral feature analysis. Remote Sens. 13:581.

Hardin, P.J. and R.R. Jensen. 2011. Small-scale unmanned aerial vehicles in environmental remote sensing: Challenges and opportunities. GISci. Remote Sens. 48:99-111.

Hartley, C., and C. van Kessel. 2003. UC Davis rice fertility management survey. Univ. of California Coop. Ext., Rice Project.

Hatfield, J.L., Prueger, J.H., Sauer, T.J., Dold, C., O'Brien, P., and K. Wacha. 2019. Applications of vegetative indices from remote sensing to agriculture: Past and future. Invent. 4:71.

Howarth, R., Chan, F., Conley, D.J., Garnier, J., Doney, S.C., Marino, R., and G. Billen. 2011. Coupled biogeochemical cycles: eutrophication and hypoxia in temperate estuaries and coastal marine ecosystems. Front. Ecol. Environ. 9:18-26.

Huang, S., Tang, L., Hupy, J.P., Wang, Y., and G. Shao. 2021. A commentary review on the use of normalized difference vegetation index (NDVI) in the era of popular remote sensing. J. Forestry Res. 32:1-6.

Hussain, F., Bronson, K.F., Yadvinder-Singh, Bijay-Singh, and S. Peng. 2000. Use of Chlorophyll Meter Sufficiency Indices for Nitrogen Management of Irrigated Rice in Asia. Agron. J. 92:875-879.

Islam, Z., Bagchi, B., and M. Hossain. 2007. Adoption of leaf color chart for nitrogen use efficiency in rice: Impact assessment of a farmer-participatory experiment in West Bengal, India. Field Crops Res. 103:70-75.

LaHue, G.T., Chaney, R.T., Adviento-Borbe, M.A., and B.A. Linquist. 2016. Alternate wetting and drying in high yielding direct-seeded rice systems accomplishes multiple environmental and agronomic objectives. Agr. Ecosyst. Environ. 229:30-39.

Ladha, J.K., Jat, M.L., Stirling, C.M., Chakraborty, D., Pradhan, P., Krupnik, T.J., Sapkota, T.B., Pathak, H., Rana, D.S., Tesfaye, K., and B. Gerard. 2020. Achieving the sustainable development goals in agriculture: The crucial role of nitrogen in cereal-based systems. Adv. Agron. 163:39-116.

Ladha, J.K., Tirol-Padre, A., Reddy, C.K., Cassman, K.G., Verma, S., Powlson, D.S., Van Kessel, C., de B Richter, D., Chakraborty, D., and H. Pathak. 2016. Global nitrogen budgets in cereals: A 50-year assessment for maize, rice and wheat production systems. Sci. Rep. 6:1-9.

Li, F., Miao, Y., Feng, G., Yuan, F., Yue, S., Gao, X., Liu, Y., Liu, B., Ustin, S.L., and X. Chen. 2014. Improving estimation of summer maize nitrogen status with red edge-based spectral vegetation indices. Field Crop. Res. 157:111-123.

Linquist, B.A., Hill, J.E., Mutters, R.G., Greer, C.A., Hartley, C., Ruark, M., and C. van Kessel. 2009. Assessing the necessity of surface applied preplant nitrogen fertilizer in rice systems. Agron. J. 101:906-915.

Linquist, B.A. and P. Sengxua. 2003. Efficient and flexible management of nitrogen for rainfed lowland rice. Nutr. Cycl. Agroecosys. 67:139-146.

Lofton, J., Tubaña, B.S., Kanke, Y., Teboh, J., and H. Viator. 2012. Predicting sugarcane response to nitrogen using a canopy reflectance-based response index value. Agron. J. 104:106-113.

Lu, J., Miao, Y., Shi, W., Li, J., Hu, X., Chen, Z., Wang, X. and K. Kusnierek. 2020. Developing a proximal active canopy sensor-based precision nitrogen management strategy for high-yielding rice. Remote Sens. 12:1440.

Lukina, E.V., Freeman, K.W., Wynn, K.J., Thomason, W.E., Mullen, R.W., Stone, M.L., Solie, J.B., Klatt, A.R., Johnson, G.V., Elliott, R.L. and W.R. Raun. 2001. Nitrogen fertilization optimization algorithm based on in-season estimates of yield and plant nitrogen uptake. J. Plant Nutr. 24:885-898.

Mullen, R.W., Freeman, K.W., Raun, W.R., Johnson, G.V., Stone, M.L., and J.B. Solie. 2003. Identifying an in-season response index and the potential to increase wheat yield with nitrogen. Agron. J. 95:347-351.

Norman, R.J., Slaton, N.A., and T.L. Roberts. 2021. Soil fertility. In: J. Hardke, editor, Rice production handbook. Misc. Publ. 192. Arkansas Coop. Ext. Serv. Little Rock. 69–101.

Peng, S., Garcia, F.V., Laza, R.C., Sanico, A.L., Visperas, R.M., and K.G. Cassman. 1996. Increased N-use efficiency using a chlorophyll meter on high-yielding irrigated rice. Field Crops Res. 47:243-252.

Pittelkow, C.M., Assa, Y., Burger, M., Mutters, R.G., Greer, C.A., Espino, L.A., Hill, J.E., Horwath, W.R., van Kessel, C. and B.A. Linquist. 2014b. Nitrogen management and methane emissions in direct-seeded rice systems. Agron. J. 106:968-980.

Pittelkow, C.M., Adviento-Borbe, M.A., van Kessel, C., Hill, J.E., and B.A. Linquist. 2014a. Optimizing rice yields while minimizing yield-scaled global warming potential. Glob Change Biol. 20:1382-1393.

Raun, W.R., Solie, J.B., Johnson, G.V., Stone, M.L., Mullen, R.W., Freeman, K.W., Thomason, W.E., and E.V. Lukina. 2002. Improving nitrogen use efficiency in cereal grain production with optical sensing and variable rate application. Agron. J. 94:815-820.

Raun, W.R., Solie, J.B., Stone, M.L., Martin, K.L., Freeman, K.W., Mullen, R.W., Zhang, H., Schepers, J.S., and G.V. Johnson. 2005. Optical sensor-based algorithm for crop nitrogen fertilization. Commun. Soil Sci. Plan. 36:2759-2781.

Saberioon, M.M., Amin, M.S.M., Gholizadeh, A., and M.H. Ezri. 2014. A review of optical methods for assessing nitrogen contents during rice growth. Appl. Eng. Agric. 30:657-669.

Singh, Y., Singh, B, Ladha, J.K., Bains, J.S., Gupta, R.K., Singh, J., and V. Balasubramanian. 2007. On-farm evaluation of leaf color chart for need-based nitrogen management in irrigated transplanted rice in northwestern India. Nutr. Cycl. Agroecosys. 78:167-176.

Toth, C. and G. Jóźków. 2016. Remote sensing platforms and sensors: A survey. ISPRS J Photogramm. 115: 22-36.

Troldahl, D. 2018. Rice growing guide. New South Wales Govt. Dept. Primary Industries. 16-19.

Tsouros, D.C., Bibi, S., and P.G. Sarigiannidis. 2019. A review on UAV-based applications for precision agriculture. Inform. 10:349.

Tubaña, B.S., Harrell, D.L., Walker, T., Teboh, J., Lofton, J. and Y. Kanke. 2012. In-season canopy reflectance-based estimation of rice yield response to nitrogen. Agron. J. 104:1604-1611.

Tubaña, B.S., Arnall, D.B., Walsh, O., Chung, B., Solie, J.B., Girma, K. and W.R. Raun. 2008. Adjusting midseason nitrogen rate using a sensor-based optimization algorithm to increase use efficiency in corn. J. Plant Nutr. 31:1393-1419.

Tubiello, F.N., Salvatore, M., Rossi, S., Ferrara, A., Fitton, N., and P. Smith. 2013. The FAOSTAT database of greenhouse gas emissions from agriculture. Environ. Res. Lett. 8:015009.

Tucker, C.J. 1979. Red and photographic infrared linear combinations for monitoring vegetation. Remote Sens. Environ. 8:127-150.

Tucker, C.J., Vanpraet, C.L., Sharman, M.J., and G. van Ittersum. 1985. Satellite remote sensing of total herbaceous biomass production in the Sengalese Sahel 1980–1984. Remote Sens. Environ. 17:233–249.

Uddling, J., Gelnag-Alfredsson, J., Piikki, K., and H. Pleijel. 2007. Evaluating the relationship between leaf chlorophyll concentration and SPAD-502 chlorophyll meter readings. Photosynth. Res. 91:37-46.

Wang, F., Yi, Q., Hu, J., Xie, L., Yao, X., Xu, T., and J. Zheng. 2021. Combining spectral and textural information in UAV hyperspectral images to estimate rice grain yield. Int. J. Appl. Earth Obs. 102:102397.

Williams, J.F. 2010. Rice nutrient management in California. UC ANR Publication 3516.

Xue, L., Cao, W., Luo, W., Dai, T., and Y. Zhu. 2004. Monitoring leaf nitrogen status in rice with canopy spectral reflectance. Agron. J. 96:134-142.

Xue, L., Li, G., Qin, X., Yang, L., and H. Zhang. 2014. Topdressing nitrogen recommendation for early rice with an active sensor in South China. Precis. Agric. 15:95-110.

Xue, J. and B. Su. 2017. Significant remote sensing vegetation indices: A review of developments and applications. J. Sens. Article ID 1353691.

Xue, L. and L. Yang. 2008. Recommendations for nitrogen fertiliser topdressing rates in rice using canopy reflectance spectra. Biosyst. Eng. 100:542-534.

Yao, Y., Miao, Y., Cao, Q., Wang, H., Gnyp, M.L., Bareth, G., Khosla, R., Yang, W., Liu, F., and C. Liu. 2014. In-season estimation of rice nitrogen status with an active crop canopy sensor. IEEE J-STARS. 7:4403-4413.

Yao, Y., Miao, Y., Huang, S., Gao, L., Ma, X., Zha, G., Jiang, R., Chen, X., Zhang, F., Yu, K., Gnyp, M.L., Bareth, G., Liu, C., Zhao, L., Yang, W., and H. Zhu. 2012. Active canopy sensor-based precision N management strategy for rice. Agron. Sustain. Dev. 32:925-933.

Yang, W.H., Peng, S., Huang, J., Sanica, A.L., Buresh, R.J., and C. Witt. 2003. Using leaf color charts to estimate leaf nitrogen status of rice. Agron. J. 95:212-217.

Zhang, C. and J.M. Kovacs. 2012. The application of small unmanned aerial systems for precision agriculture: a review. Precis. Agric. 13:693-712.

Zheng, H., Cheng, T., Li, D., Yao, X., Tian, Y., Cao, W., and Y. Zhu. 2018. Combining unmanned aerial vehicle (UAV)-based multispectral imagery and ground-based hyperspectral data for plant nitrogen concentration estimation in rice. Front. Plant Sci. 9:936.

Zheng, H., Cheng, T., Zhou, M., Li, D., Yao, X., Tian, Y., Cao, W., and Y. Zhu. 2019. Improved estimation of rice aboveground biomass combining textural and spectral analysis of UAV imagery. Precis. Agric. 20:611-629.

CHAPTER ONE

Using Normalized Difference Vegetation Index to assess N status and predict grain yield in rice

Telha H. Rehman[a], Andre Froes de Borja Reis[b], Nadeem Akbar[c], and Bruce A. Linquist[a]

[a]Department of Plant Sciences, University of California – Davis, Davis, CA 95616, USA

[b]Department of Crop Sciences, "Luiz de Queiroz" College of Agriculture, University of Sao Paulo, SP, Piracicaba, Brazil

[c] Department of Agronomy, University of Agriculture – Faisalabad, Faisalabad, Punjab 38040, Pakistan

Published in Agronomy Journal

Rehman, T.H., Borja Reis, A.F., Akbar, N., and B.A. Linquist. 2019. Use of normalized difference vegetation index to assess N status and predict grain yield in rice. Agron. J. 111:2889-2898.

Abbreviations: aboveground biomass, AGB; California, CA; N concentration; N_{CONC}; Normalized Difference Vegetation Index, NDVI; panicle initiation, PI; total nitrogen uptake, N_{UP}

ABSTRACT

Fine tuning N recommendations requires an understanding of crop N status and yield potential early enough in the growing season when changes to N management can influence yields. Recent studies have demonstrated the ability of Normalized Difference Vegetation Index (NDVI) to assess crop N status and predict yield in wheat (*Tricticum aestivum*) and maize (*Zea mays*); however, there has been relatively little such research on rice (*Oryza sativa* L.). The objectives of this study were to determine how well NDVI measured at the panicle initiation (PI) rice growth stage assesses crop N status and predicts final grain yield. Nitrogen response trials were established over a four-year period (10 site-years) at various locations throughout the Sacramento Valley rice growing region of California. Additionally, the relationship between NDVI and crop N status was characterized across 28 on-farm plots representing a range of environmental conditions and management practices. The NDVI at PI was best correlated with total N uptake (N_{UP}, $r^2 = 0.66$), followed by N concentration (N_{CONC}, $r^2 = 0.54$), and aboveground biomass (AGB, $r^2 = 0.51$). The utility of NDVI was greatest at lower values of crop N status, whereas at higher values, NDVI saturated. The NDVI at PI was positively correlated with final grain yield ($r^2 = 0.58$) indicating utility for developing in-season yield predictions. While NDVI is a potentially useful tool to improve N fertilizer management and develop in-season yield predictions in rice, alternative indices that do not saturate would likely provide a basis for a better tool.

1.1. INTRODUCTION

Despite being the most studied nutrient worldwide, nitrogen (N) use efficiency in global rice (*Oryza sativa* L.) production is only about 30 % (Ladha et al., 2005). In 2017, approximately 16 million Mg of N fertilizer was used for rice production worldwide (IFA, 2017), implying 10 million Mg of N was potentially lost to the environment. Nitrogen fertilizer losses from agricultural systems can have many adverse environmental and human health consequences. For example, nitrate leaching due to excessive N fertilization and improper water management can contaminate drinking water and lead to methemoglobinemia in infants (Di and Cameron, 2002; Harter et al., 2012). Significant amounts of greenhouse gases, such as nitrous oxide and methane, can be released from agricultural systems when N availability in the soil exceeds plant N requirements (Smith et al., 2007; Almaraz et al., 2018). Elevated N inputs to aquatic ecosystems from agricultural tailwater can result in hypoxic dead zones due to eutrophication and the proliferation of harmful algal blooms (Conley et al., 2009). Therefore, improved methods need to be designed and adopted that allow farmers to accurately assess crop N needs and make informed management decisions.

In California (CA), the average seasonal N fertilizer requirement for rice is approximately 165 kg N ha^{-1} (UC ANR, 2018), which is most efficiently utilized when injected into the soil as aqua-ammonia before planting (Linquist et al., 2009). In recent years, an increasing number of CA rice farmers have started applying additional N fertilizer as top-dress around panicle initiation (PI) growth stage. For the short duration varieties commonly grown in CA, PI typically occurs around 45 to 50 days after sowing and is considered a critical stage for N management as all pre-plant N fertilizer has been taken up (LaHue et al., 2016), and N applied at growth stages later than PI is less efficiently utilized for grain yield (DeDatta, 1981, Linquist et al., 2003). The current recommendation at PI is for farmers to first assess crop N status and apply top-dress N only if the crop is deemed N deficient (Linquist et al., 2009). However, assessing crop N status in an accurate and timely manner remains a challenge in these systems, thus most top-dress N applications take place without evaluating crop N status; possibly resulting in inefficiencies due to over application.

Some methods are available to assess midseason plant N status but have not been widely adopted by CA rice farmers due to their limitations. Plant tissue analysis provides the most direct measure; however, this technique is also time consuming and lab results are often received past the time when fertilizer decisions need to be made (Daugherty et al., 2000). Alternative technologies are available to expedite in-field N status assessment, such as the Leaf Color Chart (LCC) and the Soil Plant Analysis Development (SPAD) chlorophyll meter (Peng et al., 1996; Balasubramanian et al., 1999). The LCC estimates N content based on leaf greenness, while the SPAD chlorophyll meter measures the difference in transmittance between red and near infrared light passing through the leaf to estimate chlorophyll content (Alam et al., 2005; Uddling et al., 2007). Previous research has demonstrated the ability of these technologies to assess rice N status and promote sustainable N management (e.g. Yang et al., 2003; Islam et al., 2007; Singh et al., 2007). However, both the LCC and SPAD chlorophyll meter are inefficient as they only assess a single leaf at a time, thus requiring considerable time and effort to accurately assess a whole field (Daugherty et al., 2000; Saberioon et al., 2004; Xue et al., 2004).

More recently, remote sensing technology has been developed which utilizes canopy reflectance measurements to assess crop N status in a quick and non-destructive manner. Canopy reflectance data is collected remotely (via satellite, aircraft, or proximal sensor), and interpreted through a vegetative index. The Normalized Difference Vegetation Index (NDVI) is the most widely adopted (McFarland and van Riper, 2013) and is sensitive to photosynthetic compounds, making it a potentially useful index to measure the productivity of vegetation in a defined area (Tucker, 1979; Tucker et al., 1985).

The ability of NDVI to assess crop N status and develop in-season yield predictions has been studied extensively in wheat (*Tricticum aestivum*) and maize (*Zea mays*) production systems. Many have shown NDVI to effectively quantify plant N status across a variety of growth stages and sensor types (Reyniers and Vrindts, 2006; Li et al., 2008; Erdle et al., 2011; Li et al., 2014). Others found NDVI to be useful for developing in-season yield predictions by estimating biomass growth in wheat and maize (Raun et al., 2001; Teal et al., 2006; Inman et al., 2007). Adopting NDVI based N management in wheat and maize production systems has led to improved grain yield, N use efficiency, and net returns (Raun et al., 2002; Mullen et al., 2003; Raun et al., 2005; Tubaña et al., 2008). Comparatively, there have been relatively few such studies in rice. Some have tested the ability of NDVI to assess rice N status (Zhu et al. 2007; Gnyp et al., 2014; Yao et al., 2014; Lu et al. 2017) and few have used NDVI to develop in-season yield predictions (Harrell et al., 2011; Yao et al., 2012; Cao et al., 2016). However, most of these studies have focused their research on single sites, leaving at question the scalability of their findings to other sites representing different soils and management practices. Therefore, the objectives of this study were to determine how well NDVI at PI assesses rice N status and predicts final grain yield across a range of sites and years. Such research will provide the basis for using NDVI as a N management tool in rice.

1.2. MATERIALS AND METHODS

1.2.1 Nitrogen Response Trials

1.2.1.1 Site Description

Eight on-farm and two on-station N response trials were established during the 2015 to 2018 rice growing seasons at various locations (referred to by proximity to nearest town or station and study year) throughout the Sacramento Valley rice growing region of CA (Fig. 1.1, Table 1.1). On-station sites were established at the CA Rice Experiment Station (RES) near Biggs. The Sacramento Valley has a Mediterranean climate characterized by warm and dry conditions during the growing season (May to October). The average air temperature and precipitation during the growing season for the four years of this study were 23.4° C and 7.04 mm, respectively, based on weather data collected from a centrally located CA Irrigation Management Information Systems (CIMIS) weather station near Biggs (CIMIS, 2018). In CA, most farmers use direct water-seeding to establish the rice crop. In this case, the fields are fertilized following seedbed preparation, flooded, and then soaked seed is broadcast onto the field using an airplane.

Soil samples were collected from the plow layer (approximately 0 – 15 cm) after tillage, but prior to fertilizer application. Soil taxonomic classification and selected chemical and physical properties for each site-year are provided in Table 1.1. Most study sites consisted of soils with high clay contents (40 – 57%), typical of rice soils in CA. The only exceptions were soils at Biggs (20% clay) and Marysville (22% clay). Soil pH was measured using saturated paste (United States Salinity Laboratory Staff, 1954) and ranged from 4.6 – 7.0. Soil organic carbon and N were measured using an elemental analyzer interfaced to a continuous flow isotope ratio mass spectrometer (EA-IRMS) and ranged from 1.19% to 2.25%, and from 0.12 to 0.20%, respectively.

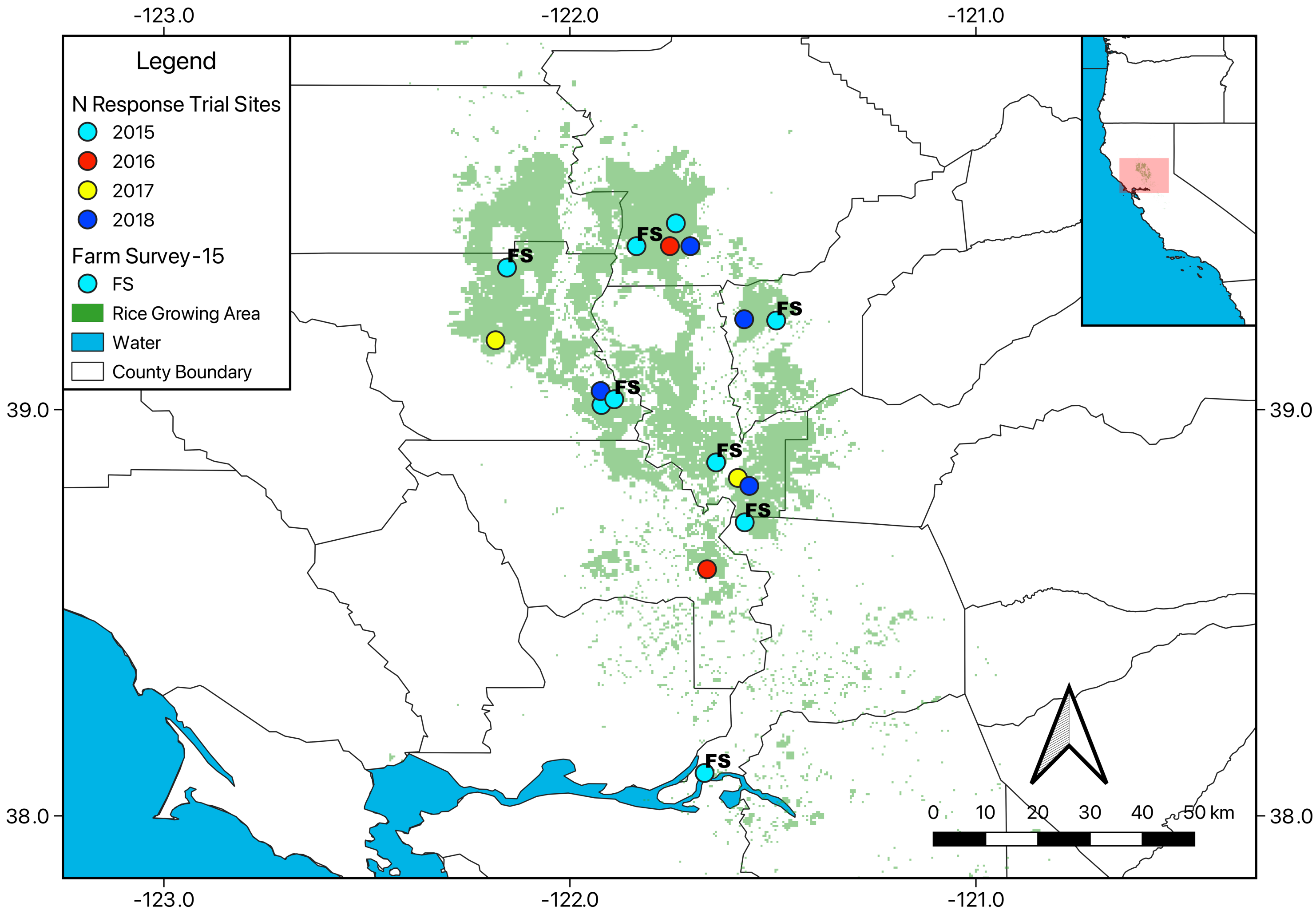

Figure 1.1. A map of N response trial sites and Farm Survey-15 locations established during the 2015 to 2018 growing seasons throughout the Sacramento Valley rice growing area of California (CA).

Table 1.1. Soil descriptions and selected properties of each N response trial site-year located throughout the Sacramento Valley

Site-Year	Soil Series	Taxonomic Classification	Texture			Organic Carbon	Total Nitrogen	pH
			Sand	Silt	Clay			
			---------- % ----------					
Arbuckle-15	Clear Lake Clay	Fine, smectitic, thermic Xeric Endoaquerts	10	33	57	2.25	0.19	6.2
RES-15	Esquon-Neerdobe	Fine, smectitic, thermic Xeric Epiaquerts	31	25	44	1.49	0.12	5.0
Davis-16	Sycamore Complex	Fine-silty, mixed, super active, nonacid, thermic Mollic Endoaquepts	13	37	50	2.22	0.20	7.0
RES-16	Esquon-Neerdobe	Fine, smectitic, thermic Xeric Epiaquerts	32	24	44	1.75	0.13	5.0
Nicolaus-17	Capay silty clay	Fine, smectitic, thermic Typic Haploxererts	19	36	45	1.44	0.13	5.5
Williams-17	Willows silty clay	Fine, smectitic, thermic Sodic Endoaquerts	21	39	40	1.79	0.16	5.0
Arbuckle-18	Clear Lake Clay	Fine, smectitic, thermic Xeric Endoaquerts	30	21	49	2.12	0.18	6.3
Biggs-18	Eastbiggs	Fine, mixed, active, thermic Abruptic Durixeralfs	50	30	20	1.52	0.12	4.9
Marysville-18	San Joaquin Loam	Fine, mixed, active, thermic Abruptic Durixeralfs	39	39	22	1.19	0.15	4.6
Nicolaus-18	Capay silty clay	Fine, smectitic, thermic Typic Haploxererts	22	36	42	1.75	0.16	4.8

1.2.1.2 Experimental Design

N response trials were arranged in a randomized complete block design with four replicates. In 2015 and 2016, plots measured 5 m by 6 m and in 2017 the plots measured 5 m by 7.5 m. A wide range of crop N status (i.e. biomass and N concentrations) was achieved by broadcasting pre-plant N fertilizer by hand at rates of 0, 75, 125, 175, and 225 kg N ha^{-1} as urea (0.46 g N g^{-1}). In 2017, additional pre-plant rates of 45 and 275 kg N ha^{-1} were included. In 2018, pre-plant N fertilizer was injected into the soil subsurface at approximately 7 to 10 cm depth as aqua-ammonia at rates of 0, 101, 135, 168, 202, 235 kg N ha^{-1}. Plot width was determined by the swath width of the harrowing implement used to apply aqua-ammonia and ranged from 6.5 m to 11.5 m. Plot length was 9.1 m at all sites and was taken from the central portion of a 21 m tractor pass to ensure uniform fertilizer application within the plots. Phosphorus (P) and potassium (K) were broadcast across all plots at a rate of 45 kg P_2O_5 ha^{-1} as triple superphosphate (0.45 g P g^{-1}) and 50 kg K_2O ha^{-1} as sulfate of potash (0.52 g K g^{-1}; 0.17 g S g^{-1}) to ensure these nutrients did not limit crop growth. Plots did not receive any additional fertilizer after pre-plant applications. Once all fertilizer was applied, fields were flooded and then aerially planted with pre-germinated seeds of medium grain rice variety M-206. Planting dates varied by site-year but were all within the normal timeframe for the Sacramento Valley (early to mid-May). Crop establishment and management followed common grower practice and was either managed by the grower (on-farm sites) or researchers (on-station sites).

1.2.2 Farm Survey

In addition to the N response trials, in 2015 a total of 28 on-farm plots (Farm Survey-15) were established to evaluate the relationship between NDVI and PI N status across a range of rice varieties, fertilizer management, soil types, microclimates, and crop establishment methods. Seven farms were selected (denoted by the nearest town or island) representing the major geographical regions of CA where rice is grown (Fig. 1.1, Table 1.2). Within each farm, two to seven plots were established. Soil samples (0 – 15 cm) were collected from each plot and taxonomic classification and selected chemical and physical characteristics are reported in Table 1.2. All farms were within the Sacramento Valley, except Twitchell Island, which has peat and mineral soils, was dry-seeded (as opposed to water seeded), and has cooler temperatures due to its proximity to the Sacramento-San Joaquin Delta.

Table 1.2. Soil description, selected properties, and rice variety grown at each Farm Survey-15 location

Farm Location (number of plots)	Rice Variety	Soil Series	Taxonomic Classification	Texture			Organic Carbon	Total Nitrogen	pH
				Sand	Silt	Clay			
				---------------------------------%	----------------------------------				
Arbuckle (2)	M-206	Clear Lake Clay	Fine, smectitic, thermic Xeric Endoaquerts	12 – 16	28 – 30	56 – 58	2.05 – 2.32	0.19	6.0– 6.5
Biggs (3)	M-205	Lofgren-Blavo	Very-fine, smectitic, thermic Xeric Duraquerts	16 – 29	15 – 25	46 – 63	1.54 – 2.17	0.12 – 0.17	4.8 – 5.6
Marysville (4)	M-401	Kimball loam	Fine, mixed, active, thermic Mollic Palexeralfs	35 – 47	29 – 37	24 – 29	1.01 – 1.64	0.10 – 0.14	4.9 – 5.1
Maxwell (3)	M-206	Willows silty clay	Fine, smectitic, thermic Sodic Endoaquerts	19 – 31	32 – 40	37 – 43	2.52 – 2.71	0.22 – 0.23	5.1 – 5.4
Robbins (4)	Koshi	Clear Lake silt loam	Fine, smectitic, thermic Xeric Endoaquerts	49 – 83	8 – 34	9 – 18	0.40 – 0.96	0.04 – 0.08	4.9 – 5.5
Sacramento (5)	M-104 & FRC-22	Clear Lake Clay / Yuvas Loam	Fine, smectitic, thermic Xeric Endoaquerts / Fine, mixed, active, thermic Abruptic Durixeralfs	21 – 33	23 – 38	36 – 49	1.64 – 1.97	0.14 – 0.17	5.0 – 5.8
Twitchell Island (7)	M-206	Rindge mucky silt loam	Euic, thermic Typic Haplosaprists	15 – 87	5 – 39	8 – 56	2.72 – 26.14	0.05 – 1.34	5.1 – 5.8

1.2.3 NDVI Measurements

A GreenSeeker handheld crop sensor (Trimble Inc., Sunnyvale, CA) was used to measure NDVI. The GreenSeeker is an active sensor which measures canopy reflectance (ρ) at specific wavelengths in the red (670 +/- 10 nm) and near infrared (780 +/- 10 nm) regions of the electromagnetic spectrum and calculates NDVI as ($\rho_{780\ nm}$ - $\rho_{670\ nm}$) / ($\rho_{780\ nm}$ + $\rho_{670\ nm}$). Measurements were taken at PI, which marks the physiological shift from vegetative to reproductive plant growth (Counce et al., 2000). For the short duration varieties, which were used in most sites in this study, PI occurs approximately 45 to 50 days after sowing and is visually determined by a dark green ring just below the initiating panicle, occurring 5 to 7 days before panicle differentiation (PD) (when the panicle becomes visible) (De Datta, 1981). Panicle initiation was visually confirmed in the field prior to measuring NDVI using the method outlined by Dunn et al. (2014). Measurements were taken by holding the GreenSeeker in the nadir position and scanning it over the biomass sampling area at a constant height of 1.0 m above the crop canopy. For each plot, the final NDVI value represented the average of three to four NDVI readings. Canopy closure was achieved by PI in all plots that received N fertilizer, thus the effect of background water or soil on NDVI measurements was considered negligible. For the 0 N plots, some influence of background water was present and was accounted for by taking the average of multiple NDVI readings.

Two GreenSeekers were used to measure NDVI (GreenSeeker 1 in 2015 and GreenSeeker 2 from 2016 to 2018). Consistent differences between the two devices were detected by plotting side by side NDVI measurements (n = 105) (Fig. S1). Differences were normalized by adjusting NDVI values based on the resulting fitted linear regression equation.

This variability across GreenSeekers is a concern and needs to be addressed when using the device in the field. Often, when using NDVI to inform N fertilizer management, a response index is developed where the NDVI of a N non-limiting plot and the field test area are measured and the ratio of the two provides the response index (Mullen et al., 2003). In such cases, the variability between GreenSeeker units in terms of direct NDVI measurements would be less a concern.

1.2.4 Biomass Sampling

Immediately following NDVI measurements, all rice plants within a 0.5 m^2 quadrat were pulled from each plot. After removing roots, the aboveground biomass was oven dried at 60° C to constant weight; after which the samples were ground in a Wiley mill and then ball-milled. Plant material from each plot was analyzed for total N using EA-IRMS. Two plant samples were collected from each of the 28 Farm Survey-15 plots in order to calculate an average for each plot. One plant sample was collected per plot for the N response trial sites. From these samples, we quantified the following parameters of crop N status: aboveground biomass (AGB, kg ha^{-1}), N concentration (N_{CONC}, g N kg^{-1}), and total N uptake (N_{UP}, kg N ha^{-1}, = AGB x N_{CONC}).

1.2.5 Grain Yield

Grain yield (kg ha^{-1}) was obtained by harvesting mature plants from a 1.0 m^2 quadrat in each plot (grain yield was not obtained for the Farm Survey-15 plots). Grains were removed from panicles, cleaned using a seed blower, dried to constant moisture at 60° C, and weighed. Final yields are reported at 14% moisture.

1.2.6 Statistical Analysis

Construction of plots, development of regression models, and the analysis thereof was performed using the statistical program R (version 3.5.2, R Core Team). The package 'ggplot2' (Wickman, 2009) was used to visualize the data and construct plots. For the purpose of analysis, data from the Farm Survey-15 plots were combined into a single site-year. The relationship between NDVI and each N status parameter was described using a quadratic linear regression model. The horizontal asymptote for each model was determined as the y-value at the vertex, which was calculated from the resulting model coefficients. Quadratic models were selected over complex higher order models as both model types explained a similar amount of variability in the data and the quadratic models allowed for direct comparisons of results with previous studies.

The relationship between N_{UP} and grain yield was described by a segmented linear regression model from the package 'segmented' (Muggeo, 2017). The segmented model identifies breakpoints in the data (i.e. significant changes in the slope parameter) and describes the data before and after the breakpoint using separate linear segments. The relationship between NDVI and grain yield was described by a simple linear regression model.

Graphical and numerical summaries were examined to ensure the assumptions of linear regression were satisfied for all regression models. Model goodness of fit was assessed by comparing adjusted coefficient of determination (r^2) and root mean squared error (RMSE), calculated as: $\mathrm{RMSE} = \sqrt{\frac{1}{n}\sum_{i=1}^{n}(y_i - y_i)^2}$.

1.3. RESULTS

1.3.1 N Response Trials

Considerable variability in crop AGB, N_{CONC} and N_{UP} was present at PI both within and across N trial sites. As expected, the within-site variability was due to the different N rates with crop AGB, N_{CONC} and N_{UP} all increasing with increasing N rate (Table 1.3). Across site-years, mean AGB ranged from 2609 kg ha^{-1} (Davis-16) to 6334 kg ha^{-1} (Arbuckle-15); N_{CONC} ranged from 21.4 g N kg^{-1} (Arbuckle-15, 18) to 29.9 g N kg^{-1} (Marysville-18); and N_{UP} ranged from 58.9 kg N ha^{-1} (Davis-16) to 147.7 kg N ha^{-1} (Nicolaus-17).

At any given N trial site, NDVI increased with increasing N rate to a point then leveled off (i.e. saturated). Therefore, the lowest NDVI values tend to represent the 0 N rate, while the highest NDVI value represented the higher N rates. Minimum NDVI varied considerably among the site-years, ranging from 0.15 (Arbuckle-18) to 0.58 (Nicolaus-18) whereas maximum NDVI only ranged from 0.72 (Davis-16) to 0.82 (Williams-17) (Table 1.3).

As expected, the lowest grain yields in the N trials were in the 0 N treatments, with grain yield increasing at most sites to a maximum and then leveling off or decreasing at higher N rates. Minimum site-year grain yield ranged from 2,948 kg ha^{-1} (Arbuckle-18) to 10,345 ka ha^{-1} (Nicolaus-17) (Table 1.4). Despite different maximum AGB, N_{CONC}, and N_{UP} at PI across site-years, maximum yields were relatively similar and ranged from 12,829 kg ha^{-1} (Williams-17) to 14,675 kg ha^{-1} (RES-16). Overall, there was no segregation in crop AGB, N_{CONC}, N_{UP}, or grain yield between site-years based on different sources of pre-plant N fertilizer (i.e. urea and aqua-ammonia).

Table 1.3. Descriptive statistics of rice N status parameters and NDVI measured at PI growth stage

		Aboveground Biomass		**N Concentration**		**Total N Uptake**		**NDVI**	
Site-Year	N	Min – Max	Mean	Min – Max	Mean	Min – Max	Mean	Min – Max	Mean
		----------- kg ha^{-1} -----------		----------- g N kg^{-1} -----------		---------- kg N ha^{-1} ----------			
Arbuckle-15	20	3400 – 8540	6334	13.6 – 30.5	21.4	48.9 – 255.8	141.4	0.49 – 0.78	0.71
Farm Survey-15	28	1260 – 7260	5090	10.9 – 33.6	21.9	13.8 – 196.4	114.9	0.18 – 0.82	0.65
RES-15	20	3520 – 6540	5084	11.9 – 37.3	23.8	41.7 – 230.5	126.5	0.53 – 0.80	0.73
Davis-16	20	1332 – 3714	2609	14.6 – 31.7	21.5	20.3– 114.7	58.9	0.56 – 0.72	0.67
RES-16	20	1466 – 4960	3428	18.5 – 38.8	28.6	30.9 – 192.6	103.2	0.36 – 0.75	0.64
Nicolaus-17	28	3970 – 7426	5559	15.5 – 36.1	25.7	61.7 – 240.2	147.7	0.49 – 0.80	0.68
Williams-17	28	2740 – 7270	5471	12.3 – 30.6	22.1	33.8 – 194.3	124.6	0.36 – 0.82	0.71
Arbuckle-18	24	730 – 8006	3397	12.1 – 30.2	21.4	9.7 – 160.6	76.5	0.15 – 0.75	0.61
Biggs-18	23	1962 – 6812	5019	10.4 – 32.9	21.5	20.4 – 193.4	113.6	0.36 – 0.79	0.69
Marysville-18	24	2384 – 5472	4604	16.1 – 37.0	29.9	38.3 – 202.4	142.0	0.45 – 0.75	0.66
Nicolaus-18	24	3242 – 7282	6069	13.1 – 30.7	23.3	46.0 – 223.5	146.0	0.58 – 0.77	0.72
All	**289**	**730 – 8540**	**4840**	**10.4 – 38.8**	**23.7**	**9.7 – 255.8**	**118.9**	**0.15 – 0.82**	**0.68**

NDVI, Normalized Difference Vegetation Index; PI, panicle initiation; N, sampling number; Min, minimum value; Max, maximum value; Mean, average value

Table 1.4. Descriptive statistics of final grain yield at the N response trial site-years (yields were not obtained for Farm Survey-15)

Site-Year	N	Grain Yield†	
		Min – Max	Mean
		---------------- kg ha^{-1} ----------------	
Arbuckle-15	20	6469 – 14529	12072
RES-15	20	5235 – 14140	11753
Davis-16	20	6664 – 13969	10599
RES-16	20	6653 – 14675	11246
Nicolaus-17	28	10345 – 13375	12005
Williams-17	28	6096 – 12829	10159
Arbuckle-18	24	2948 – 13648	9980
Biggs-18	23	6767 – 13069	11468
Marysville-18	24	8046 – 12246	11000
Nicolaus-18	24	8961 – 14391	12793
All	**231**	**2948 – 14675**	**11291**

N, sampling number; Min, minimum value; Max, maximum value; Mean, average value
†Adjusted to 14% moisture

1.3.2 Farm Survey

Crop N status data taken at PI from the Farm Survey-15 plots varied considerably, as may be expected, given the large number of farms within Farm Survey-15 and the variability among them. The range of AGB (1260 – 7260 kg ha^{-1}), N_{CONC} (10.9 – 33.6 g N kg^{-1}), and N_{UP} (13.8 – 196.4 kg N ha^{-1}) was considerably larger across Farm Survey-15 plots relative to N trial site-years (Table 1.3). Variability in crop N status was also reflected by the wide range of NDVI (0.18 to 0.82). Grain yield was not obtained for Farm Survey-15.

1.3.3 Relationship between PI N Status and NDVI

An increase in PI N status led to a corresponding increase in NDVI, until a threshold was achieved, after which, NDVI values leveled off (Fig. 1.2). NDVI saturated within a narrow range (0.76 to 0.78), when AGB, N_{CONC}, and N_{UP} exceeded 7597 kg ha^{-1}, 29.9 g N kg^{-1}, and 185 kg N ha^{-1}, respectively. Overall, the nature of the relationship between each N status parameter and NDVI was similar across the N response trials and Farm Survey-15. Of the three N status parameters, N_{UP} explained the largest amount of variation in NDVI ($r^2 = 0.66$), followed by N_{CONC} ($r^2 = 0.54$) and AGB ($r^2 = 0.51$).

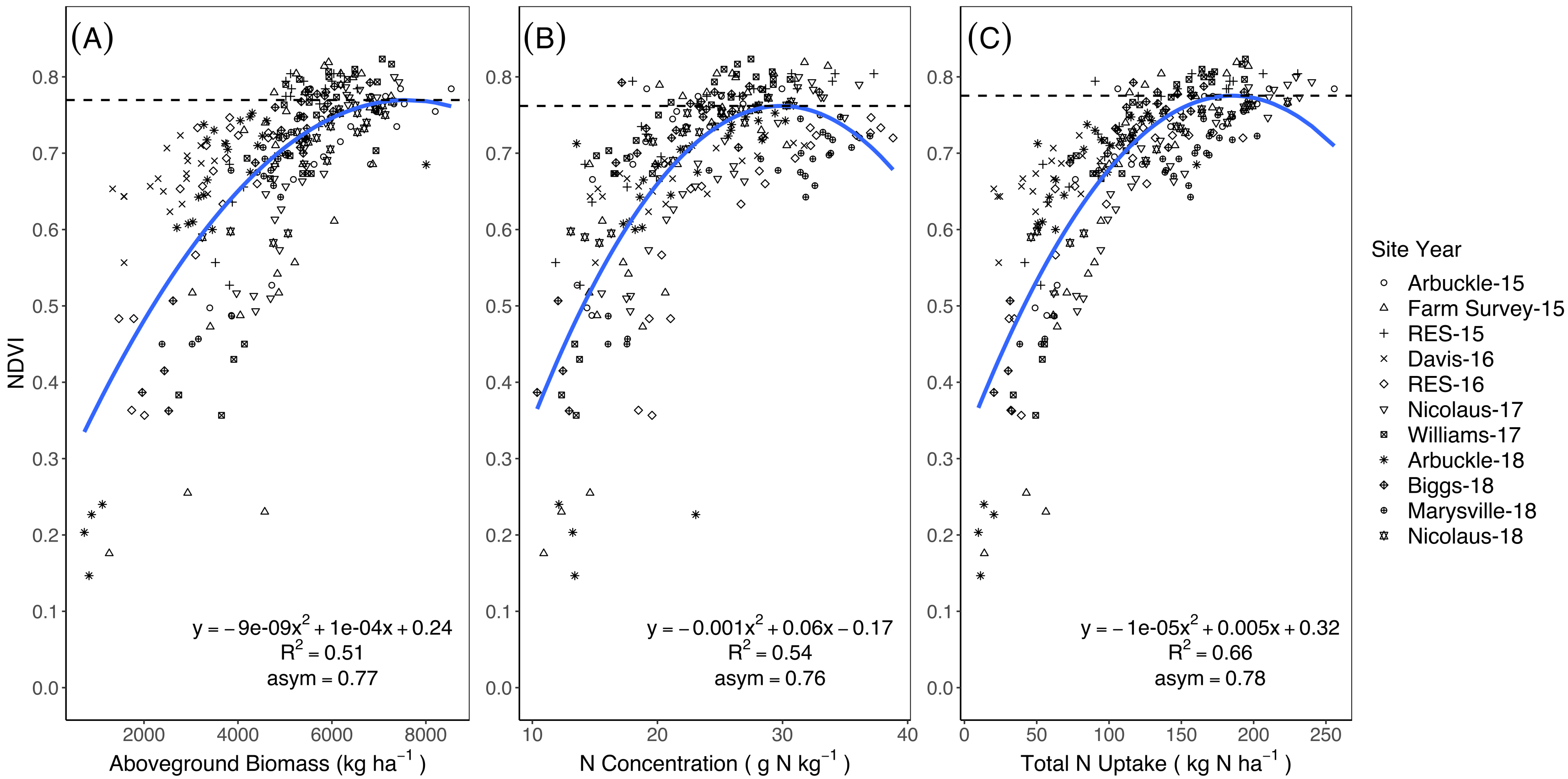

Figure 1.2. The relationship between rice **(A)** aboveground biomass, **(B)** N concentration, and **(C)** total N uptake at panicle initiation rice growth stage and Normalized Difference Vegetation Index (NDVI) as described by quadratic linear regression models. The horizontal asymptote (asym) represents the NDVI value at which the relationship saturates. Data was collected during the 2015 to 2018 growing season from ten N response trial sites and 28 on-farm plots (Farm Survey-15) throughout the Sacramento Valley rice growing region of California (CA).

1.3.4 Relationship Between PI Total N Uptake, NDVI, and Final Grain Yield

Based on the segmented model, PI N_{UP} explained a large portion of the variation in final grain yield ($r^2 = 0.63$; RMSE = 1321 kg ha^{-1}) (Fig. 1.3a). The segmented model estimated a breakpoint at 93.9 kg N ha^{-1} (95% confidence interval: 85.1 to 102.9 kg N ha^{-1}) (data not shown), indicating that an increase in crop PI N_{UP} beyond this value did not result in a significant increase in average final grain yield. The slope before the breakpoint was 81 kg kg^{-1} N, and after the breakpoint was not statistically different than a zero slope. The breakpoint of 93.9 kg N ha^{-1} corresponded to an average maximum grain yield of 12,314 kg ha^{-1}. Based on the simple linear regression model, NDVI at PI was positively correlated with final grain yield ($r^2 = 0.58$; RMSE = 1415 kg ha^{-1}) (Fig. 1.3b).

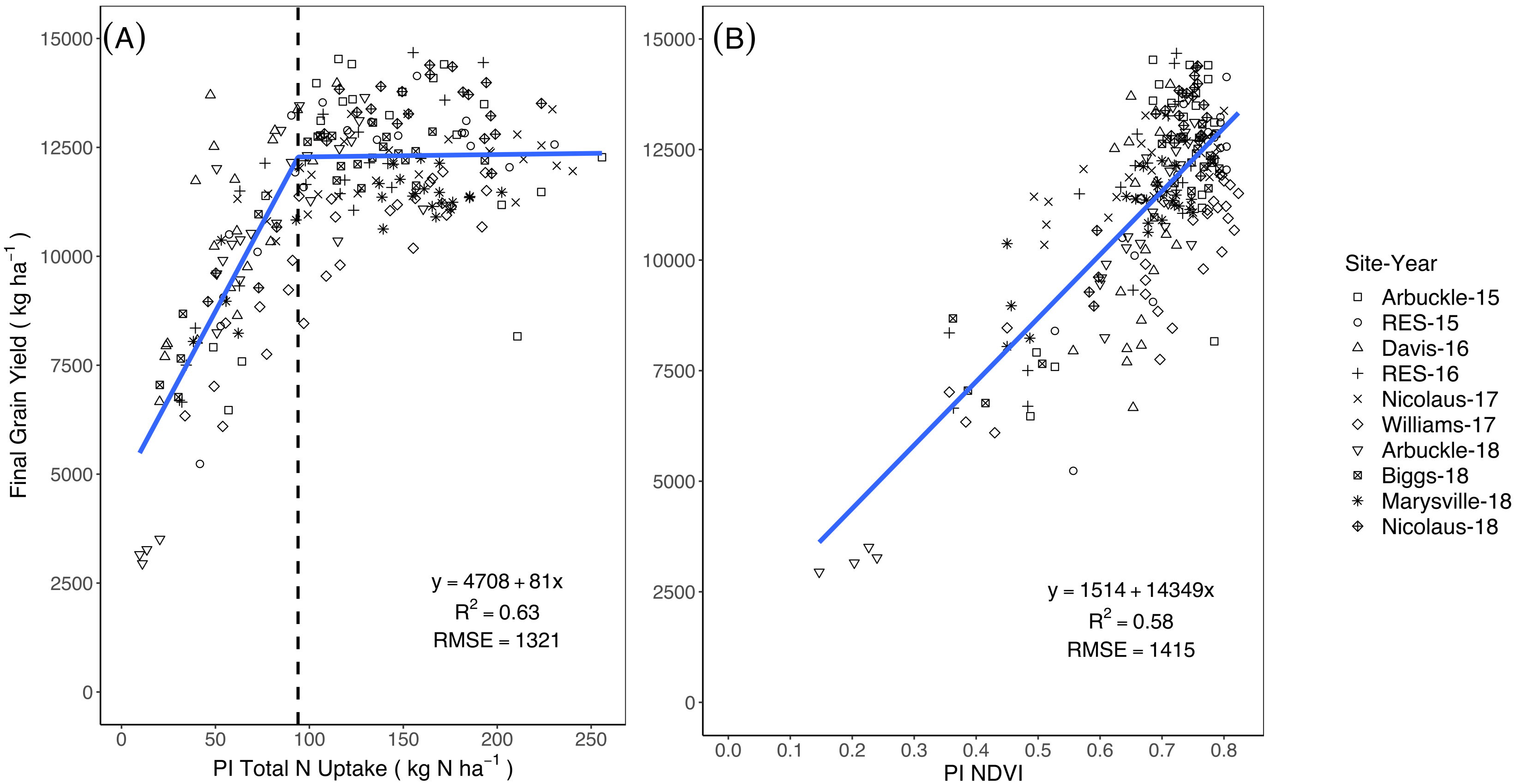

Figure 1.3. (A) The relationship between rice total N uptake at panicle initiation (PI) growth stage and final grain yield as described by a segmented model. The vertical dashed line at 93.9 kg N ha^{-1} represents the minimum amount of crop N uptake required by PI to achieve maximum grain yield. **(B)** The relationship between Normalized Difference Vegetation Index (NDVI) at PI and final grain yield as described by a simple linear regression model. Data was collected during 2015 to 2018 from ten N response trial sites throughout the Sacramento Valley rice growing area of California (CA).

1.4. DISCUSSION

1.4.1 NDVI Saturation

Quadratic linear regression models were developed to describe the relationship between NDVI and crop N status. In each case, as crop N status increased, so did NDVI, until a horizontal asymptote was reached and additional increases in crop N status led to minimal change in NDVI (Fig. 2). This saturation of two-band indices such as NDVI is a well-known phenomenon (Asrar et al., 1984; Hatfield et al., 1985; Thenkabail et al., 2000; Cao et al., 2013; Gu et al., 2013). NDVI saturation is a result of the crop reaching 100% canopy cover, but AGB and leaf area index continuing to increase (Gitelson, 2003). Once the canopy reaches 100% cover, near infrared reflectance continues to rise, but red reflectance only exhibits a modest decrease, resulting in only slight changes in the ratio (i.e. the denominator will have a much greater impact on the ratio than the numerator) (Thenkabail et al., 2000). In our study, NDVI saturated within a narrow range (0.76 to 0.78), when AGB, N_{CONC}, and N_{UP} exceeded 7597 kg ha^{-1}, 29.9 g N kg^{-1}, and 185 kg N ha^{-1}, respectively (Fig. 1.2). Our result is similar to the findings of Yao et al. (2014) who reported the relationship between NDVI and AGB and N_{UP} to saturate at about 0.80 and 0.78, respectively. Gnyp et al. (2014) reported the relationship between AGB and NDVI to saturate at approximately 0.90, which is higher than our study and may be because they simulated GreenSeeker NDVI from passive hyperspectral data, while we have used actual GreenSeeker measurements.

Recent studies suggest indices which incorporate a red-edge band (690 to 730 nm) may improve rice N status assessment by overcoming the saturation problem (Wang et al., 2012; Cao et al., 2013; Dunn et al., 2016). Cao et al. (2013) found several red-edge based indices to explain a large portion of rice N_{UP} variability when described by linear regression models. Wang et al.

(2012) developed a red-edge based three band index which estimated N_{CONC} with high accuracy while reducing saturation. Dunn et al. (2016) confirmed the strong correlation of red-edge bands with rice N_{UP} based on their analysis of fine-resolution hyperspectral data. Given the saturation of NDVI, and strong linear relationships observed between red-edge based indices and rice N status, further research is warranted to investigate the potential improvement of red-edge based indices over NDVI to assess rice N status.

1.4.2 Assessing PI N Status with NDVI

Of the three N status parameters, N_{UP} explained the largest amount of variation in NDVI ($r^2 = 0.66$), followed by N_{CONC} ($r^2 = 0.54$) and AGB ($r^2 = 0.51$) (Fig. 1.2). The relationship between NDVI and crop N status was similar across the N trial site-years and Farm Survey-15, indicating NDVI assessed crop N status consistently across the wide range of environmental conditions and management practices included in this study. Importantly, within the observations in this study, AGB at NDVI saturation was closer to the maximum observed AGB, whereas NDVI saturated earlier for N_{CONC} and N_{UP} (Fig 2). This suggests at PI, NDVI saturation may pose less of a limitation when assessing AGB as it would with N_{CONC} or N_{UP}. That said, the relationship between NDVI and AGB is still poorer than for N_{CONC} or N_{UP}.

The relationship between NDVI and crop N status observed in this study is similar in strength to what others have found in wheat and maize (Reyniers and Vrindts, 2006; Li et al., 2008; Erdle et al., 2011; Li et al., 2014). To our knowledge, only one other study has examined the relationship between NDVI and AGB, N_{CONC}, and N_{UP} in rice. In that study, Yao et al. (2014) reported the strongest correlation between NDVI and AGB ($r^2 = 0.76$), followed by N_{UP} ($r^2 = 0.70$), and N_{CONC} ($r^2 = 0.38$). This is in contrast to our study where NDVI predicted N_{UP} and

N_{CONC} better than AGB. We are not sure why this difference between studies, but it may be because Yao et al. (2014) conducted all their research at a single location, thus resulting in less variation of AGB during the course of their study. Others have looked at the relationship between NDVI and N_{CONC} and have reported both strong ($r^2 = 0.81$) and weak ($r^2 = 0.08$) correlations (Zhu et al., 2007; Lu et al., 2017), which may be due to differences in rice varieties or the growth stage when data was collected. In other studies, Gnyp et al. (2014) examined the relationship between NDVI and AGB and reported the same correlation ($r^2 = 0.51$) as our study; while Li et al. (2018) examined the relationship between leaf N_{UP} and NDVI and found a similar correlation ($r^2 = 0.70$) to our study with plant N_{UP}.

The strength of our study relative to most of the other studies mentioned above is that it considered multiple N status parameters over a large range of sites and years. The strong correlation observed between NDVI and rice N status in this study suggests that the GreenSeeker could be a scalable tool to assess N status. However, as previously discussed, NDVI saturation limits its utility to lower values of crop N status, suggesting alternative indices that do not saturate could potentially improve N status assessment.

1.4.3 Predicting Final Grain Yield at PI with N_{UP} and NDVI

The utility of NDVI to develop regional scale rice yield predictions has received considerable attention (e.g. Huang et al., 2013; Son et al., 2014; Pagani et al., 2019), while fewer studies have focused on the farm scale. The ability to estimate rice yield early in the season is of interest to farmers and private companies for a number of reasons, including refining N fertilizer recommendations, planning harvest, forecasting milling and storage needs, and defining marketing strategies.

We observed a positive correlation ($r^2 = 0.63$) between PI N_{UP} and final grain yield (Fig. 1.3a). Yields increased strongly with increasing N_{UP} until they reached a plateau at a breakpoint of 93.9 kg N ha^{-1} (Fig. 1.3a). This breakpoint represents the average minimum amount of crop PI N_{UP} required to achieve average maximum grain yield. Across sites the actual N_{UP} value varied as indicated by the 95% confidence interval ranging from 85.1 to 102.9 kg N ha^{-1} (data not shown) and final grain yield at the breakpoint also varied considerably (Fig 3a). Part of this variability may be explained by differences in soil indigenous N supply after PI. For example, achieving the average maximum grain yield at the breakpoint (12,314 kg ha^{-1}) requires a total seasonal N_{UP} of approximately 215 kg N ha^{-1} (assuming N concentrations in rice grain and straw of 1.10% and 0.65%, respectively; Dobermann and Fairhurst, 2007), indicating that an additional 121 kg N ha^{-1} is required after PI. Given that pre-plant N fertilizer is completely taken up by PI (LaHue et al., 2016), and additional N fertilizer was not applied, this requirement must have been satisfied by soil indigenous N. Previous studies have shown that indigenous N supply from rice soils can vary significantly across sites and over time; and is closely linked with soil properties such as organic carbon (Cassman et al., 1998; Espe et al., 2015). In theory, the breakpoint of 93.9 kg N ha^{-1} N_{UP} and corresponding NDVI could potentially serve as a target for farmers when assessing midseason crop N requirements. However, accounting for site-specific differences in soil N supply may be needed to refine this target and further research could explore this. In this study, N_{UP} of 93.9 kg N ha^{-1} corresponds to a NDVI value for 0.66 (derived from Fig 2c); and importantly, this NDVI value is below the saturation value.

Given the relationship between PI N_{UP} and final grain yield (Fig 3a) and PI N_{UP} and NDVI (Fig. 1.2c), the positive correlation between NDVI at PI and final grain yield ($r^2 = 0.58$) was expected (Fig. 1.3b). This is similar to Cao et al. (2015), who found a comparable correlation ($r^2 = 0.63$) in their experiments at a single location. Others (e.g. Harrell et al., 2011; Yao et al., 2012) have reported a poorer relationship between NDVI and grain yield with r^2 values ranging from 0.36 to 0.44.

Importantly, for short duration varieties grown in CA, PI usually occurs about 45 to 50 days after seeding; thus, only one-third of the entire growing season. Grain yield can be altered in a number of ways after PI due to many abiotic and biotic factors. For example, in CA and elsewhere, cold nighttime temperatures at meiosis (between PI and heading) causes floret sterility and reduced grain yields (Board et al., 1980, Espe et al., 2016). High temperatures at flowering can result in yield losses in many rice growing areas, including CA (Espe et al., 2016, Fahad et al., 2018). Additionally, differences in soil N supply late in the season can affect yields as discussed above. Biotic factors such as insects and diseases can all negatively affect yields after PI (Sesma and Osbourne, 2004; Brooks et al., 2009; Hasanuzzaman et al., 2018). The greater the variability in these stresses across sites or years, the poorer the relationship will be between NDVI at PI and final grain yield. Given this, one should not expect the relationship between final grain yield and any plant measurement taken at PI to be very high. However, if those relationships were developed under optimal conditions where post PI stresses did not limit grain yield, then such measurements may provide a good estimate of yield potential. Although, the incidence of these stresses was not measured directly in this study, the fact that maximum grain yields were similar across all site-years suggests that post PI stresses did not have a significant impact on yields, thus providing optimal conditions to predict final grain yield at PI using NDVI.

1.5. CONCLUSION

The significant correlation between GreenSeeker NDVI and crop N status suggests that it may be developed into a useful tool to guide midseason N management decisions. However, NDVI saturated at high values of crop N status, suggesting further research in alternative indices (e.g. red-edge based NDVI) is warranted and could potentially improve estimates of midseason N status. Interestingly, in this study we identified an N_{UP} value at PI (93.9 kg N ha^{-1}) at which average maximum grain yield was achieved. This value could serve as a midseason target in similar systems and may identify when further N applications are needed. The NDVI corresponding to this N_{UP} value is 0.66 which, importantly, is below the saturation point. Finally, as technology advances, future research focusing on large scale production systems will likely shift away from handheld proximal sensors, like the GreenSeeker used in this study, in favor of sensors that can be mounted to drones or satellites.

1.6. ACKNOWLEDEMENTS

We would like to thank the California Rice Research Board for supporting this research, Cesar G. Abrenilla and the entire Agroecosystems Lab for their generous help with field work and data collection, John Ray Stogsdill and the entire staff at the California Rice Experiment Station, and the California rice growers who participated in this study.

REFERENCES

Alam, M.M., Ladha, J.K., Khan, S.R., Foyjunnessa, Harun-ur-Rashid, Khan, A.H., and R.J. Buresh. 2005. Leaf color chart for managing nitrogen fertilizer in lowland rice in Bangladesh. Agron. J. 97:949-959.

Almaraz, M., Bai, E., Wang, C., Trousdell, J., Conley, S., Faloona, I., and B.Z. Houlton. 2018. Agriculture is a major source of NO_x pollution in California. Sci. Adv. 4:8.

Asrar, G., Fuchs, M., Kanemasu, E.T., and J.L. Hatfield. 1984. Estimating absorbed photosynthetic radiation and leaf area index from spectral reflectance in wheat. Agron. J. 76:300-306.

Balasubramanian, V., Morales, A.C., Cruz, R.T., and S. Abdulrachman. 1999. On-farm adaptation of knowledge-intensive nitrogen management technologies for rice systems. Nutr Cycl Agroecosys. 53:59-69.

Board, J.E., Peterson, M.L., and E. Ng. 1980. Floret sterility in rice in a cool environment. Agron. J. 72:483-487.

Brooks, S.A., Anders, M.M., and K.M. Yeater. 2009. Effect of cultural management practices on the severity of false smut and kernel smut of rice. Plant Dis. 93:1202-1208.

Cassman, K.G., Peng, S., Olk, D.C., Ladha, J.K., Reichardt, W., Dobermann, A., and U. Singh. 1998. Opportunities for increased nitrogen-use efficiency from improved resource management in irrigated rice systems. Field Crops Res. 56:7-39.

Cao, Q., Miao, Y., Shen, J., Yu, W., Yuan, F., Cheng, S., Huang, S., Wang, H., Yang, W., and F. Liu. 2016. Improving in-season estimation of rice yield potential and responsiveness to topdressing nitrogen application with Crop Circle active crop canopy sensor. Precis. Agric. 17:136-154.

Cao, Q., Miao, Y., Wang, H., Huang, S., Cheng, S., Khosla, R., and R. Jiang. 2013. Non-destructive estimation of rice plant nitrogen status with crop circle multispectral active canopy sensor. Field Crops Res. 154:133-134.

CIMIS. 2018. California Irrigation Management Information System. Internet Resource. (http://www.cimis.water.ca.gov/WSNReportCriteria.aspx) (accessed 17 Nov. 2018).

Conley D.J., Paerl, H.W., Howarth, W.R., Boesch, D.F., Seitzinger, S.P., Haven, K.E., Lancelot, C., and G.E. Likens. 2009. Controlling eutrophication: Nitrogen and phosphorus. Science. 323:1014-1015

Counce, P.A., Keisling, T.C., and A.J. Mitchell. 2000. A uniform, objective, and adaptive system for expressing rice development. Crop Sci. 40:436-443.

Daughtry, C.S.T., Walthall, C.L., Kim, M. S., Brown de Colstoun, E., and J.E. McMurtrey III. 2000. Estimating corn leaf chlorophyll concentration from leaf and canopy reflectance. Remote Sens. Environ. 74:229-239.

S.K. DeDatta. Principles and practices of rice production. 1981. John Wiley & Sons. Singapore.

Di, H.J. and K.C. Cameron. Nitrate leaching in temperate agroecosystems: sources, factors, and mitigating strategies. Nutr. Cycl. Agroecosys. 46:237-256.

Dobermann, A., and T.H. Fairhurst. 2000. Rice: Nutrient disorders and nutrient management. Potash & Phosphate Inst., Potash & Phosphate Inst. Of Canada, and International Rice Research Inst. Oxford Graphic Printers PTE, LTD. Singapore.

Dunn, B.W., Dehaan, R., Schmidtke, L.M., Dunn, T.S., and R. Meder. 2016. Using field-derived hyperspectral reflectance measurement to identify the essential wavelengths for predicting nitrogen uptake of rice at panicle initiation. J. Near Infrared Spec. 24:473-483.

Dunn, T., Dunn, B., and R. Whitworth. 2014. Identifying panicle initiation in rice. NSW Department of Primary Industries.

Erdle, K., Mistele, B., and U. Schmidhalter. 2011. Comparison of active and passive spectral sensors in discrimination biomass parameters and nitrogen status in wheat cultivars. Field Crops Res. 124:74-84.

Espe, M.B., Yang, H., Cassman, K.G., Guilpart, N., Sharifi, H., and B.A. Linquist. 2016. Estimating yield potential in temperate high-yielding, direct-seeded US rice production systems. Field Crops Res. 193:123-132.

Espe, M.B., Kirk, E., van Kessel, C., Horwath, W.H., and B.A. Linquist. 2015. Indigenous nitrogen supply of rice is predicted by soil organic carbon. Soil Sci. Soc. Am. J. 79:569-576.

Fahad, S., Ishan, M.Z., Khaliq, A., Duar, I., Saud, S., Alzamanan, S., Nasim, W., Abdullah, M., Khan, I.A., Wu, C., Wang, D., and J. Huang. 2018. Consequences of high temperature under changing climate optima for rice pollen characteristics-concepts and perspectives. Arch. Agron. Soil Sci. 64:1473-1488.

Gitelson, A.A. 2003. Wide dynamic range vegetation index for remote quantification of biophysical characteristics of vegetation. J. Plant Physiol. 161:163-173.

Glass, A.D.M. 2003. Nitrogen use efficiency of crop plants: Physiological constraints upon nitrogen absorption. Crit. Rev. Plant Sci. 22:453-470.

Gnyp, M.L., Miao, Y., Yuan, F., Ustin, S.L., Yu, K., Yao, Y., Huang, S., and G. Bareth. Hyperspectral canopy sensing of paddy rice aboveground biomass at different growth stages. Field Crops Res. 155:42-55.

Gu, Y., Wylie, B.K., Howard, D.M., Phuyal, K.P., and L. Ji. 2013. NDVI saturation adjustment: A new approach for improving cropland performance estimates in the Greater Platte River Basin, USA. Ecol. Indic. 30:1-6.

Harrell, D.L., Tubaña, B.S., Walker, T.W., and S.B. Phillips. 2011. Estimating rice grain yield potential using Normalized Difference Vegetation Index. Agron. J. 103:1717-1723.

Harter, T., Lund, J.R., Darby, J., Fogg, G.E., Howitt, R., Jessoe, K.K., Pettygrove G.S., Quinn, J.F., Viers, J.H., Boyle, D.B., Canada, H.E., DeLaMora, N., Dzurella, K.N., Fryjoff-Hung, A., Hollander, A.D., Honeycutt, K.L., Jenkins, M.W., Jensen, V.B., King, A.M., Kourakos, G., Liptzin, D., Lopez, E.M., Mayzelle, M.M., McNally, A., Medellin-Azuara, J., and T. S. Rosenstock. 2012. Addressing nitrate in California's drinking water with a focus on Tulare Lake Basin and Salinas Valley groundwater. Report for the State Water Resources Control Board Report to the Legislature. Center for Watershed Sciences, University of California, Davis. 78 p.

Hasanuzzaman, M., Fujita, M., Nahar, K., and J. Biswas. 2018. Advances in rice research for abiotic stress tolerance. Woodhead Publishing. United Kingdom.

Hatfield J.L., Kanemasu, E.T., Asrar, G., Jackson, R.D., Pinter, P.J., Reginato, R.J., and S.B. Idso. 1985. Leaf-area estimates from spectral measurements over various planting dates of wheat. Int. J. Remote Sens. 6:167-175.

Huang, J., Wang, X., Li, X., Tian, H., and Z. Pan. 2013. Remotely sensed rice yield prediction using multi-temporal NDVI data derived from NOAA’s AVHRR. PLoS ONE. 8:8.

Inman, D., Khosla, R., Reich, R.M., and D.G. Westfall. 2007. Active remote sensing and grain yield in irrigated maize. Precis. Agric. 8:241-252.

International Fertilizer Association (IFA). 2017. Assessment of fertilizer use by crop at the global level. International Fertilizer Association and International Plant Nutrition Institute. Paris.

Islam, Z., Bagchi, B., and M. Hossain. 2007. Adoption of leaf color chart for nitrogen use efficiency in rice: Impact assessment of a farmer-participatory experiment in West Bengal, India. Field Crops Res. 103:70-75.

Ladha, J.K., Pathak, H., Krupnik, T.J., Six, J., and C. van Kessel. 2005. Efficiency of fertilizer nitrogen in cereal production: Retrospects and prospects. Adv. Agron. 87:85-156.

LaHue, G.T., Chaney, R.T., Adviento-Borbe, M.A., and B.A. Linquist. 2016. Alternate wetting and drying in high yielding direct-seeded rice systems accomplishes multiple environmental and agronomic objectives. Agr. Ecosyst. Environ. 229:30-39.

Li, S., Ding, X., Kuang, Q., Ata-Ul-Karim, S.T., Cheng, T., Liu, X., Tian, Y., Zhu, Y., Cao, W., and Q. Cao. 2018. Potential of UAV-based active sensing for monitoring rice leaf nitrogen status. Front. in Plant Sci. 9:1834.

Li, F., Gnyp, M.L., Jia, L., Miao, Y., Yu, Z., Koppe, W., Bareth, G., Chen, X., and F. Zhang. 2008. Estimating N status of winter wheat using a handheld spectrometer in the North China Plain. Field Crops Res. 106:77-85.

Li, F., Miao, Y., Feng, G., Yuan, F., Yue, S., Gao, X., Liu, Y., Liu, B., Ustin, S.L., and X. Chen. 2014. Improving estimation of summer maize nitrogen status with red edge-based spectral vegetative indices. Field Crops Res. 157:111-123.

Lu, J., Miao, Y., Shi, W., Li, J., and F. Yuan. 2017. Evaluating different approaches to non-destructive nitrogen status diagnosis of rice using portable RapidSCAN active canopy sensor. Sci. Rep. 7:14073

Linquist, B.A., Hill, J.E., Mutters, R.G., Greer, C.A., Hartley, C., Ruark, M., and C. van Kessel. 2009. Assessing the necessity of surface applied preplant nitrogen fertilizer in rice systems. Agron. J. 101:906-915.

Linquist, B.A. and P. Sengxua. 2003. Efficient and flexible management of nitrogen for rainfed lowland rice. Nutr. Cycl. Agroecosys. 67:139-146.

McFarland, T. M. and C. van Riper III. 2013. Use of normalized difference vegetation index NDVI habitat models to predict breeding birds on the San Pedro River, Arizona. U.S. Geological Survey Open-File Report 1100:42

V.M.R. Muggeo. 2017. segmented: An R package to fit regression models with broken-line relationships. (https://cran.r-project.org/doc/Rnews/)

Mullen, R.W., Freeman, K.W., Raun, W.R., Johnson, G.V., Stone, M.L., and J.B. Solie. 2003. Identifying an in-season response index and the potential to increase wheat yield with nitrogen. Agron. J. 95:347-351.

Pagani, V., Guarneri, T., Busetto, L., Ranghetti, L., Boschetti, M., Movedi, E., Campos-Taberner, M., Garcia-Haro, F.J., Katsantonis, D., Stavrakoudis, D., Ricciardelli, E., Romano, F., Holecz, F., Collivignarelli, F., Granell, C., Casteleyn, S., and R. Confalonieri. 2019. A high-resolution, integrated system for rice yield forecasting at district level. Agr. Syst. 168:181-190.

Peng, S., Garcia, F.V., Laza, R.C., Sanico, A.L., Visperas, R.M., and K.G. Cassman. 1996. Increased N-use efficiency using a chlorophyll meter on high-yielding irrigated rice. Field Crops Res. 47:243-252.

R Core Team 2019. R: A language and environment for statistical computing. R Foundation for Statistical Computing, Vienna, Austria. (https://www.R-project.org/)

Raun, W.R., Soilie, J.B., Johnson, G.V., Stone, M.L., Lukina, E.V., Thomason, W.E., and J.S. Schepers. 2001. In-season prediction of potential grain yield in winter wheat using canopy reflectance. Agron. J. 93:131-138.

Raun, W.R., Solie, J.B., Johnson, G.V., Stone, M.L., Mullen, R.W., Freeman, K.W., Thomason, W.E., and E.V. Lukina. 2002. Improving nitrogen use efficiency in cereal grain production with optical sensing and variable rate application. Agron. J. 94:815-820.

Raun, W.R., Solie, J.B., Stone, M.L., Martin, K.L., Freeman, K.W., Mullen, R.W., Zhang, H., Schepers, J.S., and G.V. Johnson. 2005. Optical sensor-based algorithm for crop nitrogen fertilization. Commun. Soil Sci. Plan. 36:2759-2781.

Reyniers, M. and E. Vrindts. 2006. Measuring wheat nitrogen status from space and ground-based platform. Int. J. of Remote Sens. 27:549-567.

Saberioon, M.M., Amin, M.S.M., Gholizadeh, A., and M.H. Ezri. 2014. A review of optical methods for assessing nitrogen contents during rice growth. Appl. Eng. Agric. 30:657-669.

Sesma, A., and A.E. Osbourne. 2004. The rice leaf blast pathogen undergoes development processes typical of root-infecting fungi. Nature. 431:582-586.

Singh, Y., Singh, B, Ladha, J.K., Bains, J.S., Gupta, R.K., Singh, J., and V. Balasubramanian. 2007. On-farm evaluation of leaf color chart for need-based nitrogen management in irrigated transplanted rice in northwestern India. Nutr. Cycl. Agroecosys. 78:167-176.

Son, N.T., Chen, C.F., Chen, C.R., Minh, V.Q., and N.H. Trung. 2014. A comparative analysis of multitemporal MODIS EVI and NDVI data for large-scale rice yield estimation. Agr. Forest Meteorol. 197:52-64.

Smith, P., Martingo, D., Cai, Z., Gwary, D., Janzen, H., Kumar, P., McCarl, B., Ogle, S., O'Mara, F., Rice, C., Scholes, B., Sirotenko, O., Howden, M., McAllister, T., Pan, G., Romanenkov, V., Schneider, U., Towprayoon, S., Wattenbach, M., and J. Smith. 2007. Greenhouse gas mitigation in agriculture. Philos. T. Roy. Soc. B. 363:789-813.

Teal, R.K., Tubaña, B., Girma, K., Freeman, W., Arnall, D.B., Walsh, O., and W.R. Raun. 2006. In-season prediction of corn grain yield potential using normalized difference vegetation index. Agron. J. 98:1488-1494.

Thenkabail, P.S., Smith, R.B., and E.D. Pauw. 2000. Hyperspectral vegetation indices and their relationships with agricultural crop characteristics. Remote Sens. Environ. 71:158-182.

Tubaña, B.S., Arnall, D.B., Walsh, O., Chung, B., Solie, J.B., Girma, K., and W.R. Raun. 2008. Adjusting midseason nitrogen rate using a sensor-based optimization algorithm to increase use efficiency in corn. J. Plant Nutr. 31:1393-1419.

C.J. Tucker. 1979. Red and photographic infrared linear combinations for monitoring vegetation. Remote Sens. Environ. 8:127-150.

Tucker, C.J., Vanpraet, C.L., Sharman, M.J., and G. van Ittersum. 1985. Satellite remote sensing of total herbaceous biomass production in the Sengalese Sahel 1980–1984. Remote Sens. Environ. 17:233–249.

Uddling, J., Gelnag-Alfredsson, J., Piikki, K., and H. Pleijel. 2007. Evaluating the relationship between leaf chlorophyll concentration and SPAD-502 chlorophyll meter readings. Photosynth. Res. 91:37-46.

United States Salinity Laboratory Staff. 1954. Diagnosis and improvement of saline and alkali soils. USDA Agric. Handb. 60. U.S. Gov. Print. Office, Washington, D.C.

University of California, Division of Agriculture and Natural Resources (UC ANR). 2018. California Rice Production Workshop Manual.

Wang, W., Yao, X., Yao, X., Tian, Y., Liu, X., Ni, J., Cao, W., and Y. Zhu. 2012. Estimating leaf nitrogen concentration with three-band vegetation indices in rice and wheat. Field Crops Res. 129:90-98.

H. Wickham. 2009. ggplot2: Elegant graphics for data analysis. Springer-Verlag. New York.

Xue, L., Cao, W., Luo, W., Dai, T., and Y. Zhu. 2004. Monitoring leaf nitrogen status in rice with canopy spectral reflectance. Agron. J. 96:134-142.

Yang, W.H., Peng, S., Huang, J., Sanica, A.L., Buresh, R.J., and C. Witt. 2003. Using leaf color charts to estimate leaf nitrogen status of rice. Agron. J. 95:212-217.

Yao, Y., Miao, Y., Cao, Q., Wang, H., Gnyp, M.L., Bareth, G., Khosla, R., Yang, W., Liu, F., and C. Liu. 2014. In-season estimation of rice nitrogen status with an active crop canopy sensor. IEEE J-STARS. 7:4403-4413.

Yao, Y., Miao, Y., Huang, S., Gao, L., Ma, X., Zha, G., Jiang, R., Chen, X., Zhang, F., Yu, K., Gnyp, M.L., Bareth, G., Liu, C., Zhao, L., Yang, W., and H. Zhu. 2012. Active canopy sensor-based precision N management strategy for rice. Agron. Sustain. Dev. 32:925-933.

Zhu, Y., Zhou, D., Yao, X., Tian, Y., and W. Cao. 2007. Quantitative relationships of leaf nitrogen status to canopy spectral reflectance in rice. Aust. J. Agr. Res. 58:1077-1085.

CHAPTER TWO

Sensitivity of vegetative indices derived from proximal and aerial sensors for assessing the N status and predicting grain yield of rice

Telha H. Rehman[a], Mark E. Lundy[a], and Bruce A. Linquist[a]

[a]Department of Plant Sciences, University of California – Davis, Davis, CA 95616, USA

Abbreviations: greenseeker, GS; index value, IV; panicle initiation, PI; Sufficiency Index, SI; unmanned aerial system, UAS

ABSTRACT

Remotely sensed vegetative indices can be valuable tool in assessing N status and predicting crop yields. This is a rapidly expanding field and numerous sensors and indices are available that can be used either proximally or aerially. While the Normalized Difference Vegetation Index (NDVI) is a reliable index to assess vegetative growth, it can saturate at high biomass or N levels and the Normalized Difference Red Edge Index (NDRE) has been shown to be a better index in this regard. Few have explored how aerial sensors compare to proximal sensors. The objective of this study was to evaluate the potential improvement of aerially sensed NDVI and NDRE and proximally sensed NDVI when assessing total N uptake (N_{UP}) at panicle initiation (PI) and grain yield in rice. Nitrogen response trials were established over a 3-yr. period (10 site-years) at various locations throughout the Sacramento Valley rice growing region of California. At PI, an unmanned aerial system (UAS) was used to measure $NDVI_{UAS}$ and $NDRE_{UAS}$, and a proximal GreenSeeker (GS) sensor recorded $NDVI_{GS}$. Each index was normalized by calculating the Sufficiency Index (SI) using a non-N limiting plot. Kernel density distributions indicated that $NDVI_{UAS}$ SI had a stronger saturation relative to the $NDVI_{GS}$ SI and $NDRE_{UAS}$ SI. Quadratic-plateau models were developed to describe the relationship between each SI and PI N_{UP} and found that the relationship between PI N_{UP} and $NDVI_{UAS}$ SI saturated the earliest (96 kg N ha^{-1}), followed by the $NDVI_{GS}$ SI (kg N ha^{-1}) and $NDRE_{UAS}$ SI (129 kg N ha^{-1}). Linear mixed effects models were developed to describe the relationship between each SI and grain yield. The resulting model for $NDVI_{UAS}$ SI was least sensitive to changes in final grain yields and thus had the steepest slope (25.3 Mg ha^{-1}), while the $NDVI_{GS}$ SI (9.5 Mg ha^{-1}) and $NDRE_{UAS}$ SI (11.7 Mg ha^{-1}) demonstrated greater sensitivity. Our results indicate that the $NDRE_{UAS}$ and $NDVI_{GS}$ were the most reliable indices and were superior to $NDVI_{UAS}$.

2.1. INTRODUCTION

Remote sensing has emerged as a powerful technology to inform sustainable agronomic management by providing an accurate and timely assessment of the health and status of developing crops (**Hatfield et al., 2008**). Remote sensing of crops is based on the collection of canopy reflectance spectra at specific wavelengths in the electromagnetic spectrum, usually corresponding to regions where the plant canopy experiences strong absorption or reflectance of incoming radiation (**Xue and Su, 2017)**. A common method to interpret the data and evaluate crop status is to place the wavelengths into vegetative indices, which are mathematical combinations of wavelengths related to specific biophysical characteristics of the plant (**Hatfield et al., 2019**). Over the past decade, the rapid development of new sensors with higher spatial and spectral sensing abilities, as well as new platforms that can carry such sensors and easily maneuver over the object space have led to a significant broadening of remote sensing applications in many fields including agriculture (**Toth and Jóźków, 2016**). As such, some of the current applications of remotely sensed data in agriculture include biomass estimation, assessing crop nutritional status, detecting plant stress, identifying disease incidence, scouting fields for weeds, and predicting potential yield among others.

An important application of remote sensing in rice (*Oryza sativa* L.) is the assessment of crop nitrogen (N) status and the prediction of final grain yield. Nitrogen is an essential element for plant growth and an adequate supply of N is fundamental to maximizing rice grain yield and quality (**De Datta, 1981**). However, over application of N fertilizer in rice and other crops has been associated with harmful impacts on the environment through nitrate leaching (**Tamagno et al., 2021**), greenhouse gas emissions (**Pittelkow et al., 2014)**, or eutrophication of downstream aquifers (**Smith et al., 2021**). The most accurate method to assess plant N status is by plant tissue analysis, but this technique is time consuming and lab results are often received past the time when decisions need to be made (**Daughtry et al., 2000**). Alternative methods to assess N status in rice include using the Soil Plant Analysis Development (SPAD) chlorophyll meter (**Balasubramanian et al., 2000**) or the Leaf Color Chart (**Witt et al., 2005**). While these tools are useful, they are limited by their single leaf sampling method, thus making it difficult to utilize these tools to accurately assess crop N status over large areas (**Daughtry et al., 2000; Saberioon et al., 2014**). The development of remote sensing techniques provides a promising alternative to assess crop N status and better manage N resources.

Remote sensing data can be collected using several different platforms including proximal handheld sensors or aerial sensors which can be mounted to airplanes, satellites, or unmanned aircraft vehicles (UAV; sensor mounted to an UAV is referred to as an unmanned aircraft system, UAS) (**Toth and Jóźków, 2016)**. Over the past two decades, most of the research in agricultural remote sensing has focused on the use of proximal sensors, especially those that utilize an active light source (**Saberioon et al., 2014).** However, with the recent expansion of compact aerial sensors that can be easily mounted to an UAV, an increasing number of studies have shifted toward utilizing UAS based platforms (**Colomina and Molina, 2014**). Relative to proximal and UAS based remote sensing, airplane and satellite-based measurements are less frequently used in agricultural applications due to the high operational complexity and costs of flying an airplane, and insufficient spatial and temporal resolution of satellite imagery (**Zheng et al., 2018**). However, despite being far more convenient than airplane and satellite based remote sensing, both proximal and UAS based remote sensing also come with their own unique advantages and disadvantages.

Among proximal sensors, one of the most often used in agricultural research has been the GreenSeeker (GS) HandHeld (Trimble Inc., Sunnyvale, CA, USA), which is an active canopy sensor, thus allowing it to collect reflectance data at any time during the day regardless of ambient light conditions or cloud cover (**Saberioon et al., 2014)**. The GreenSeeker measures canopy reflectance at specific bands in the red (670 nm) and near infrared (780 nm) spectral regions and displays the Normalized Difference Vegetation Index (NDVI), which is the most commonly measured index in remote sensing applications and has been used widely to assess vegetative growth (**Huang et al., 2021**). Among studies that have tested the ability of GS NDVI ($NDVI_{GS}$) to assess crop N status and predict yields, **Yao et al. (2014)** and **Rehman et al. (2019)** both reported strong correlations between $NDVI_{GS}$ and aboveground biomass and total N uptake in rice, and the latter study also showed that $NDVI_{GS}$ was useful to accurately predict grain yields. Others have reported similar results for wheat (*Triticum aestivum*) (**Li et al., 2010)** and maize (*Zea mays)* (**Teal et al., 2006; Xia et al. 2016)**. However, a key disadvantage of the GS, as was noted by each of the studies mentioned above, as well as many others, is that $NDVI_{GS}$ loses sensitivity (i.e. saturates) once crop biomass exceeds a certain threshold (**Huang et al., 2020**).

When collecting canopy reflectance data aerially, a passive multispectral sensor (in most cases) is mounted to an UAV and flown in a grid-style pattern over the field or experimental area; thus, facilitating the assessment of larger areas more efficiently and potentially identifying the spatial variability that is often present within a field (**Tsouros et al., 2019; Delavarpour et al., 2021; Fu et al., 2021**). A multispectral sensor that is frequently used in agricultural applications is the MicaSense Red-Edge M (MicaSense, Inc., Seattle, WA, USA) which is a passive sensor and collects canopy reflectance across five spectral bands (blue, green, red, red edge, and near infrared) (**Esposito et al., 2021**). The additional bands included in multispectral sensors such as the MicaSense sensor provide an important advantage over proximal sensors like the GS as they permit the calculation of a wide range of vegetative indices, including red edge based indices, among which the Normalized Difference Red Edge Index (NDRE) is the most commonly used (**Dunn et al., 2016).** The NDRE is based on the same calculation as the NDVI but incorporates a red edge band in place of red, which allows the NDRE to be more resistant to the saturation problem inherent with NDVI (**Li et al, 2014; Dunn et al., 2016).** However, aerial based remote sensing also has its own limitations, among which some include the narrow timeframe around solar noon during which data must be collected, UAS platforms are often more expensive than proximal sensors, and the UAS can experience technical issues mid-air, such as loss of power or an engine breakdown (**Hardin and Jensen, 2011; Zhang and Kovacs, 2012**).

Among the studies that used aerial sensors to assess N status in rice, **Dunn et al., 2016** reported strong correlations between NDVI and NDRE and total N uptake but noted that the NDRE was less saturated than the NDVI. Similarly, **Zheng et al. (2019**) and **Wang et al. (2021)** reported stronger correlations between NDRE and red edge chlorophyll index when estimating rice total N uptake and N-index (ratio of N concentration between fertilized and non-fertilized plants), respectively, relative to the NDVI. In similar experiments on other crops, **Walsh et al. (2018)** found that the red edge based indices measured in their study exhibited a higher correlation with wheat N concentration than red based indices. **Becker et al. (2020)** did not evaluate NDVI in their study but reported a stronger correlation between NDRE and grain yield relative to the other indices in their study in maize.

Although numerous studies have demonstrated the ability of NDVI and NDRE to assess crop status measured using either a proximal sensor or an aerial sensor, few studies have compared proximal and aerial sensors side-by-side. In rice, **Zheng et al. (2019)** reported that NDVI measured using an aerial multispectral sensor was better correlated with plant N concentration than NDVI measured with proximal hyperspectral sensor. **Sumner et al. (2021)** measured NDVI and NDRE in maize using a proximal and aerial sensor and found that both the NDVI and NDRE both exhibited a similar correlation with N fertilizer rate when each index was compared across the two sensors. In wheat, **Hassan et al. (2018)** and **Duan et al. (2017)** found the NDVI measured with a proximal and aerial sensor to be well correlated across a wide range of growth stages.

Given the interest and the promise of this technology along with the lack of studies comparing different platforms, the objective of this study was to evaluate the sensitivity of aerially sensed NDVI and NDRE over proximally sensed NDVI in assessing rice crop status when quantified as total N uptake at PI and final grain yield. This was accomplished through field studies over a 3-yr. period at ten locations throughout the Sacramento Valley rice growing region of California (CA), USA.

2.2. MATERIALS AND METHODS

2.2.1 Site Description

Ten replicated N response trials (nine on-farm; one on-station) were established during the 2017 to 2019 rice growing seasons (referred to by proximity to nearest town or station and study year) throughout the Sacramento Valley rice growing region of California (CA) (**Fig. 2.1; Table 2.1**). The on-station site was established at the CA Rice Experiment Station (RES) near Biggs. The Sacramento Valley has a Mediterranean climate characterized by warm and dry conditions during the growing season (May to October). The average air temperature and precipitation during the three years of this study were 23.2° C and 5.9 mm, respectively (**CIMIS 2020** – Biggs Station). Pre-season soil samples were collected from the plow layer (approximately 0 – 15 cm) after tillage and prior to fertilizer applications at each site and analyzed for pH, particle size, organic C, and total N. The soil properties at each site were typical for rice soils in this region (**Table 2.1**).

2.2.2 Experimental Design

Each N response trial was arranged as a randomized complete block design with four replicates. Treatments were pre-plant N fertilizer rates. In 2017, pre-plant N fertilizer was applied as urea at rates ranging from 0 to 275 kg N ha^{-1}, and in 2018 and 2019 pre-plant N fertilizer was applied as aqua-ammonia at rates ranging from 0 to 235 kg N ha^{-1}. Potassium (K) and phosphorus (P) fertilizers were broadcast across all plots at rates of 50 kg K_2O ha^{-1} as sulfate of potash and 45 kg P_2O_5 ha^{-1} as triple superphosphate to ensure these nutrients did not limit crop growth. The rice crop was established using water-seeding at all sites which is the common practice in CA (**Hill et al., 2006)**. In this case, the fields are fertilized

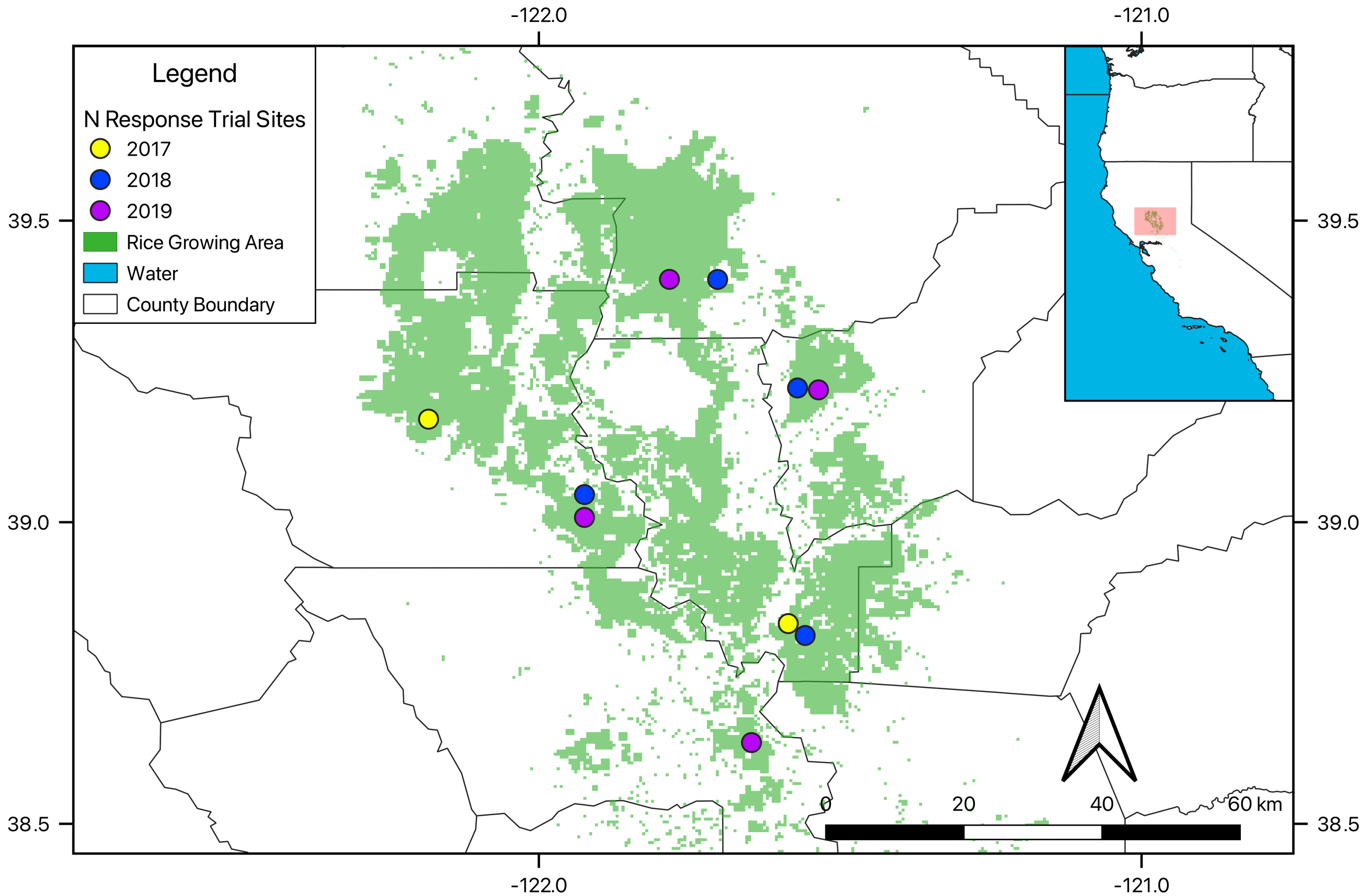

Figure 2.1. A map of N response trial sites established during the 2017 to 2019 growing seasons throughout the Sacramento Valley rice growing area of California, USA.

Table 2.1. Soil descriptions and selected properties of each N response trial site-year located throughout the Sacramento Valley, California.

Site-Year	Soil Series	Taxonomic Classification	Texture (%)			Organic Carbon (%)	Total Nitrogen (%)	pH
			Sand	Silt	Clay			
Nicolaus-17	Capay	Fine, smectitic, thermic Typic Haploxererts	19	36	45	1.51	0.12	5.5
Williams-17	Willows	Fine, smectitic, thermic Sodic Endoaquerts	21	39	40	1.75	0.15	5.0
Arbuckle-18	Clear Lake	Fine, smectitic, thermic Xeric Endoaquerts	30	21	49	1.95	0.16	6.3
Biggs-18	Eastbiggs	Fine, mixed, active, thermic Abruptic Durixeralfs	50	30	20	1.60	0.12	4.9
Marysville-18	San Joaquin	Fine, mixed, active, thermic Abruptic Durixeralfs	39	39	22	1.64	0.13	4.6
Nicolaus-18	Capay	Fine, smectitic, thermic Typic Haploxererts	22	36	42	1.67	0.14	4.8
Arbuckle-19	Clear Lake	Fine, smectitic, thermic Xeric Endoaquerts	8	38	55	1.99	0.16	6.3
Davis-19	Sycamore	Fine-silty, mixed, super active, nonacid, thermic Mollic Endoaquepts	9	38	53	1.98	0.18	6.3
Marysville-19	San Joaquin	Fine, mixed, active, thermic Abruptic Durixeralfs	35	41	24	1.54	0.12	4.7
RES-19	Esquon-Neerdobe	Fine, smectitic, thermic Xeric Epiaquerts	30	26	44	1.38	0.11	5.3

following seedbed preparation, flooded, and then soaked seed is broadcast onto the field by airplane. The medium grain rice variety M-206, which is commonly grown in CA, was planted at all sites. Herbicide and irrigation management followed common grower practice and was either managed by the growers (on-farm sites) or researchers (on-station site). The fields remained flooded until three weeks before harvest when they are drained.

2.2.3 Plant Sampling and Analysis

Biomass was collected at panicle initiation (PI) after canopy reflectance data was collected (see below) by pulling all rice plants within a 0.5 m^2 quadrat from every main plot. Within 24 hr of collecting the samples, the biomass was washed to remove any residual soil, the roots were removed, and the aboveground shoots were oven dried to constant weight at 60° C; after which the samples were ground to pass a 4-mm sieve and then ball-milled. Plant material was analyzed for total N using an elemental analyzer interfaced to a continuous flow isotope ratio mass spectrometer (EA-IRMS) (**Sharp, 2005**). From these samples, we quantified total N uptake (N_{UP}) as the product of aboveground biomass and N concentration.
Grain yield was determined at physiological maturity by harvesting all plants from a 1.0 m^2 quadrat in every main plot. Grains were removed from panicles, cleaned using a seed blower, dried to constant moisture at 60° C, and then weighed. Grain yields are reported at 14% moisture.

2.2.4 Measuring Canopy Reflectance

The Normalized Difference Vegetation Index (NDVI) and Normalized Difference Red-Edge (NDRE) were measured for each main plot at PI using a proximal and/or aerial sensor

(**Table 2.2**). The proximal sensor used in this study was the GreenSeeker (GS) handheld crop sensor (Trimble Inc., Sunnyvale, CA). The GS is an active sensor and measures canopy

Table 2.2. Summary of the proximal and aerial sensors used to measure the Normalized Difference Vegetative Index (NDVI) and the Normalized Difference Red Edge (NDRE) at the panicle initiation (PI) rice growth stage.

Vegetative Index	**Sensor Type**	**Year**	**Sensor**	**Light Source**	**Spectral Band**	**Central Wavelength (nm)**	**Bandwidth† (nm)**	**Formula**	**Reference**
NDVI	Proximal	2017-2019	GreenSeeker	Active	Red	670	10	$\frac{(Near\ IR - Red)}{(Near\ IR + Red)}$	Rouse 1974? Tucker (1979)
					Near Infrared	780	10		
	Aerial	2017	SlantRange 3P	Passive	Red	650	40		
					Near Infrared	850	100		
		2018 & 2019	MicaSense RedEdge-M	Passive	Red	668	10		
					Near Infrared	840	40		
NDRE	Aerial	2017	SlantRange 3P	Passive	Red Edge	710	20	$\frac{(Near\ IR - Red\ Edge)}{(Near\ IR + Red\ Edge)}$	Barnes et al. (2000)
					Near Infrared	850	100		
		2018 & 2019	MicaSense Red Edge-M	Passive	Red Edge	717	10		
					Near Infrared	840	40		

†full width at half maximum

reflectance at two specific spectral wavelengths (red and near infrared) and then automatically calculates and displays the NDVI. The GS NDVI ($NDVI_{GS}$) measurements were taken by holding the sensor in the nadir position at a constant height of 1.0 m above the crop canopy while walking steadily along the edges of each plot. For each plot, the final $NDVI_{GS}$ value represented the average of four $NDVI_{GS}$ readings. Canopy closure was achieved by PI in all plots that received N fertilizer, thus the effect of background water or soil on canopy reflectance measurements was considered negligible in those plots.

Two different aerial sensors were used in this study (**Table 2.2**). In 2017, canopy reflectance was measured using a SlantRange 3P (SlantRange Inc., San Diego, CA) passive multispectral sensor. The autonomous flight mission was loaded onto the unmanned aircraft system (UAS) using the DroneDeploy mobile app and images were captured at a height of 117 m above ground level (AGL) with 55% forward and side overlap. SlantView software (version 2.16.0) was used to process the multispectral imagery into a georeferenced orthomosaic with an average ground sampling distance of 4.8 cm pixel^{-1}. The SlantView software was also used to extract plot level canopy reflectance values for each of the spectral bands.

In 2018 and 2019, a MicaSense Red-Edge M (MicaSense Inc., Seattle, WA) passive multispectral sensor was used to capture aerial imagery. The mobile app Pix4Dcapture was used to upload the flight mission onto the sUAS, and images were captured at a height of 50 m AGL with 85% forward and side overlap. The software Pix4DMapper (version 4.2.27) was used to process the imagery into a georeferenced orthomosaic with an average ground sampling distance of 3.5 cm pixel^{-1}. Plot level reflectance values were extracted from the orthomosaic image using the recommended method of **Haghighattalab et al. (2016)** as modified by **Nelsen (2019).**

In all years, the aerial sensor was mounted to a Matrice 100 UAS (DJI, Shenzhen, China). All flights occurred within 1 hr. of solar noon. Before beginning each flight, images of a calibration reflectance panel were taken to calibrate for ambient light conditions. There was also an upwelling light sensor on-board the sUAS that calibrated for incoming irradiance. Plot-level canopy reflectance values were converted into NDVI ($NDVI_{UAS}$) and Normalized Difference Red-Edge Index ($NDRE_{UAS}$) using the formulas provided in **Table 2.2**.

2.2.5 Sufficiency-Index

In order to directly compare the ability of each vegetative index to predict PI N_{UP} and final grain yield, the raw IV from the three indices were normalized by calculating the SI. Calculating the SI is an important step to qualify comparisons across differing sensors, vegetative indices, fields, varieties, and years all on a common scale (**Lu et al., 2017; Chen et al., 2019)**. At each site-year, the SI was calculated by dividing the raw IV of each N treatment by the mean IV of the highest N rate (**Lu et al., 2017; Chen et al., 2019)**. Using the mean IV of the highest N rate resulted in some main plots of the higher N rates to have a SI greater than 1.00, in which case, the SI was adjusted to equal 1.00, thus allowing data to be reported on a scale (0 to 1) that coincides with previous work in this area.

2.2.6 Data Analysis

Data analysis was performed using the statistical program R (version 4.0.5, **R Core Team, 2021**). The package *dplyr* (**Wickham et al., 2021**) was used to process the data, and the package *ggplot2* (**Wickham, 2016**) was used to visualize the data and construct plots. The relationship between pre-plant N rate and both mean PI N_{UP} and mean final grain yield at each site-year was described by unique quadratic simple linear regression models. The univariate density distribution of raw IV and SI for each index was illustrated as kernel density plots developed from the *geom_density()* function in the package *ggplot2* (**Wickham, 2016**). The relationship between each SI and PI N_{UP} was described by unique quadratic-plateau linear regression models also using the *nls()* function from the *stats* package (**R Core Team, 2021**) and following the method outlined by **Mangiafico (2016)**. The resulting model coefficients were used to identify the critical x-value (i.e. PI N_{UP}) where each SI reaches a plateau (i.e. point of saturation for each index). The function *nagelkerke()* from the *rcompanion* package (**Mangiafico, 2022)** was used to calculate a pseudo coefficient of determination (R^2) for each quadratic-plateau and the linear-plateau model using the method described by **Cox and Snell (2018)**. The relationship between each SI and final grain yield was described by unique linear mixed-effects regression models using the function *lme( )* in the *nlme* package (**Pinheiro et al., 2021**). Each mixed-effects model contained a fixed-effect for SI and random-effects of site-year for both the slope and intercept. The response variable was final grain yield in each mixed-effect model. A pseudo R^2 was calculated for the mixed-effects models using the function *r.squaredGLMM( )* in the *MuMIn* package (**Bartoń, 2020**) with the conditional R^2 representing the variability explained by the entire model (fixed and random effects), the marginal R^2 representing the variability explained only by the fixed-effects, and the portion of variability explained by the random-effects represented as the difference in conditional and marginal R^2. The package *emmeans* (**Lenth, 2021**) was used to derive estimated marginal means (emmeans) from the mixed-effects model coefficients. For all regression models in this study, graphical and numerical summaries were examined to ensure the models satisfied the assumptions of linear regression.

2.3. RESULTS

2.3.1 PI Total N Uptake and Grain Yield

Mean PI N_{UP} was lowest in the 0N treatment at all site-years, with values ranging from 15 kg N ha^{-1} (Arbuckle-18) to 75 kg N ha^{-1} (Nicolaus-17) across all sites (**Fig. 2.2, left axis)**. At each site-year, mean PI N_{UP} increased with increasing pre-plant N rate; however, the magnitude of increase varied considerably across all sites. For example, at Davis-19 mean PI N_{UP} only increased by a maximum of 61 kg N ha^{-1}, whereas at Nicolaus-18 mean PI N_{UP} increased by 140 kg N ha^{-1}. This variability in magnitude of N_{UP} across site-years resulted in the maximum PI N_{UP} to also range considerably, with values ranging from 94 kg N ha^{-1} (Davis-19) up to 209 kg N ha^{-1} (Nicolaus-17) across all sites. At most site-years, maximum PI N_{UP} was observed in the highest N rate, with the only exceptions being at Biggs-18 and RES-19 where it was observed in the second highest N rate.

At every site-year, grain yield was also lowest in the 0N treatment, with values ranging from 3.2 Mg ha^{-1} (Arbuckle-18) up to 10.6 Mg ha^{-1} (Nicolaus-17) (**Fig. 2.2, right axis).** Across all sites, yields increased with increasing pre-plant N rate up to a maximum and either leveled off or decreased. The magnitude of increase in grain yields in response to fertilizer N varied strongly across site-years, with yields at Nicolaus-17 only increasing by 1.6 Mg ha^{-1}, whereas at Arbuckle-18 final grain yield increased by 9.5 Mg ha^{-1} across N rates. Despite these differences in the grain yield response to pre-plant N fertilizer across site-years, maximum final grain yields were relatively similar across all sites and ranged from 9.1 Mg ha^{-1} (RES-19) to 13.3 Mg ha^{-1} (Nicolaus-18).

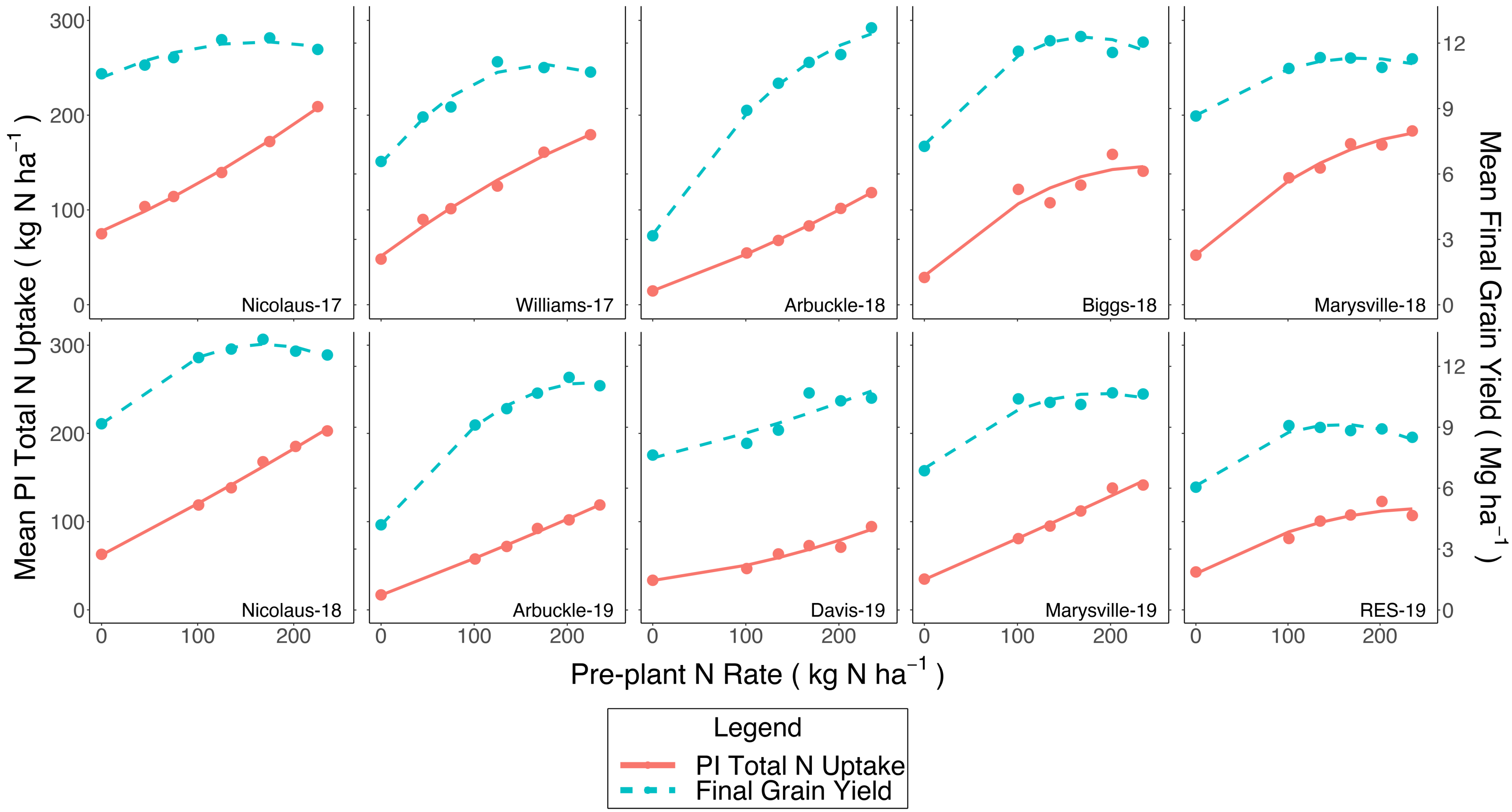

Figure 2.2. The relationship between pre-plant N rate and mean panicle initiation (PI) total N uptake (N_{UP}) (left axis), and mean final grain yield (right axis), as described by unique quadratic linear regression models

2.3.2 Canopy Reflectance Data

There were considerable differences in the kernel density distributions among the three indices in this study, both in terms of raw IV and SI (**Fig. 2.3**). With respect to raw IV, the $NDVI_{UAS}$ exhibited the strongest saturation among the three indices, as seen by the relatively high and narrow peak of $NDVI_{UAS}$ IV observations centered around 0.90 (**Fig. 2.3a**). The $NDRE_{UAS}$ exhibited the least amount of saturation as the peak of $NDRE_{UAS}$ IV values was the lowest and generally broader relative to the other two indices. The $NDVI_{GS}$ was more saturated stronger saturation than the $NDRE_{UAS}$, as seen by the higher and narrower peak of $NDVI_{GS}$ IV observations centered around 0.72. However, both the $NDRE_{UAS}$ and $NDVI_{GS}$ exhibited considerably less saturation relative to the $NDVI_{UAS}$.

The relative differences in saturation among the three indices in terms of raw IV were evident in the density distributions developed from SI data. The strong saturation of $NDVI_{UAS}$ IV resulted in 88% of the $NDVI_{UAS}$ SI observations to fall between 0.90 and 1.00, resulting in the $NDVI_{UAS}$ SI to also have the narrowest range (0.63 to 1.00) among the three indices in this study (**Fig. 2.3b**). Among the $NDVI_{GS}$ and the $NDRE_{UAS}$, the $NDVI_{GS}$ SI had a larger range of observations (0.28 to 1.00) as compared to the $NDRE_{UAS}$ SI (0.49 to 1.00). However, similar to the trend seen with respect to raw IV, the $NDVI_{GS}$ SI was slightly more saturated than the $NDRE_{UAS}$ SI, as seen by the relatively higher overall peak, and larger proportion of $NDVI_{GS}$ SI values falling between 0.90 and 1.00 (66%) as compared to the $NDRE_{UAS}$ (62%).

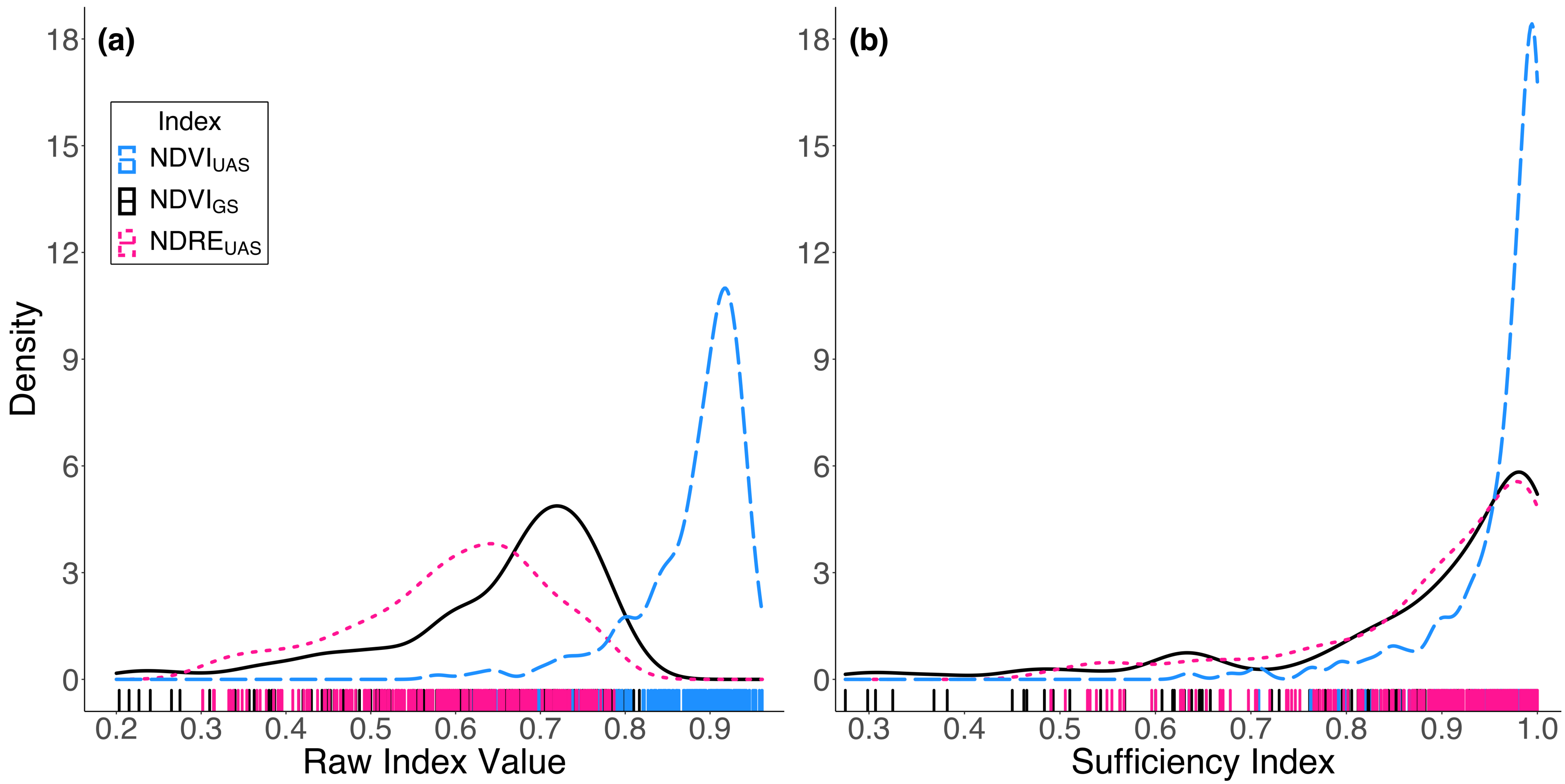

Figure 2.3. Kernel density distributions of raw index values (IV) and the Sufficiency Index (SI) of each vegetative index measured at the panicle initiation (PI) rice growth stage. Note the differences in scale of the x-axis. Some colors of the rug are not visible due to overlap.

2.3.3 Relationship between PI N_{UP} and Sufficiency-Index

Unique quadratic-plateau linear regression models were developed to describe the relationship between PI N_{UP} and each SI (**Fig. 2.4**). All quadratic-plateau regression models had a R^2 of 0.73 or greater, suggesting that each model described the data appropriately. In each case, the quadratic-plateau model increased with increasing PI N_{UP} up to a threshold, after which the model reached a plateau. Among the three indices in this study, the quadratic-plateau regression model for the $NDVI_{UAS}$ SI saturated (i.e., plateaued) the earliest (96 kg N ha^{-1}), and the $NDVI_{UAS}$ SI was also the least sensitive to changes in PI N_{UP} as seen by its narrow range of observations along the y-axis (0.63 to 0.99) (**Fig. 2.4c)**. In contrast, the quadratic-plateau models for both the $NDVI_{GS}$ SI and $NDRE_{UAS}$ SI saturated at higher N_{UP} values and were more sensitive to changes in PI N_{UP} prior to their respective points of saturation (**Fig. 2.4a, 4b**). The quadratic-plateau model for $NDVI_{GS}$ SI saturated earlier than $NDRE_{UAS}$ SI (113 kg N ha^{-1} and 129 kg N ha^{-1}, respectively), but the $NDVI_{GS}$ SI was more sensitive to changes in PI N_{UP} prior to its point of saturation (0.28 to 0.96, left axis) relative to the $NDRE_{UAS}$ SI (0.49 to 0.97, left axis).

2.3.4 Relationship between Sufficiency-Index and Final Grain Yield

Results from the unique linear mixed-effects models that were developed to describe the relationship between each SI and yield show that each SI was positively correlated with yield (**Fig. 2.5)**. However, the relative amount of saturation for each SI seen in **Fig. 2.3b** had an effect on the ability of each SI to quantify changes in

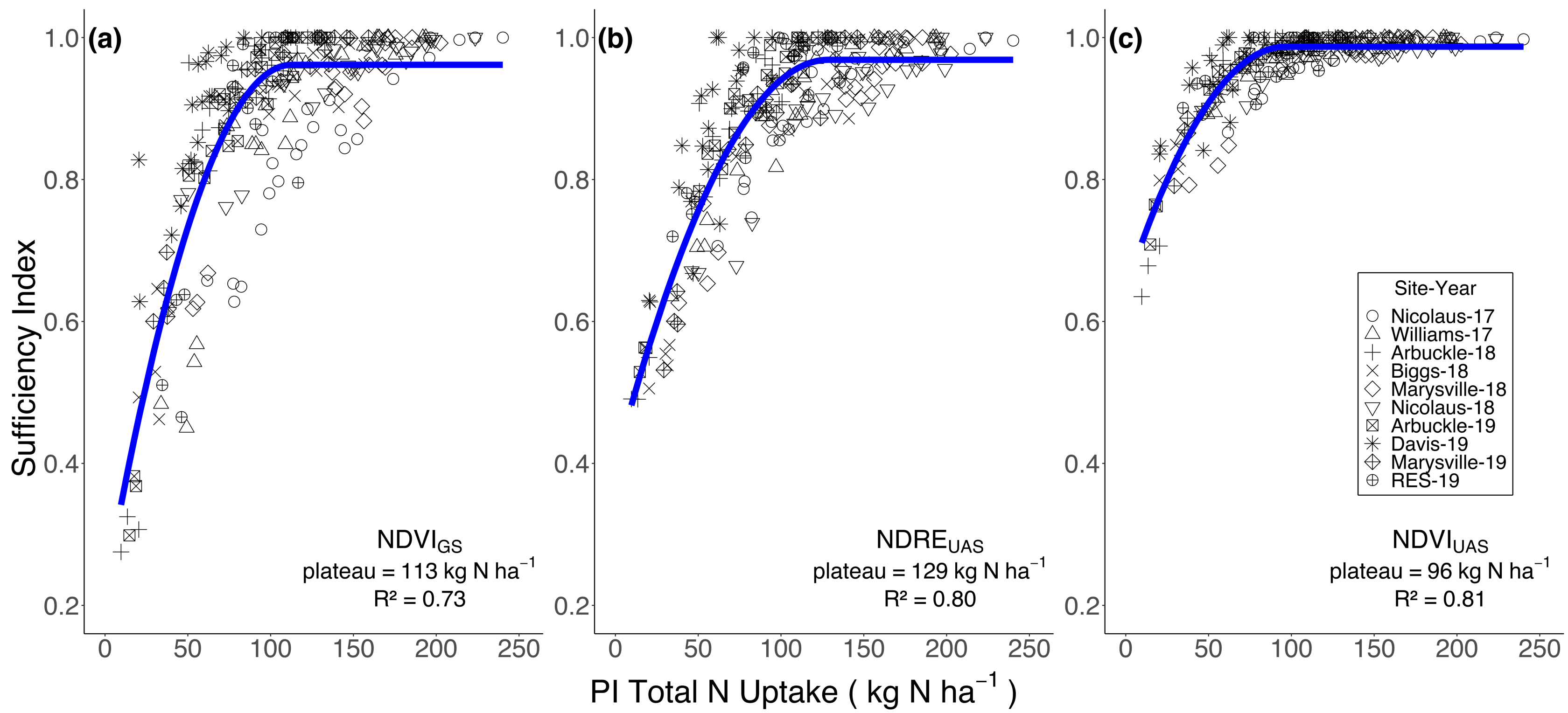

Figure 2.4. The relationship between panicle initiation (PI) total N uptake (N_{UP}) and **(a)** GreenSeeker Normalized Difference Vegetation Index ($NDVI_{GS}$) Sufficiency-Index (SI), **(b)** small unmanned aerial system Normalized Difference Red-Edge Index ($NDRE_{UAS}$) SI, and **(c)** $NDVI_{UAS}$ SI as described by unique quadratic-plateau linear regression models. The plateau value reported in each panel represents the PI N_{UP} value where the regression model reached a plateau (i.e. the point of saturation for each index). Data were collected during the 2017 to 2019 growing season from ten N response trial site-years established throughout the Sacramento Valley rice growing region of California.

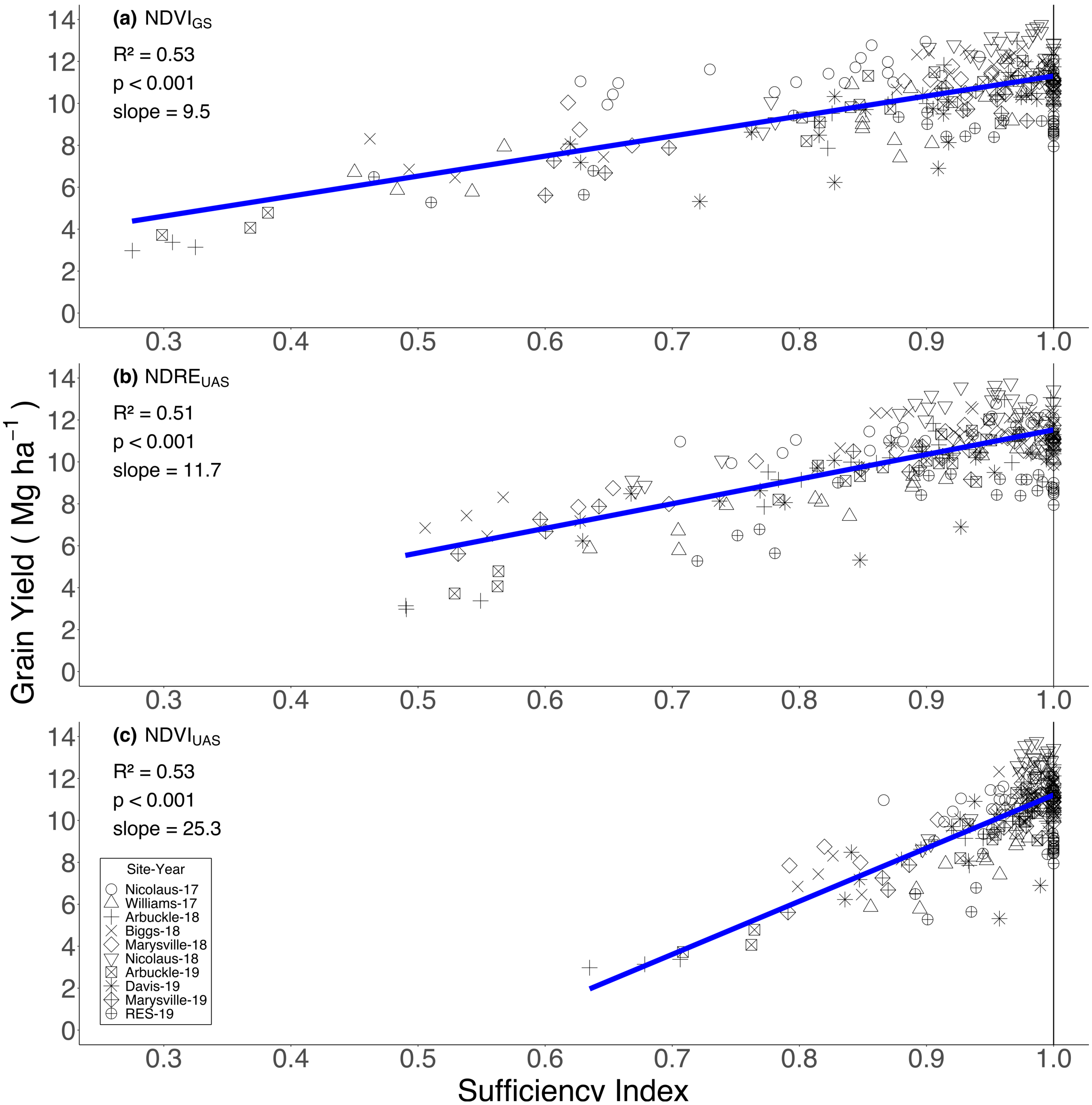

Figure 2.5. The relationship between **(a)** GreenSeeker Normalized Difference Vegetation Idnex ($NDVI_{GS}$) Sufficiency Index (SI) **(b)** small unmanned aerial system Normalized Difference Red-Edge Index ($NDRE_{UAS}$) SI, and **(c)** $NDVI_{UAS}$ SI and rice final grain yield as described by unique linear mixed-effects models. The coefficient of determination (R^2) reported in each panel represents the proportion of variability explained by the model fixed effects only. Data were collected during the 2017 to 2019 from ten N response trial site-years throughout the Sacramento Valley rice growing region of California.

grain yield. For example, the $NDVI_{UAS}$ SI which was the most saturated among the three indices, was also the poorest predictor of grain yields (**Fig. 2.5c).** Due to the high degree of saturation of $NDVI_{UAS}$ SI values, a large portion of grain yield observations were clustered between a $NDVI_{UAS}$ SI of 0.95 and 1.00. With respect to the portion of data that was not saturated, the $NDVI_{UAS}$ SI was least sensitive to changes in grain yield, as seen by the relatively large change in yields explained over a narrow range of $NDVI_{UAS}$ SI values. As a result, the mixed-effects model for $NDVI_{UAS}$ SI had the highest slope (25.3 Mg ha^{-1}) among the three indices in this study. As seen in **Fig. 2.3b**, both the $NDVI_{GS}$ SI and $NDRE_{UAS}$ SI were relatively less saturated than the $NDVI_{UAS}$ SI, which resulted in the $NDVI_{GS}$ SI and $NDRE_{UAS}$ SI to measure changes in grain yields more effectively than the $NDVI_{UAS}$ SI **(Fig. 2.5a, 5b).** The $NDVI_{GS}$ SI and $NDRE_{UAS}$ SI both explained the change in grain yield over a wider range of SI values relative to the $NDVI_{UAS}$ SI, thus resulting in the slope of the mixed-effects model for the $NDVI_{GS}$ SI and $NDRE_{UAS}$ SI to be considerably lower (9.5 Mg ha^{-1} and 11.7 Mg ha^{-1}, respectively). While the slopes of the mixed-effect model for the $NDVI_{GS}$ SI and $NDRE_{UAS}$ SI were generally similar, the slope for $NDVI_{GS}$ SI was slightly lower than for the $NDRE_{UAS}$ SI due to the $NDVI_{GS}$ SI having a larger range of observations. Overall, each mixed-effects model explained over 50% of the variability in grain yield, suggesting that the models appropriately described the data.

2.4. DISCUSSION

2.4.1 Crop Response to N Fertilizer

Applying pre-plant N fertilizer led to an increase in crop PI N_{UP} and grain yield at every site; however, there were considerable differences in the magnitude of increase across sites (**Fig 2)**. Across all sites, the net increase in PI N_{UP} due to pre-plant N fertilizer ranged from 61 kg N ha^{-1} to 140 kg N ha^{-1}, and the grain yield response to pre-plant N fertilizer ranged from 1.6 Mg ha^{-1} to 9.5 Mg ha^{-1}. Observed variability in N_{UP} and grain yields across sites in this study is not unexpected, given that they were established over a 3-yr. period at varying locations with differing soils and micro-climates. That being said, the strong variability in crop response to N fertilizer measured across sites in this study highlights the need to develop tools that take into account site and year specific differences and can develop an accurate prediction of crop status early in the season when decisions are made.

Despite the variability in the yield response to pre-plant N fertilizer, maximum grain yields were similar across all sites in this study, especially at those sites where rice was planted in May (all except RES-19), which is typically when rice is planted in CA (**Hill et al., 2006)**. For sites where rice was planted in May, maximum yields ranged from 11.3 Mg ha^{-1} to 13.8 Mg ha^{-1} (**Fig 2**), while at RES-19 maximum yield was 9.6 Mg ha^{-1}, likely due to late planting in June. However, maximum yields at all sites fall within 75% of the maximum yield potential for this region (**Espe et al., 2016**), suggesting that the sites received proper management and were not significantly affected by diseases or pests.

2.4.2 Index Saturation

Saturation of red-based two-band indices, such as NDVI, is a well-documented problem (**Hatfield and Pruger, 2010; Huang et al., 2020)**, and a growing body of research is reporting that red edge based indices, such as the NDRE, are less affected by saturation and can provide a better estimation of crop status than NDVI, especially at higher levels of crop biomass (**Amaral et al., 2014; Li et al, 2014; Dunn et al., 2016**).

There were considerable differences in the relative amount of saturation observed among the three indices in this study, both with respect to raw IV and SI (**Fig. 2.3**). With respect to raw IV, both NDVI based indices ($NDVI_{UAS}$ and $NDVI_{GS}$) saturated more than the NDRE based index, as illustrated by the relatively higher and narrower peaks of the NDVI based indices (**Fig. 2.3a**). These differences in saturation also effected the relative saturation of each index with respect to SI (**Fig. 2.3b**). Among the three indices evaluated in this study, the $NDVI_{UAS}$ SI exhibited the greatest degree of saturation, with over 80% of observations falling within a SI range of 0.90 and 1.00, as compared to 66% and 62% of $NDVI_{GS}$ SI and $NDRE_{UAS}$ SI observations falling within the same range, respectively.

Saturation of NDVI is attributed to the crop reaching 100% canopy cover, but crop biomass beneath the canopy continuing to increase (**Gitelson, 2004, Huang et al., 2020**). Once the crop reaches 100% canopy cover, near infrared reflectance continues to rise, but red reflectance remains relatively constant due to strong absorption by chlorophyll at the top of the canopy, thus resulting in a minimal change in the overall ratio (i.e. the denominator will have a greater impact on the ratio than the numerator) (**Hatfield et al., 1985; Thenkabail et al., 2000; Gitelson, 2004**). Red edge radiation can penetrate deeper into the crop canopy due to relatively lower chlorophyll absorption, causing it to be more sensitive to chlorophyll content within the entire canopy, especially at higher biomass levels (**Li et al., 2014**; **Miller et al., 2018)** Given this greater sensitivity to total chlorophyll content within the canopy, to a certain degree, red edge based indices are able to overcome the saturation problem inherent to NDVI (**Van Niel and McVicar, 2004; Nguy-Robertson et al., 2012**). The results of our study are consistent with the findings of the aforementioned studies, as we also found the NDRE to be less saturated than both NDVI based indices in our study, with respect to both raw IV and SI.

In addition to the differences in saturation observed between NDVI and NDRE, a difference in saturation was observed between the two NDVI based indices in our study, with the $NDVI_{UAS}$ saturating to a greater degree than the $NDVI_{GS}$, both with respect to raw IV and SI (**Fig. 2.3**). **Duan et al. (2017)** observed a similar result in their wheat breeding trials where they measured $NDVI_{GS}$ and $NDVI_{UAS}$ at various time points throughout the growing period and found that $NDVI_{UAS}$ measurements were strongly correlated with $NDVI_{GS}$, but the $NDVI_{UAS}$ readings were offset by about 0.2 units higher and were more compressed. A likely explanation for this difference in sensitivity among the two indices could be that compared to the $NDVI_{GS}$ which is measured using a proximal sensor close to the canopy, the lower resolution of the multispectral camera used to measure $NDVI_{UAS}$ cannot sample the small amount of background noise from a higher altitude which results in a higher $NDVI_{UAS}$ value with a smaller range (**Duan et al., 2017**).

2.4.3 Predicting PI N_{UP} and Final Grain Yield with SI

The objective of this study was to compare the utility of vegetative indices measured using aerial and proximal sensors at assessing rice crop status quantified as PI N_{UP} and final grain yield. Predicting crop N_{UP} and final grain yields early in the season is of interest to farmers and agricultural stakeholders for a number of reasons, including refining fertilizer management, planning harvest, forecasting milling and storage needs, and directing marketing strategies. In order to directly compare the ability of each index to predict PI N_{UP} and final grain yield, the raw IV from the three indices were normalized by calculating the SI. Unique quadratic-plateau models were developed to describe the relationship between each SI and PI N_{UP} (**Fig. 2.4),** and unique linear mixed effects models were developed to describe the relationship between each SI and final grain yield (**Fig. 2.5**). As we had hypothesized, the relative degree of saturation across the three indices (as seen in **Fig. 2.3b),** significantly affected the ability of each SI to predict PI N_{UP} and final grain yield. The $NDVI_{UAS}$ SI was the most saturated index among the three indices in this study and was also the poorest predictor of PI N_{UP} and final grain yield, as the relationship between N_{UP} and $NDVI_{UAS}$ SI saturated (i.e. reached a plateau) the earliest (plateau = 96 kg N ha^{-1}) (**Fig. 2.4c**), the range of SI values before its point of saturation was the narrowest (**Fig. 2.4c, left axis**), and the $NDVI_{UAS}$ SI was least sensitive to changes in final grain yield, as seen by the slope of the resulting mixed-effects models being the steepest (slope = 25.3 Mg ha^{-1}) (**Fig. 2.5c).** The $NDRE_{UAS}$ SI, which was the least saturated index in this study, was the best predictor of PI N_{UP}, as illustrated by the relationship between N_{UP} and $NDRE_{UAS}$ SI saturating the latest (plateau = 129 kg N ha^{-1}) (**Fig. 2.4b**), and the relatively large range of SI values before its point of saturation (**Fig. 2.4b, left axis**), and the $NDRE_{UAS}$ SI was more sensitive to changes in final grain yield, as it explained changes in final grain yield over a larger SI range, which resulted in the model to have a much lower slope (slope = 11.7 Mg ha^{-1}, **Fig 2.5b**). Our finding that the $NDRE_{UAS}$ saturates less than the $NDVI_{UAS}$, which results in superior ability of the former to assess crop status is in agreement with what others have previously observed in rice (**Dunn et al., 2016; Zheng et al. 2019**; **Wang et al. 2021**) and also in wheat (**Chen et al., 2019; Walsh et al., 2018).**

Although we found the $NDRE_{UAS}$ SI to be generally superior to the $NDVI_{GS}$ SI at assessing crop status, our results suggest that both the $NDRE_{UAS}$ and $NDVI_{GS}$ are reliable options to assess rice crop status at PI and are far superior to the $NDVI_{UAS}$. As seen in **Fig. 2.3b,** The $NDVI_{GS}$ SI was slightly more saturated than the $NDRE_{UAS}$ SI, which led the relationship between PI N_{UP} and $NDVI_{GS}$ SI to also saturate (plateau = 113 kg N ha^{-1}) relatively sooner (**Fig. 2.4a)**. However, with respect to predicting final grain yield, the $NDRE_{UAS}$ SI and $NDVI_{GS}$ SI were similarly sensitive to changes in final grain yield, as seen by the relatively similar slope for both mixed effects models (slope = 11.7 Mg ha^{-1} and 9.5 Mg ha^{-1}, respectively) (**Fig. 2.5a, 2.5b).** The $NDVI_{GS}$ SI did have a relatively larger range of SI values before its point of saturation (**Fig. 2.4a, left axis**), and predicted final grain yield across a relatively larger range of SI values than the $NDRE_{UAS}$ SI (**Fig. 2.5**), however this was in large part due to $NDVI_{GS}$ SI observations in the 0N treatment at the Arbuckle sites which experienced a strong effect of background water (due to the close proximity of the sensor and sparse crop), resulting in very low $NDVI_{GS}$ SI measurements.

2.5. CONCLUSION

To the best of our knowledge, the current study is the first effort to have compared the ability of NDVI and NDRE measured using a proximal and aerial sensor at assessing N_{UP} and final grain yield in rice, wheat, or maize. Our finding that both the $NDRE_{UAS}$ SI and $NDVI_{GS}$ SI measured PI rice crop status effectively is quite encouraging, considering that the former was measured using an aerial sensor at least 50 m. from the crop, while the latter was measured using a proximal sensor within 1 m. of the crop canopy. The ability to assess crop status effectively across different sensors provides a unique advantage for end-users as it allows them the flexibility to choose the sensor most suitable for their goals. This is especially important considering the significant differences among the sensors and how they are used to record canopy reflectance data. Given the relatively small number of studies that have explored this topic, additional studies are required to better understand how these results may be affected by the choice of vegetative indices, growth stages, biophysical parameters, or crops.

2.6. ACKNOWLEDGEMENTS

We would like to thank the California Rice Research Board for supporting this research, Cesar Abrenilla and fellow members of the Agroecosystems Lab at UC Davis, Ray Stogsdill and the entire staff at the California Rice Experiment Station, visiting scholars Muhammad Ishfaq, Kevin Cassman, and Wencheng Ding, and the California rice growers who participated in this study.

REFERENCES

Amaral, L.R., Molin, J.P. and J.S. Schepers. 2015. Algorithm for variable-rate nitrogen application in sugarcane based on active crop canopy sensor. Agron. J. 107:1513-1523.

Balasubramanian, V., Morales, A.C., Cruz, R.T., and S. Abdulrachman. 1999. On-farm adaptation of knowledge-intensive nitrogen management technologies for rice systems. Nutr. Cycl. Agroecosys. 53:59-69.

Becker, T., Nelsen, T.S., Leinfelder-Miles, M. and Lundy, M.E., 2020. Differentiating between Nitrogen and Water Deficiency in Irrigated Maize Using a UAV-Based Multi-Spectral Camera. Agronomy, 10(11), p.1671.

Chen, Z., Miao, Y., Lu, J., Zhou, L., Li, Y., Zhang, H., Lou, W., Zhang, Z., Kusnierek, K. and Liu, C., 2019. In-season diagnosis of winter wheat nitrogen status in smallholder farmer fields across a village using unmanned aerial vehicle-based remote sensing. Agronomy, 9(10), p.619.

CIMIS. 2020. California Irrigation Management Information System. Internet Resource. (http://www.cimis.water.ca.gov/WSNReportCriteria.aspx) (accessed 01 Sept. 2020).

Colomina, I. and Molina, P., 2014. Unmanned aerial systems for photogrammetry and remote sensing: A review. ISPRS Journal of photogrammetry and remote sensing, 92, pp.79-97.

Cox, D.R. and Snell, E.J., 2018. Analysis of binary data. Routledge.

Daughtry, C.S.T., Walthall, C.L., Kim, M. S., Brown de Colstoun, E., and J.E. McMurtrey III. 2000. Estimating corn leaf chlorophyll concentration from leaf and canopy reflectance. Remote Sens. Environ. 74:229-239.

De Datta, S.K., 1981. Principles and practices of rice production. Int. Rice Res. Inst.

Delavarpour, N., Koparan, C., Nowatzki, J., Bajwa, S. and X. Sun. 2021. A technical study on UAV characteristics for precision agriculture applications and associated practical challenges. Remote Sens. 13:1204.

Duan, T., Chapman, S.C., Guo, Y. and Zheng, B., 2017. Dynamic monitoring of NDVI in wheat agronomy and breeding trials using an unmanned aerial vehicle. Field Crops Research, 210, pp.71-80.

Dunn, B.W., Dehaan, R., Schmidtke, L.M., Dunn, T.S. and R. Meder. 2016. Using field-derived hyperspectral reflectance measurement to identify the essential wavelengths for predicting nitrogen uptake of rice at panicle initiation. J. Near Infrared Spec. 24:473-483.

Dunn, B.W., Dunn, T.S., Hume, I., Orchard, B.A., Dehaan, R., and A. Robson. 2016a. Remote sensing PI nitrogen uptake in rice. IREC Newsletter. 195:48-50.

Dzurella, K.N., Pettygrove, G.S., Fryjoff-Hung, A., Hollander, A., and T. Harter. 2015. Potential to assess nitrate leaching vulnerability of irrigated cropland. J. Soil Water Conserv. 70: 63-72.

Esposito, M., Crimaldi, M., Cirillo, V., Sarghini, F. and Maggio, A., 2021. Drone and sensor technology for sustainable weed management: A review. Chemical and Biological Technologies in Agriculture, 8(1), pp.1-11.

Espe, M.B., Yang, H., Cassman, K.G., Guilpart, N., Sharifi, H. and Linquist, B.A., 2016. Estimating yield potential in temperate high-yielding, direct-seeded US rice production systems. Field Crops Research, 193, pp.123-132.

Fu, Y., Yang, G., Song, X., Li, Z., Xu, X., Feng, H. and Zhao, C., 2021. Improved estimation of winter wheat aboveground biomass using multiscale textures extracted from UAV-based digital images and hyperspectral feature analysis. Remote Sensing, 13(4), p.581.

Gitelson, A.A., 2004. Wide dynamic range vegetation index for remote quantification of biophysical characteristics of vegetation. Journal of plant physiology, 161(2), pp.165-173.

Haghighattalab, A., Pérez, L.G., Mondal, S., Singh, D., Schinstock, D., Rutkoski, J., Ortiz-Monasterio, I., Singh, R.P., Goodin, D. and J. Poland. 2016. Application of unmanned aerial systems for high throughput phenotyping of large wheat breeding nurseries. Plant Methods. 12:1-15.

Hardin, P.J. and R.R. Jensen. 2011. Small-scale unmanned aerial vehicles in environmental remote sensing: Challenges and opportunities. GISci. Remote Sens. 48:99-111.

Hassan, M.A., Yang, M., Rasheed, A., Yang, G., Reynolds, M., Xia, X., Xiao, Y. and He, Z., 2019. A rapid monitoring of NDVI across the wheat growth cycle for grain yield prediction using a multi-spectral UAV platform. Plant science, 282, pp.95-103.

Hatfield, J.L., Gitelson, A.A., Schepers, J.S. and C.L. Walthall. 2008. Application of Spectral Remote Sensing for Agronomic Decisions. Agron. J. 100:117-131.

Hatfield, J.L. and Prueger, J.H., 2010. Value of using different vegetative indices to quantify agricultural crop characteristics at different growth stages under varying management practices. Remote Sensing, 2(2), pp.562-578.

Hatfield, J.L., Prueger, J.H., Sauer, T.J., Dold, C., O’Brien, P. and Wacha, K., 2019. Applications of vegetative indices from remote sensing to agriculture: Past and future. Inventions, 4(4), p.71.

Hill, J.E., Williams, J.F., Mutters, R.G., and C.A. Greer. 2006. The California rice cropping system: agronomic resource issues for long-term sustainability. Paddy Water Environ. 4: 13-19.

Huang, S., Tang, L., Hupy, J.P., Wang, Y. and Shao, G., 2021. A commentary review on the use of normalized difference vegetation index (NDVI) in the era of popular remote sensing. Journal of Forestry Research, 32(1), pp.1-6.

Li, F., Miao, Y., Feng, G., Yuan, F., Yue, S., Gao, X., Liu, Y., Liu, B., Ustin, S.L. and Chen, X., 2014. Improving estimation of summer maize nitrogen status with red edge-based spectral vegetation indices. Field Crops Research, 157, pp.111-123.

Lu, J., Miao, Y., Shi, W., Li, J., and F. Yuan. 2017. Evaluating different approaches to non-destructive nitrogen status diagnosis of rice using portable RapidSCAN active canopy sensor. Sci. Rep. 7:14073.

Mangiafico, S. and Mangiafico, M.S., 2017. Package 'rcompanion'. Cran Repos, 20, pp.1-71.

Miller, J.J., Schepers, J.S., Shapiro, C.A., Arneson, N.J., Eskridge, K.M., Oliveira, M.C. and Giesler, L.J., 2018. Characterizing soybean vigor and productivity using multiple crop canopy sensor readings. Field Crops Research, 216, pp.22-31.

Nelsen, T. 2019. Drone-Data-in-Agricultural-Research: Information and script for working with multispectral drone-based data in agricultural research settings. San Francisco, CA: GitHub.

Nguy-Robertson, A., Gitelson, A., Peng, Y., Viña, A., Arkebauer, T. and Rundquist, D., 2012. Green leaf area index estimation in maize and soybean: Combining vegetation indices to achieve maximal sensitivity. Agronomy Journal, 104(5), pp.1336-1347.

Pittelkow, C.M., Adviento-Borbe, M.A., van Kessel, C., Hill, J.E., and B.A. Linquist. 2014. Optimizing rice yields while minimizing yield-scaled global warming potential. Glob Change Biol. 20:1382-1393.

R Core Team. 2021. R: A language and environment for statistical computing. R Foundation for Statistical Computing, Vienna, Austria. (https://www.R-project.org/)

Rehman, T.R., Reis, A.F.B., Akbar, N., and B.A. Linquist. 2019. Use of Normalized Difference Vegetation Index to assess N status and predict grain yield in rice. Agron. J. 111:2889-2898.

Saberioon, M.M., Amin, M.S.M., Gholizadeh, A., and M.H. Ezri. 2014. A review of optical methods for assessing nitrogen contents during rice growth. Appl. Eng. Agric. 30:657-669.

Smith, J., Sutula, M., Bouma-Gregson, K., and M. Van Dyke. 2021. California Water Boards' Framework and Strategy for Freshwater Harmful Algal Bloom Monitoring: Executive Synthesis. Southern California Coastal Water Research Project Technical Report 1141.A

Sharp, Z. 2017. Principles of stable isotope geochemistry. 2nd edition. Univ. of New Mexico Press, Albuquerque.

Sumner, Z., Varco, J.J., Dhillon, J.S., Fox, A.A., Czarnecki, J. and Henry, W.B., 2021. Ground versus aerial canopy reflectance of corn: Red-edge and non-red edge vegetation indices. Agronomy Journal, 113(3), pp.2782-2797.

Tamagno, S., Eagle, A.J., McLellan, E.L., van Kessel, C., Linquist, B.A., Ladha, J.K. and C.M. Pittelkow. 2022. Quantifying N leaching losses as a function of N balance: A path to sustainable food supply chains. Agric. Ecosyst. Environ. 324:107714.

Teal, R.K., Tubana, B., Girma, K., Freeman, K.W., Arnall, D.B., Walsh, O. and Raun, W.R., 2006. In-season prediction of corn grain yield potential using normalized difference vegetation index. Agronomy Journal, 98(6), pp.1488-1494.

Thenkabail, P.S., Smith, R.B. and E. De Pauw. 2000. Hyperspectral vegetation indices and their relationships with agricultural crop characteristics. Remote Sens. Environ. 71: 158-182.

Toth, C. and Jóźków, G., 2016. Remote sensing platforms and sensors: A survey. ISPRS Journal of Photogrammetry and Remote Sensing, 115, pp.22-36.

Tsouros, D.C., Bibi, S. and Sarigiannidis, P.G., 2019. A review on UAV-based applications for precision agriculture. Information, 10(11), p.349.

Van Niel, T.G. and McVicar, T.R., 2004. Determining temporal windows for crop discrimination with remote sensing: a case study in south-eastern Australia. Computers and electronics in agriculture, 45(1-3), pp.91-108.

Walsh, O.S., Shafian, S., Marshall, J.M., Jackson, C., McClintick-Chess, J.R., Blanscet, S.M., Swoboda, K., Thompson, C., Belmont, K.M. and Walsh, W.L., 2018. Assessment of UAV based vegetation indices for nitrogen concentration estimation in spring wheat. Advances in Remote Sensing, 7(2), pp.71-90.

Wang, L., Chen, S., Li, D., Wang, C., Jiang, H., Zheng, Q. and Peng, Z., 2021. Estimation of paddy rice nitrogen content and accumulation both at leaf and plant levels from UAV hyperspectral imagery. Remote Sensing, 13(15), p.2956.

Witt, C., Pasuquin, J.M.C.A., Mutters, R., and R.J. Buresh. 2005. New leaf color chart for effective nitrogen management in rice. Better Crops. 89: 36-39.

Xia, T., Miao, Y., Wu, D., Shao, H., Khosla, R. and Mi, G., 2016. Active optical sensing of spring maize for in-season diagnosis of nitrogen status based on nitrogen nutrition index. Remote sensing, 8(7), p.605.

Xue, J. and Su, B., 2017. Significant remote sensing vegetation indices: A review of developments and applications. Journal of sensors, 2017.

Yao, Y., Miao, Y., Cao, Q., Wang, H., Gnyp, M.L., Bareth, G., Khosla, R., Yang, W., Liu, F., and C. Liu. 2014. In-season estimation of rice nitrogen status with an active crop canopy sensor. IEEE J-STARS. 7:4403-4413.

Zhang, C. and J.M. Kovacs. 2012. The application of small unmanned aerial systems for precision agriculture: a review. Precis. Agric. 13:693-712.

Zheng, H., Cheng, T., Zhou, M., Li, D., Yao, X., Tian, Y., Cao, W. and Y. Zhu. 2019. Improved estimation of rice aboveground biomass combining textural and spectral analysis of UAV imagery. Precis. Agric. 20:611-629.

CHAPTER THREE

Using NDVI Response-Index to Inform Sustainable Top-dress N Fertilization in Direct-Seeded Rice

Telha H. Rehman[a], Mark E. Lundy[a], Nadeem Akbar[b], Daniel C. Olk[c], Andre Froes de Borja Reis[d], and Bruce A. Linquist[a]

[a]Department of Plant Sciences, University of California – Davis, Davis, CA 95616, USA

[b]Department of Agronomy, University of Agriculture – Faisalabad, 38040, Pakistan

[c]USDA-ARS, National Laboratory for Agriculture and the Environment, Ames, IA 50011, USA

[d]Department of Agronomy, Kansas State University, Manhattan, KS 66506, USA

Abbreviations: indigenous N supply, INS; normalized difference vegetation index, NDVI; panicle initiation, PI; response-index, RI

ABSTRACT

Accurately detecting nitrogen (N) deficiency and determining the need for additional N fertilizer is a key challenge to achieving precise in-season N fertilizer management in many crops including rice (*Oryza sativa* L.). In many direct-seeded rice systems, like in California (CA) and other regions of the world, the recommendation for N is to apply the N rate required for an average growing season at the beginning of the season and then assess the crop at panicle initiation (PI) to determine its N status and the potential need for a N top-dress to achieve maximum yields. However, accurately assessing rice N status and determining the need for top-dress N is a challenge for farmers as the current tools are constrained by their small-scale sampling method. Our objective was to develop a method to accurately predict rice N deficiency and the need for top-dress N at PI using canopy reflectance measurements. Nitrogen fertilizer response trials were established over a 3-yr period (8 site-years) throughout the Sacramento Valley rice growing region of CA. The Normalized Difference Vegetation Index (NDVI) Response-Index (RI_{NDVI}) was measured by dividing the NDVI of an area that is not N limited by the NDVI of the area of interest. The RI_{NDVI} ranged from 1.00 (not N deficient) to higher, with higher numbers indicating greater N deficiency. A linear mixed-effects model was developed to describe the relationship between RI_{NDVI} at PI and the grain yield response to top-dress N. Results showed that the grain yield response to top-dress N increased with increasing RI_{NDVI} until a threshold was achieved, after which the response leveled off. Based on an economic analysis, a grain yield increase of 0.26 Mg ha^{-1} was required for top-dress N applications to be economically feasible. This yield increase was achieved when crop RI_{NDVI} had exceeded 1.07 by PI. Based on these findings, this RI_{NDVI} could serve as a robust tool for farmers to inform precise mid-season N fertilizer management in direct-seeded rice systems.

3.1. INTRODUCTION

Annually, about 60 Tg of nitrogen (N) fertilizer is applied to soils worldwide to produce the three staple food crops (rice, wheat, and maize), with less than half of this amount being removed at the end of the season in the harvested grain (**Ladha et al., 2020**). This disparity between N fertilizer inputs and outputs negatively impacts the biosphere in many ways. For example, excessive N fertilization can result in nitrate leaching (**Dzurella et al., 2015)**, increased greenhouse gas emissions (**Almaraz et al., 2018; Pittelkow et al., 2014a**), and elevated N levels in agricultural tailwater causing eutrophication **(Smith et al., 2021).** Given the intensification of global agriculture required to feed the growing world population, these negative impacts on the biosphere will likely worsen unless new practices are developed and adopted that allow farmers to more efficiently utilize N fertilizer.

In California (CA), where rice (*Oryza sativa* L.) is predominantly water-seeded, the recommended practice is to apply the average seasonal N fertilizer requirement (typically 150 to 200 kg N ha^{-1}) before flooding and planting (**Linquist et al., 2009; Williams et al., 2010**). Aqua ammonia (NH_4OH) is the primary preplant N fertilizer used and it is injected 7 to 10 cm deep in the soil, after which the fields are flooded and remain so continuously until harvest, thus keeping the N fertilizer protected from denitrification and ammonia volatilization losses until the crop needs it (**Broadbent and Mikkelsen, 1968; Chuong et al., 2020**). **Linquist et al. (2009)** reported from 14 on-farm studies that N applied in this manner led to an average fertilizer N recovery in the crop of 53%. Similarly, in dry-seeded systems in the mid-southern USA and Australia, it is also recommended to apply the total N requirement early in the season, prior to the establishment of permanent flood (**Dunn et al., 2014a, 2016; Norman et al., 2021; Troldahl, 2018**). In both these systems, it is recommended to assess the crop at panicle initiation

(PI) to determine whether the crop requires additional N fertilizer inputs to achieve maximum yields (**Pittelkow et al., 2014b; Williams, 2010**). Panicle initiation is considered a critical stage for in-season N management as N applications later than PI are less efficiently utilized for grain yield (**DeDatta, 1981; Linquist and Sengxua, 2003**), and most, if not all, of the pre-plant N fertilizer has been taken up by this stage in both water-seeded (**LaHue et al., 2016)** and dry-seeded systems **(Norman et al., 2021)**. Because preplant N fertilizer has been taken up by this stage, further N uptake between PI and harvest relies on late season soil indigenous N supply (INS) and any top-dress fertilizer that may have been applied. If required, in CA typical PI top-dress rates range from 22 to 45 kg N ha^{-1} (**Williams, 2010**) with the average application being around 34 kg N ha^{-1} (**Hartley and van Kessel, 2003**). While the N rate applied at this stage is relatively low, it is still an important adjustment in a year where yield potential may be higher than average. Importantly, by PI, the yield components of tiller and panicle number have been determined, so major deficiencies due to initially low N rates would be too late to correct by this stage (**DeDatta, 1981; Dunn et al., 2016**).

Tools currently available to assess crop N status at PI include the Leaf Color Chart (LCC) and Soil Plant Analysis Development (SPAD) chlorophyll meter (**Saberioon et al., 2014**). The LCC estimates N content based on leaf greenness, while the SPAD meter measures the difference in transmittance between red and near infrared light passing through the leaf to estimate chlorophyll content (**Alam et al., 2005; Uddling et al., 2007**). Both the LCC and SPAD meter are simple diagnostic tools that have been shown to accurately estimate leaf N content and aid in the development of in-season top-dress N fertilizer recommendations (**Balasubramanian et al., 1999; Peng et al., 1996; Singh et al., 2014; Turner and Jund, 1991)**. While the LCC and SPAD meter are useful, these tools have not seen large scale adoption in rice systems outside of

Asia as tools are constrained by a single leaf sampling method and thus can only assess a small fraction of the field, which in CA, can be over 50 ha in size (**Daughtry et al., 2000; Saberioon et al., 2014**). Consequently, developing an accurate assessment of crop N status at PI and determining the need for a N top-dress application remains a challenge in CA rice systems.

More recently, the development of remotely sensed vegetation indices, such as the Normalized Difference Vegetation Index (NDVI), have shown promise to accurately assess crop N status over larger areas (**Foster et al., 2017)**. The NDVI is calculated by measuring crop canopy reflectance remotely (via a satellite, aircraft, or proximal sensor) at specific wavelengths in the red and near infrared regions of the electromagnetic spectrum and reported as a ratio (**Tucker, 1979; Tucker et al., 1985**). Among the different sensors used to measure NDVI, the GreenSeeker is one of the most commonly used as it is a portable handheld sensor with an active light source and can instantly display the NDVI measurement of the crop on its built-in screen (**Saberioon et al., 2014**). Several previous studies have reported strong correlations between GreenSeeker NDVI and rice N status at the PI growth stage (**Gnyp et al., 2014; Rehman et al., 2019; Yao et al., 2014**). Although the simplicity and efficiency of the GreenSeeker provide several advantages to end users; one disadvantage of the GreenSeeker is that the device only measures NDVI, which a number of previous studies have shown to saturate once crop biomass exceeds a certain threshold (**Asrar et al., 1984; Hatfield et al., 1985; Thenkabail et al., 2000)**. **Rehman et al. (2019);** however**,** reported that NDVI saturation occurs at rice biomass levels that are in excess of overall crop PI N requirements, suggesting that NDVI saturation would likely not occur at levels of crop biomass where farmers would make N top-dress fertilization decisions.

While NDVI measurements are useful to assess the N status of a crop, a single measurement does not indicate the likelihood of a crop to respond to additional N (**Rehman et al., 2019)**. To address this issue, an N-enriched area, which is non-limiting with respect to N, can be used (**Colaço and Bramley, 2018; Hussain et al., 2000**). If the crop outside the N-enriched area has a lower NDVI than the N-enriched area, it is inferred that the crop may respond to additional N inputs (**Raun et al., 2002; Tubaña et al., 2012)**. **Mullen et al. (2003)** developed an NDVI Response-Index (RI_{NDVI}) by dividing the NDVI from the N-enriched area by the NDVI from an adjacent area in the field. The RI_{NDVI} values will usually be > 1.0 with higher numbers indicating increased potential for N responsiveness. The N-enriched area and RI_{NDVI} have been used in many different applications across a wide range of crops and have been shown to be a robust indicator of crop responsiveness to N **(Arnall et al., 2009; Cao et al., 2016; Lofton et al., 2012; Lu et al., 2020; Tubaña et al., 2008).**

In situations where N fertilizer may be split throughout the season, previous studies have used a N fertilization optimization algorithm (NFOA) to determine N needs throughout the season (**Lukina et al., 2001; Raun et al., 2002; Raun et al., 2005)**. This approach also uses a N-enriched area, but the basic estimation of N needs is based on a mass balance calculation of the optimal N rate required for an expected yield **(Colaço and Bramley, 2018**). Several studies have demonstrated that this approach improves nitrogen use efficiency in rice relative to standard farmer practice by producing similar grain yields with less N fertilizer (**Ali et al., 2014; Bijay-Singh et al., 2015; Xue et al., 2014; Xue and Yang, 2008; Yao et al., 2012**). While this approach has a strong theoretical basis, it is based on several assumptions (e.g. seasonal N_{UP}, grain yield potential, and N use efficiency) that vary considerably across fields and over time.

Such an approach is also not easy to employ by a farmer who may not have access to such information.

Our objective was to develop a simple and rapid approach using the RI_{NDVI} which can be easily and reliably used on-farm for making top-dress N decisions in direct-seeded rice systems where the average seasonal N fertilizer requirement has been applied preplant and a decision is being made whether to top-dress at PI. This objective was pursued via field studies conducted over three years at eight different locations.

3.2. MATERIALS AND METHODS

3.2.1 Site Description

Six on-farm and two on-station N response trials were established during the 2016, 2017, and 2019 growing seasons (named by proximity to the nearest town or research station and study year), with sites located throughout the Sacramento Valley rice growing region of CA (Fig. 3.1, Table 3.1). On-station sites were established at the CA Rice Experiment Station (RES) near Biggs. The Sacramento Valley has a Mediterranean climate characterized by warm and dry conditions during the growing season (May to October). The average air temperature and precipitation during the growing season for the three years of this study were 22.8° C and 10.9 mm, respectively (**CIMIS, 2020 –** Biggs station).

Pre-season soil samples were collected from the plow layer (approximately 0 – 15 cm) after tillage and prior to fertilizer application at each site. Samples were analyzed for soil pH using saturated paste (**United States Salinity Laboratory Staff, 1954**), particle size using the hydrometer method (**Carter and Gregorich, 2007**), and soil organic C (SOC) and total N using an elemental analyzer interfaced to a continuous flow isotope ratio mass spectrometer (EA-IRMS) (**Sharp, 2017**). Soil properties were typical for rice soils in this region. Most soils had high clay contents (40 – 55%) (Table 3.1). The only exception was at Marysville-19 (24% clay). Across sites, soil pH ranged from 4.7 – 7.0, and SOC and total N ranged from 13.8 to 19.9 g kg^{-1}, and from 1.1 to 1.9 g kg^{-1}, respectively.

3.2.2 Experimental Design and Management

Each N response trial was arranged as a split-plot randomized complete block design with four replicates. The main plot treatment was the pre-plant N fertilizer rate and the subplot

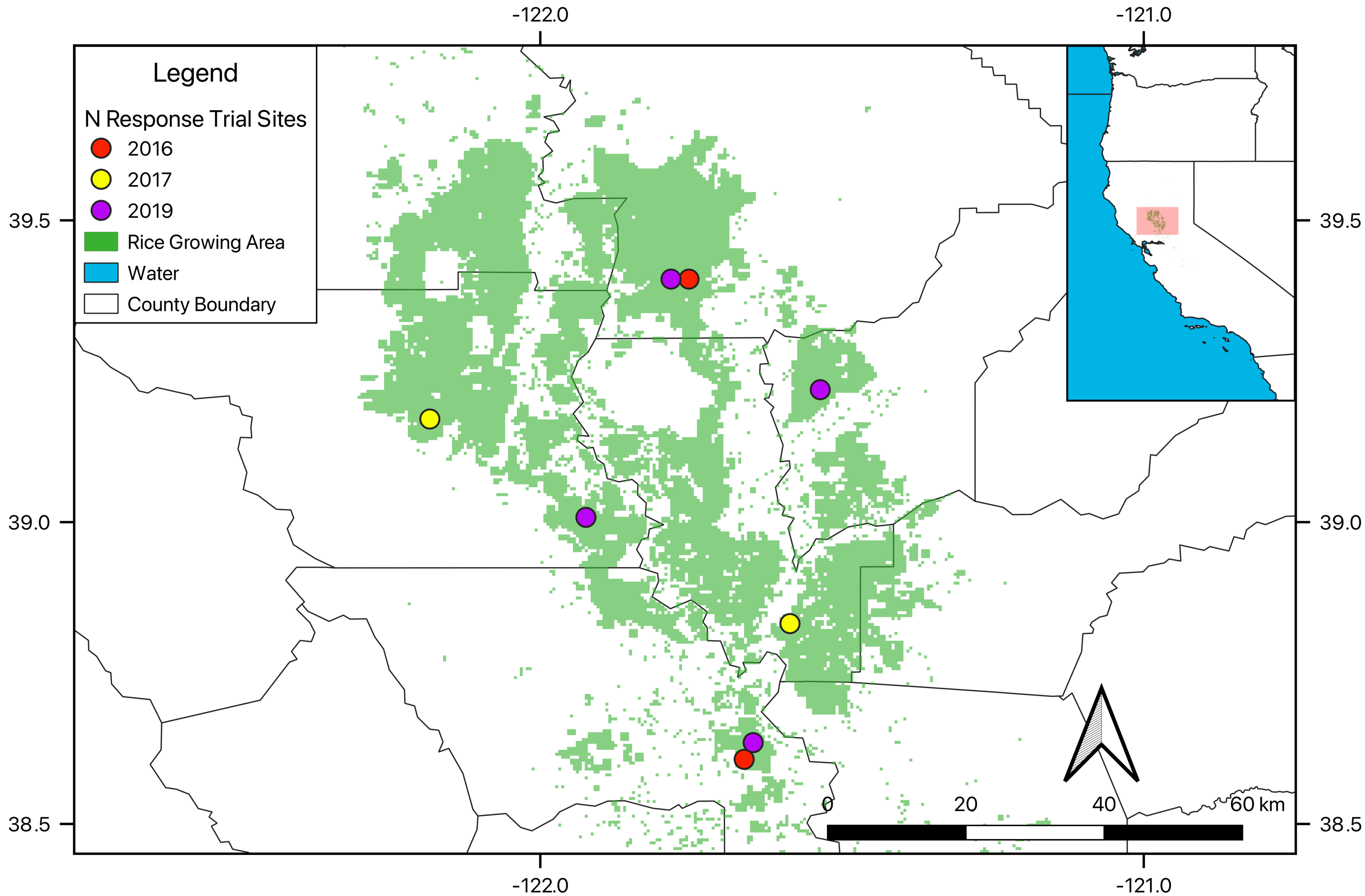

Figure 3.1. A map of N response trial sites established during the 2016, 2017, and 2019 growing seasons throughout the Sacramento Valley rice growing area of California, USA.

Table 3.1. Soil descriptions and selected properties of each N response trial site-year located throughout the Sacramento Valley, California.

Site-Year	**Soil Series**	**Taxonomic Classification**	**Texture (%)**			**Organic Carbon (g kg^{-1})**	**Total Nitrogen (g kg^{-1})**	**pH**
			Sand	**Silt**	**Clay**			
Davis-16	Sycamore	Fine-silty, mixed, super active, nonacid, thermic Mollic Endoaquepts	13	37	50	19.6	1.9	7.0
RES-16	Esquon-Neerdobe	Fine, smectitic, thermic Xeric Epiaquerts	32	24	44	16.2	1.1	5.0
Nicolaus-17	Capay	Fine, smectitic, thermic Typic Haploxererts	19	36	45	15.1	1.2	5.5
Williams-17	Willows	Fine, smectitic, thermic Sodic Endoaquerts	21	39	40	17.5	1.5	5.0
Arbuckle-19	Clear Lake	Fine, smectitic, thermic Xeric Endoaquerts	8	38	55	19.9	1.6	6.3
Davis-19	Sycamore	Fine-silty, mixed, super active, nonacid, thermic Mollic Endoaquepts	9	38	53	19.8	1.8	6.3
Marysville-19	San Joaquin	Fine, mixed, active, thermic Abruptic Durixeralfs	35	41	24	15.4	1.2	4.7
RES-19	Esquon-Neerdobe	Fine, smectitic, thermic Xeric Epiaquerts	30	26	44	13.8	1.1	5.3

treatment was the top-dress N rate applied at PI. In 2016 and 2017, pre-plant N fertilizer was broadcast by hand as urea at rates of 0, 75, 125, 175, and 225 kg N ha^{-1}. In 2017, an additional pre-plant N rate of 45 kg N ha^{-1} was also included. In 2019, pre-plant N fertilizer was injected into the soil (7 to 10 cm depth) as aqua-ammonia at rates of 0, 101, 135, 168, 202, and 235 kg N ha^{-1}. Top-dress N fertilizer was broadcast by hand at PI as ammonium sulfate at rates of 0, 25, and 50 kg N ha^{-1} in 2016 and 2017; and 0 and 34 kg N ha^{-1} in 2019. The decision to utilize only one top-dress N rate in 2019, was made because there was not a significant difference between the 25 and 50 kg N ha^{-1} N rates in 2016 and 2017. In 2016 and 2017, main plots were at least 30 m^2 and the three subplots at least 10 m^2. In 2019, main plot width was determined by the width of the implement used to apply aqua-ammonia and ranged from 3.0 m to 11.5 m. Each main plot was at least 9 m long and the area of the two subplots were at least 3.3 m^2. Phosphorus (P) and potassium (K) were broadcast across all plots at a rate of 45 kg P_2O_5 ha^{-1} as triple superphosphate and 50 kg K_2O ha^{-1} as potassium sulfate to ensure these nutrients were not limiting. The rice crop was established by water-seeding which is the common practice in CA (**Hill et al., 2006**). In this case, the fields are fertilized following seedbed preparation, flooded, and then soaked seed is broadcast onto the field by airplane. The medium grain rice variety M-206, which is commonly grown in CA, was planted at all sites. While planting dates varied by site, all sites were planted within the normal timeframe for the region (early to mid-May) with the exception of Davis and the RES in 2019, where planting was delayed until early June due to excessive rain in mid-May. Herbicide and irrigation management followed common grower practice and were managed by either the grower (on-farm sites) or researchers (on-station sites). No presence of disease or pests was identified in the plots during the course of the experiments.

At physiological maturity, grain yield was measured by harvesting mature plants from a 1.0 m^2 quadrat in each subplot. Grains were removed from panicles, cleaned using a seed blower, dried to constant moisture at 60° C, and then weighed. Final yields are reported at 14% moisture.

3.2.3 NDVI and Response-Index

The NDVI was measured in every main plot using a GreenSeeker handheld crop sensor (Trimble Inc., Sunnyvale, CA) at PI (was visually confirmed in the field using the method outlined by **Dunn et al. (2014b)**). Measurements were taken by holding the GreenSeeker in the nadir position at a constant height of 1.0 m above the crop canopy while walking steadily along the edges of each main plot. For each main plot, the final NDVI value represented the average of four NDVI readings. Canopy closure was achieved by PI in all plots that received N fertilizer, thus the effect of background water or soil on NDVI measurements was considered negligible.

For each main plot, RI_{NDVI} was calculated using the following equation as outlined by **Mullen et al. (2003):**

$$(1) \qquad \mathrm{RI_{NDVI}} = \left(\mathrm{NDVI_{N\ enriched\ plot}}\right) / \left(\mathrm{NDVI_{N\ treatment}}\right)$$

The main plot with the highest observed NDVI at each site served as the N enriched plot. At most sites, the highest NDVI was observed in a main plot with the highest pre-plant N rate (the only exceptions were at Davis-16 and Davis-19 where it was a main plot with the second highest pre-plant N rate). In all cases, the N enriched plot had the maximum yields or was in an N treatment which was above that required for maximum yields; both indicating that the plot was N enriched and not limited by N.

3.2.4 Data Analysis

Data analysis was performed using the statistical program R (version 4.0.2, **R Core Team, 2021**). The package *dplyr* (**Wickham et al., 2021**) was used to transform the data, and the package *ggplot2* (**Wickham, 2016**) was used to visualize the data and to construct figures. The relationship between pre-plant N rate and final grain yield at each top-dress N rate was described by a quadratic linear regression model. The function *lme( )* in the *nlme* package (**Pinheiro et al., 2021**) was used to develop a linear mixed-effects model to describe the relationship between PI RI_{NDVI}, top-dress N rate, and final grain yield. Given the shape of the relationship between RI_{NDVI} and final grain yield, RI_{NDVI} values were inverted to permit the inclusion of a quadratic term within the mixed-effects model. After fitting the model, $(RI_{NDVI})^{-1}$ values were reverted to RI_{NDVI} for the purpose of reporting results in units that coincide with previous work on this topic. The equation of the resulting mixed-effects model is provided below:

(2) $$Final\ Grain\ Yield =$$

$$fixed\ = (RI_{NDVI})^{-1} : top-dress\ N\ rate\ +\ [(RI_{NDVI})^{-1}]^2,$$

$$random\ =\ \sim top-dress\ N\ rate\ |\ site-year$$

Graphical and numerical summaries were examined to ensure the resulting model satisfied the assumptions of linear regression. Pseudo R^2 were calculated for the mixed-effects model using the function *r.squaredGLMM( )* in the *MuMIn* package (**Bartoń, 2020**) with the conditional R^2 representing the variability explained by the entire model (fixed and random effects), the marginal R^2 representing the variability explained only by the fixed-effects, and the portion of variability explained by the random-effects (in this study site-year slope and intercept) represented as the difference in conditional and marginal R^2. The package *emmeans* (**Lenth, 2021**) was used to derive estimated marginal means from the model coefficients. Hypothesis testing of the resulting marginal means followed the method outlined by the **UCLA Statistical Consulting Group (2021)**. Top-dress N rate was included in the model as a continuous variable to allow for estimation of final grain yield at any given top-dress N rate within the range of rates included in this study (0 – 50 kg N ha^{-1}). We did not detect a significant difference in grain yield response among top-dress rates in our study and thus elected to define the grain yield response to top-dress N as the difference in model estimated final grain yield between 0 and 34 kg N ha^{-1}; the latter being a typical top-dress N rate in CA (**Hartley and van Kessel, 2003**).

An economic analysis was performed to identify the break-even point for top-dress N applications (i.e., the amount of grain yield response needed to recover the cost of applying top-dress N). Based on the cost of fertilizer and its application, and the market value of medium grain rice, a grain yield response of 0.26 Mg ha^{-1} was identified as the break-even point for top-dress N applications. For the analysis, ammonium sulfate ($(NH_4)_2SO_4$; 0.21 g N g^{-1}) was used as the top-dressing N source at US\$ 0.40 kg^{-1} (current fertilizer price based on a survey of five local chemical suppliers). At a N composition of 21%, an application rate of 160 kg $(NH_4)_2SO_4$ ha^{-1} would be required to achieve a top-dress rate of 34 kg N ha^{-1}. In California, top-dress N is applied with an airplane for US\$ 32 ha^{-1} (**UC-ANR, 2015**). The 5-yr (2015 to 2019) historical market value of medium grain rice was US\$ 369 Mg^{-1} (**USDA NASS, 2021**). Therefore, the break-even point was calculated using the following equations:

(3) $$\text{Fertilizer cost (US\$ ha}^{-1}\text{): US\$ 0.40 kg}^{-1}\text{ (price)} \times 160\text{ kg }(\text{NH}_4)_2\text{SO}_4\text{ ha}^{-1}\text{ (rate)} = \text{US\$ 63 ha}^{-1}$$

Adding the fertilizer cost (US\$ 63 ha^{-1}) from Eqn. 3 above and the aviation cost of US\$ 32 ha^{-1} (**UC-ANR, 2015**):

(4) $$\text{Total application cost (US\$ ha}^{-1}\text{): US\$ 63 ha}^{-1}\text{(fertilizer)} + \text{ US\$ 32 ha}^{-1}\text{ (aviation)}$$
$$= \text{US\$ 95 ha}^{-1}$$

The following equation illustrates how to calculate the top-dress break-even point:

(5) $$\text{Top} - \text{dress break} - \text{even point (Mg ha}^{-1}\text{): US\$ 95 ha}^{-1}\text{ (application costs) } \times$$
$$\text{(XX Mg ha}^{-1}\text{) (required yield response)} = \text{ US\$ 369 Mg}^{-1}\text{ (rice price)}$$

Re-writing Eqn. 5 to isolate the required yield response:

(6) $$\text{Top} - \text{dress break} - \text{even point (Mg ha}^{-1}\text{): US\$ 95 ha}^{-1}\text{ (application costs)} \div$$
$$\text{US\$ 369 Mg}^{-1}\text{ (rice price)} = \text{(XX Mg ha}^{-1}\text{) (required yield response)} = 0.26\text{ Mg ha}^{-1}$$

Using the estimated marginal means derived from the mixed effects model, a t-test was performed to calculate the probability of the model estimated grain yield response exceeding the break-even point at each RI_{NDVI}. The t-statistic was calculated as follows: $t_{\hat{\beta}} = \left|\frac{\hat{\beta} - \beta_O}{s.e.\ (\hat{\beta})}\right|$, with $\hat{\beta}$ representing the model estimated grain yield response at a given RI_{NDVI}; β_O representing the break-even yield response (0.26 Mg ha^{-1}), and *s.e.* ($\hat{\beta}$) representing the standard error of the model. The p-value associated with the resulting t-statistic was calculated using the function *pt( )*

from the *base* package (**R Core Team, 2021**), which returns the cumulative density function based on the Student's t-distribution.

3.3. RESULTS

3.3.1 Grain yield response to N fertilizer

Minimum grain yields ranged widely from 4.3 Mg ha^{-1} (Arbuckle-19) to 10.6 Mg ha^{-1} (Nicolaus-17) while maximum grain yields ranged from 9.6 Mg ha^{-1} (RES-19) to 12.6 Mg ha^{-1} (RES-16) (Fig. 3.2). Across all sites, the lowest grain yields were in the 0 N pre-plant treatment. Where no top-dress N was applied, yields increased with increasing pre-plant N rate to a maximum and then leveled off or decreased at higher N rates. Applying top-dress N at PI led to an increase in grain yields in the lower pre-plant N rates at all sites; however, the magnitude of the yield response varied considerably across sites. For example, the mean yield response to top-dress N in the 0 N pre-plant treatment ranged from 0.1 Mg ha^{-1} (Nicolaus-17) to 2.4 Mg ha^{-1} (RES-19), with the mean response across all site-years equaling 1.7 Mg ha^{-1}. Overall, the grain yield response to top-dress N decreased with increasing pre-plant N rate across all site-years. The mean yield response to top-dress N in the highest pre-plant N rate also varied strongly across sites with values ranging from -1.1 Mg ha^{-1} (RES-16) to 0.6 Mg ha^{-1} (Nicolaus-17), with the mean response across all site-years equaling 0.0 Mg ha^{-1}. No differences in final grain yields were seen between sites that received urea versus aqua-ammonia as the pre-plant N fertilizer source.

3.3.2 Informing mid-season N management using RI_{NDVI}

At most sites, the highest pre-plant N rate represented the N non-limiting treatment, as a RI_{NDVI} of 1.00 (resulting from the N non-limiting plot being compared to itself) was observed in the highest pre-plant N rate (Table 3.2). The only exceptions were at Davis-16 and Davis-19 where a RI_{NDVI} of 1.00 occurred in the second highest N rate.

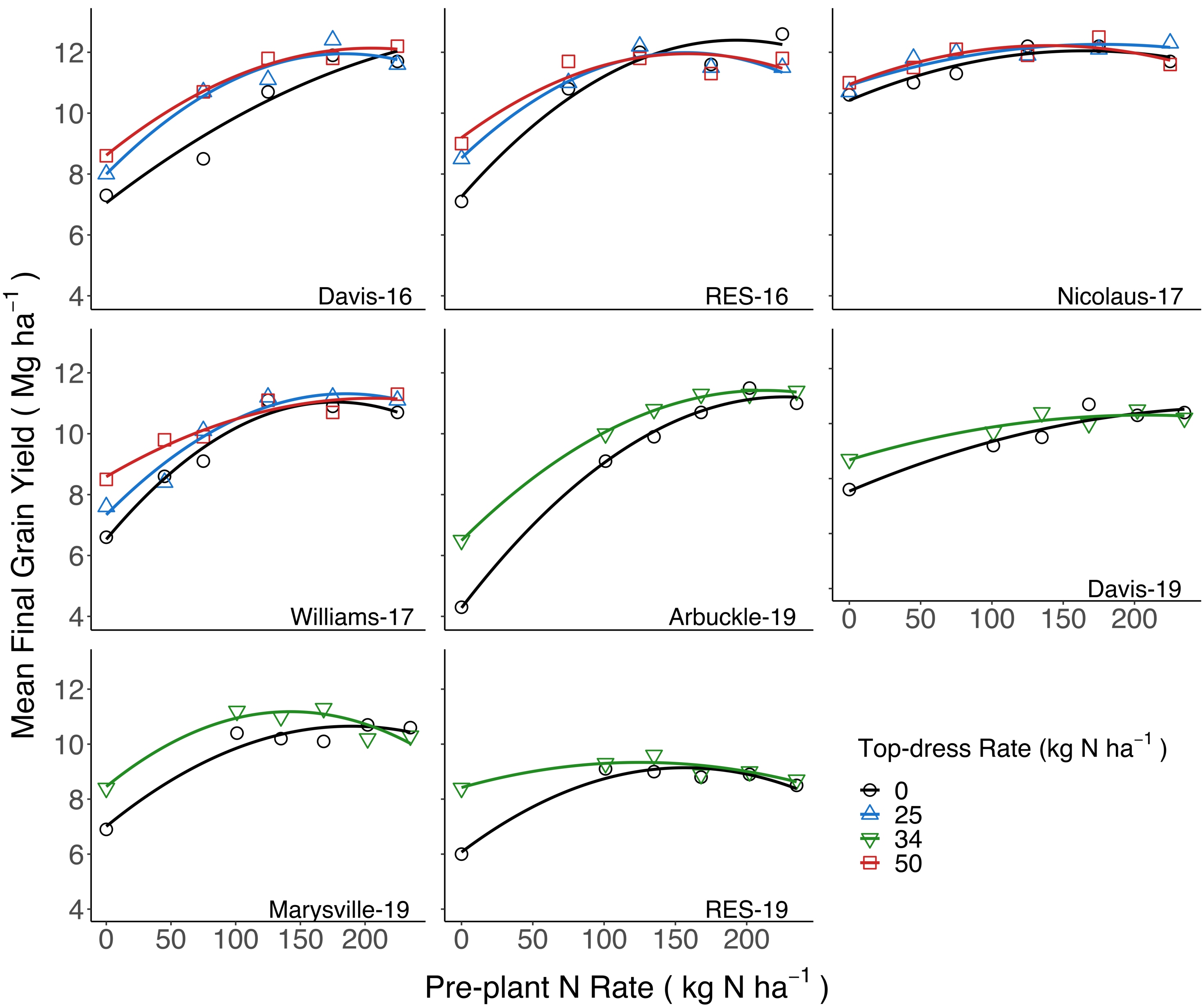

Figure 3.2. Relationship between pre-plant N rate with and without top-dress N and final grain yield for each site-year.

Table 3.2. Descriptive statistics (minimum, maximum, and mean) of GreenSeeker Normalized Difference Vegetative Index (NDVI) Response-Index measured at the panicle initiation rice growth stage from each N response trial site-year.

NDVI Response Index

Pre-plant N rate (kg N ha^{-1})	Davis-16		RES-16		Nicolaus-17		Williams-17	
	min – max	mean	min – max	mean	min – max	mean	min – max	mean
0	1.11 – 1.30	1.16	1.54 – 2.09	1.81	1.53 – 1.61	1.56	1.81 – 2.29	2.03
45	--	--	--		1.16 – 1.29	1.23	1.14 – 1.18	1.16
75	1.08 – 1.14	1.11	1.14 – 1.32	1.19	1.11 – 1.38	1.22	1.06 – 1.21	1.18
125	1.05 – 1.16	1.10	1.02 – 1.13	1.08	1.16 – 1.20	1.18	1.03 – 1.23	1.10
175	1.00 – 1.12	1.05	1.03 – 1.08	1.04	1.01 – 1.12	1.06	1.01 – 1.06	1.03
225	1.01 – 1.05	1.03	1.00 – 1.04	1.02	1.00 – 1.02	1.01	1.00 – 1.06	1.03
All	1.00 – 1.30	1.09	1.00 – 2.09	1.23	1.00 – 1.61	1.21	1.00 – 2.29	1.26

Pre-plant N rate (kg N ha^{-1})	Arbuckle-19		Davis-19		Marysville-19		RES-19	
	min – max	mean	min – max	mean	min – max	mean	min – max	mean
0	2.72 – 4.10	3.28	1.37 – 1.80	1.51	1.45 – 1.69	1.59	1.76 – 2.42	2.04
101	1.24 – 1.29	1.27	1.25 – 1.83	1.47	1.09 – 1.11	1.10	1.14 – 1.25	1.19
135	1.13 – 1.23	1.17	1.18 – 1.24	1.22	1.06 – 1.09	1.07	1.07 – 1.25	1.13
168	1.04 – 1.22	1.10	1.04 – 1.37	1.21	1.01 – 1.06	1.03	1.09 – 1.42	1.20
202	1.03 – 1.15	1.07	1.00 – 1.24	1.14	1.00 – 1.05	1.02	1.05 – 1.28	1.11
235	1.00 – 1.10	1.04	1.09 – 1.17	1.13	1.00 – 1.03	1.01	1.00 – 1.23	1.13
All	1.00 – 4.10	1.49	1.00 – 1.83	1.29	1.00 – 1.69	1.14	1.00 – 2.42	1.30

Across all site-years, the mean RI_{NDVI} decreased with increasing pre-plant N rate. Overall, strong variability in RI_{NDVI} values was seen across sites, with site-year maximum RI_{NDVI} ranging from 1.30 (Davis-16) to 4.10 (Arbuckle-19).

There was a significant response to top-dress N applications; however, as discussed earlier, there was not a significant difference in grain yield response among the top-dress N rates in this study. Given the lack of significant difference among the top-dress N rates in our study, we elected to define the grain yield response to top-dress N as the difference in model estimated final grain yield between top-dress rates of 0 and 34 kg N ha^{-1}; with the latter representing a typical top-dress N rate in CA (**Hartley and van Kessel, 2003**). Based on the liner mixed-effects model, the estimated grain yield response to top-dress N was 0.48 Mg ha^{-1} when averaged across all RI_{NDVI} observations (i.e. without using RI_{NDVI} as a predictor), and the model standard error around this estimate was ± 0.11 Mg ha^{-1} (Fig. 3.3a). However, when RI_{NDVI} was incorporated as a predictor of grain yield response, the estimated yield response ranged widely, from 0.10 Mg ha^{-1} at a RI_{NDVI} of 1.00 up to 2.02 Mg ha^{-1} at a RI_{NDVI} of 4.10 (Fig. 3.3b). Overall, the mixed-effects model explained 66% of the variability in final grain yields, with 46% being explained by the model fixed effects (top-dress N rate and RI_{NDVI}), and 20% being explained by the site-year random effect (Table 3.3); and the mean model standard error was ± 0.19 Mg ha^{-1} when averaged across the entire range of RI_{NDVI} observations. Overall, the grain yield response to top-dress N increased rapidly with increasing RI_{NDVI} until a threshold was achieved, after which the yield response leveled off (Fig. 3.3b). The range of RI_{NDVI} between 1.00 and 1.25 represents the area where N fertilizer management decisions are most likely to be made. For every 0.05 increase in

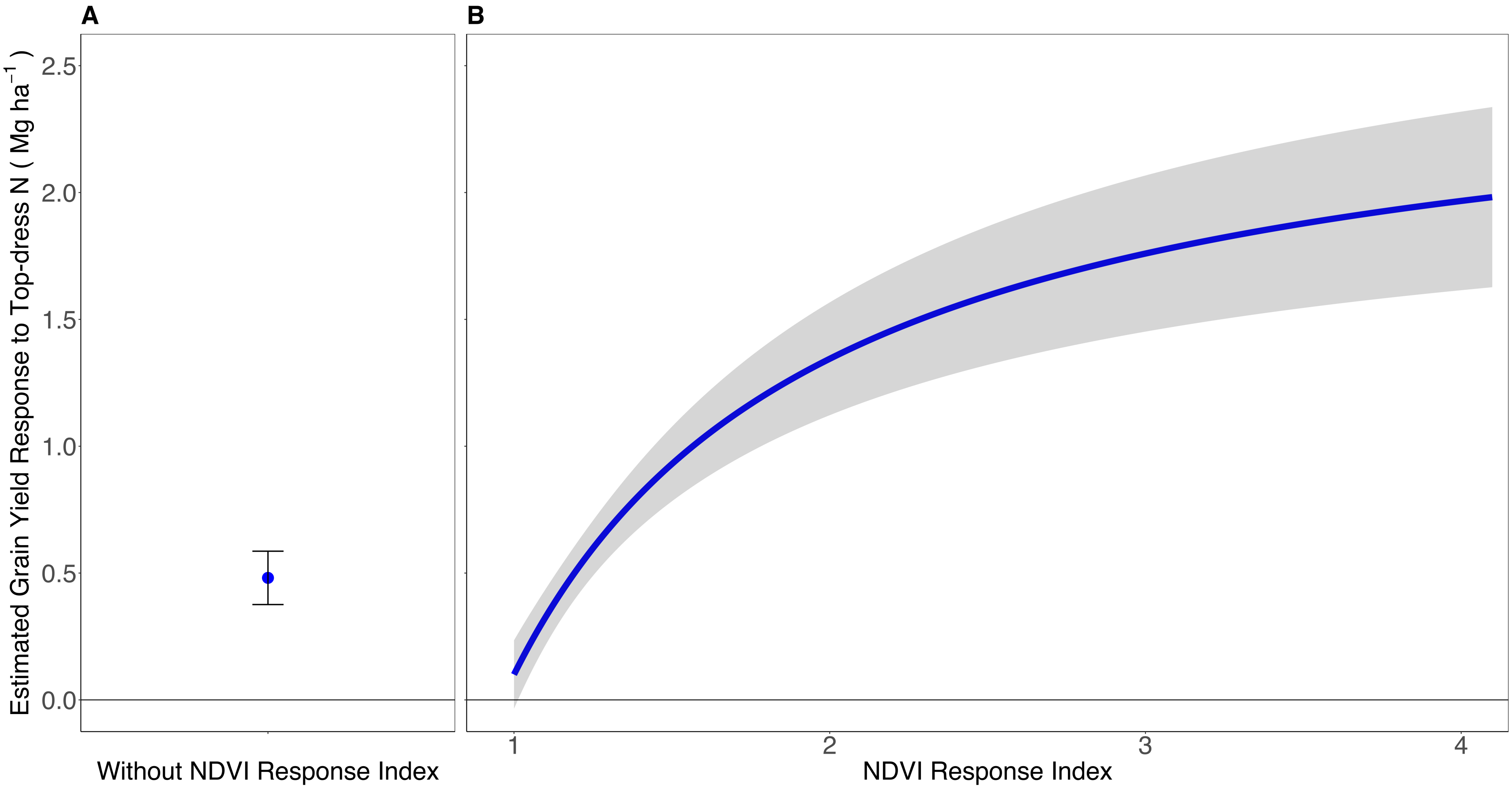

Figure 3.3. The relationship between the estimated rice grain yield response to top-dress N applied at 34 kg N ha^{-1} (typical grower rate in California) (**A**) when averaged across all NDVI Response Index (RI_{NDVI}) observations (i.e. without using RI_{NDVI} as a predictor) and (**B**) the RI_{NDVI} measured at the panicle initiation growth stage as described by a linear mixed-effects model. The error bar (panel A) and the gray shading (panel B) represents the standard error around the estimated grain yield response.

Table 3.3. Model parameters of the linear mixed-effects model developed to describe the relationship between NDVI Response-Index (RI) and the rice grain yield response to top-dress N applied at the panicle initiation (PI) growth stage.

Number of Site-Years		8
Number of Observations		456
Range of RI		1.00 – 4.10
R^2†		
	Fixed Effects	.46
	Random Effects	.20
	Entire Model	.66
Mean Model Standard Error (Mg ha^{-1})‡		± 0.19
Slope (Mg ha^{-1})§		
	RI 1.00 – 1.25	0.10
	RI 1.25 – 2.50	0.04
	RI 2.50 – 4.10	0.01
RI at break-even point¶		1.07
Model Standard Error at break-even point (Mg ha^{-1})		± 0.12

† proportion of variability explained by model fixed effects, random effects, and the entire model (fixed and random effects)
‡ averaged across the entire range of observations
§ increase in the estimated grain yield response to top-dress N per 0.05 increase in RI within each corresponding range
¶ top-dress break-even point of 0.26 Mg ha^{-1}, which represents the amount of grain yield response required to recover the cost of applying top-dress N

RI_{NDVI} between 1.00 and 1.25, applying top-dress N added 0.10 Mg ha^{-1} in final grain yield (Table 3.3, Fig. 4, left axis). Between a RI_{NDVI} of 1.25 and 2.50, the estimated yield response to N top-dress increased by 0.04 Mg ha^{-1} per 0.05 increase in RI_{NDVI}, and at a RI_{NDVI} greater than 2.50, the increase in yield response to top-dress N per 0.05 RI_{NDVI} was marginal (0.01 Mg ha^{-1}).

Based on the economic analysis and assumptions provided in the Materials and Methods, a grain yield response of 0.26 Mg ha^{-1} was required to recover the costs of applying top-dress N fertilizer (i.e. break-even point). A grain yield increase of 0.26 Mg ha^{-1} corresponded to a RI_{NDVI}

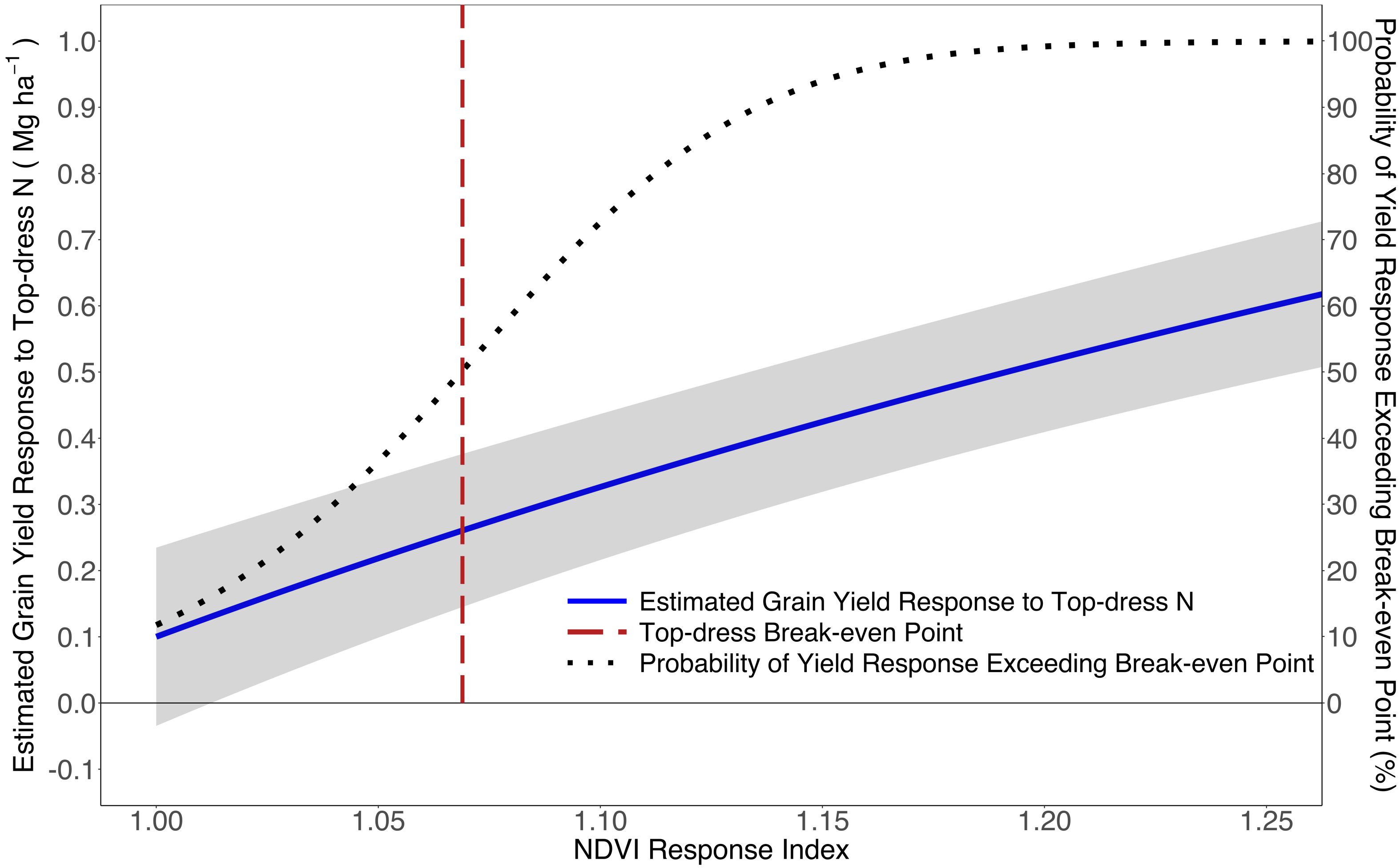

Figure 3.4. The relationship between NDVI Response Index (RI_{NDVI}) and the estimated rice grain yield response to top-dress N applied at 34 kg N ha^{-1} (typical grower rate in California) at the panicle initiation growth stage as described by a linear mixed effects model (solid blue line). The gray shading around the line represents the standard error of the estimated yield response. The vertical red dashed line at a RI_{NDVI} of 1.07 corresponds to the top-dress break-even point of 0.26 Mg ha^{-1} which represents the amount of grain yield response needed for a farmer to recover the cost of applying top-dress N. The dotted line represents the probability of the grain yield response to top-dress N exceeding the break-even point.

of 1.07, and the model standard error at this RI_{NDVI} was ± 0.12 Mg ha^{-1} (Table 3.3, Fig. 4, left axis). The probability of the grain yield response exceeding the break-even point was 50% considering the uncertainty of the estimate at RI_{NDVI} = 1.07 (Fig. 4, right axis). The probability of the grain yield response exceeding the break-even point increased steadily with increasing RI_{NDVI} until it surpassed 90% at a RI_{NDVI} of 1.14, where the estimated yield response at that RI_{NDVI} was 0.40 Mg ha^{-1} (Fig. 4, both vertical axes).

3.4. DISCUSSION

3.4.1 Grain yield response to N fertilizer

The maximum grain yields observed in this study were greater than 11 Mg ha^{-1} with the exception of RES-19 where yields were 9.6 Mg ha^{-1} (Fig. 3.2). These yields are close to 85% of the yield potential for this region (**Espe et al., 2016**), which should be achievable with good management practices. In CA, most rice is planted in May (**Hill et al., 2006**), and the late planting date (June 12th) may have contributed to the lower yields at RES-19.

At all sites, maximum yields in response to N were achieved as indicated by the leveling off of the N response curves. At two locations (Davis-16 and -19) the response curve did not level off where no top-dress N fertilizer was applied; however, looking more closely at the data points, maximum yields were achieved at these sites as the yields in the highest pre-plant N rate were numerically lower than yields in the next highest rate. Importantly, the leveling off of grain yield in the highest pre-plant N rates which did not receive a top-dress N application indicates that these plots were not N limited and thus serve as a valid N-rich plot for the development of the RI_{NDVI}.

3.4.2 Informing mid-season N management using RI_{NDVI}

The RI_{NDVI} presented here provides an improved tool for farmers to make precise mid-season N management decisions in rice. Although, developed within a CA context, this approach can be adopted by similar rice production systems, such as in the mid-southern USA and Australia, where it is also common to apply the recommended N rate early in the season and assess the need to apply a top-dress mid-season (**Dunn et al., 2014a, 2016; Norman et al., 2021; Troldahl, 2018**). This approach is less suited to rice systems where N fertilizer applications are intentionally split throughout the season (**Dobermann et al., 2002; Peng et al., 2006**). In situations where N fertilizer may be split throughout the season, previous studies have used a N fertilization optimization algorithm (NFOA) to determine N needs throughout the season (**Lukina et al., 2001; Raun et al., 2002; Raun et al., 2005)** and several studies have demonstrated that this approach improves nitrogen use efficiency in rice relative to standard farmer practice by producing similar grain yields with less N fertilizer (**Ali et al., 2014; Bijay-Singh et al., 2015; Xue et al., 2014; Xue and Yang, 2008; Yao et al., 2012**). The difference in the approach employed here is that the optimal seasonal N rate for an average year is applied in a single application at the start of the season, as it is known that it is used relatively efficiently (**Linquist et al., 2009**). The RI_{NDVI} is then used midseason to determine whether a small amount of additional N fertilizer is needed to achieve maximum yields.

While the RI_{NDVI} presented here provides a good tool for farmers to make precise mid-season N management decisions in rice, there is considerable variability in the estimated grain yield response across the range of RI_{NDVI} values as seen by the standard error around the yield response (Fig. 3.3). One explanation for the variability in yield response to top-dress may be the variability in late season soil INS across all the sites in our study. The use of the RI_{NDVI} approach presented here, as well as others such as the previously mentioned NFOA, assumes that late season INS is similar across fields. Previous experiments in rice systems have shown that by PI all or most of preplant N fertilizer has been taken up by the crop (**LaHue et al., 2016; Norman et al., 2021**), thus the supply of N to rice after PI, in the absence of top-dress N, is primarily from the soil INS. Late season soil INS may impact the decision about whether to apply a top-dress N application, as sites with soils that have a high INS would be relatively less responsive to top-dress N than sites with soils that have a low INS. Previous studies have shown that INS from rice soils can vary significantly across sites and over time (**Cassman et al., 1996; Cassman et al., 1998; Espe et al., 2015**), and is linked to the accumulation of phenolic compounds in the soil (**Olk et al., 1996; 1998; 1999; 2000**). Phenols are lignin derived compounds present in rice roots and shoots and have been shown to chemically stabilize N into compounds that would be less available to growing rice plants (**Stevenson, 1994; Thorn et al., 1996; Thorn and Mikita, 1992**). In CA, after harvest farmers typically incorporate phenol-rich rice straw into the soil and flood the field during the winter to facilitate rice straw decomposition (**Linquist et al., 2006**). Previous rice studies have shown that such practices which promote anaerobic decomposition cause phenols to accumulate in the soil; subsequently leading to a significant decrease in crop N uptake (**Olk et al. 2007; Olk et al., 2009a, 2009b**). This would suggest that understanding late season INS could help further refine late season N management decisions, in addition to the RI_{NDVI}. While quantifying phenols in the soil is likely to be too time consuming and expensive, understanding management practices that alter soil phenol concentration would be beneficial and a good area for future research.

3.5. CONCLUSION

A RI_{NDVI} based mixed-effects model was developed to assess the N status of a rice crop at PI and determine the need for a N top-dress. This approach is superior to the Leaf Color Chart or SPAD meter approach as it allows for a more rapid assessment over a larger area. A drawback to the tool developed here is that a grower would need to have a N-enriched strip in a representative portion of the field. Importantly, this approach is limited to situations where the seasonal N rate is applied at the beginning of the season and an assessment is made at PI to determine if a relatively small amount of N may be required to achieve maximum yields. Understanding management practices that influence late season soil INS would allow for an even more robust decision support tool and is worthy of further research. Finally, as technology advances, future research in this area is likely to focus on drone or satellite-based RI's which facilitate the assessment of larger areas more efficiently than the handheld proximal sensor used in this study.

3.6. ACKNOWLEDGEMENTS

We would like to thank the California Rice Research Board for supporting this research, Cesar Abrenilla and fellow members of the Agroecosystems Lab at UC Davis, Ray Stogsdill and the entire staff at the California Rice Experiment Station, visiting scholars Muhammad Ishfaq, Kevin Cassman, and Wencheng Ding, and the California rice growers who participated in this study.

REFERENCES

Almaraz, M., Bai, E., Wang, C., Trousdell, J., Conley, S., Faloona, I., and B.Z. Houlton. 2018. Agriculture is a major source of NO_x pollution in California. Sci. Adv. 4:8.

Ali, A.M., Thind, H.S., Singh, V., and B., Singh. 2014. A framework for refining nitrogen management in dry direct-seeded rice using GreenSeeker optical sensor. Comput. Electron. Agric. 110:114-120.

Arnall, D.B., Tubaña, B.S., Holtz, S.L., Girma, K., and W.R. Raun. 2009. Relationship between nitrogen use efficiency and response index in winter wheat. J. Plant Nutr. 32:502-515.

Balasubramanian, V., Morales, A.C., Cruz, R.T., and S. Abdulrachman. 1999. On-farm adaptation of knowledge-intensive nitrogen management technologies for rice systems. Nutr. Cycl. Agroecosys. 53:59-69.

Bartoń, K. 2020. MuMIn: Multi-Model Inference. R package version 1.43.17. https://CRAN.R-project.org/package=MuMIn

Bijay-Singh, Varinderpal-Singh, Purba, J., Sharma, R.K., Jat, M.L., Yadvinder-Singh, Thind, H.S., Gupta, R.K., Chaudhary, O.P., Chandna, P., Khurana, H.S., Kumar, A., Jagmohan-Singh, Uppal, H.S., Uppal, R.K., Vashistha, M., and R. Gupta. 2015. Site-specific fertilizer nitrogen management in irrigated transplanted rice (*Oryza sativa*) using and optical sensor. Precis. Agric. 16:455-475.

Broadbent, F.E. and D.S. Mikkelsen. 1968. Influence of placement on uptake of tagged nitrogen by rice. Agron. J. 60:674-677.

Cao, Q., Miao, Y., Shen, J., Yu, W., Yuan, F., Cheng, S., Huang, S., Wang, H., Yang, W., and F. Liu. 2016. Improving in-season estimation of rice yield potential and responsiveness to topdressing nitrogen application with Crop Circle active crop canopy sensor. Precis. Agric. 17:136-154.

Carter, M.R. and E.G. Gregorich. 2007. Soil sampling and methods of analysis. Lewis Publishers. Boca Raton, FL.

Cassman, K.G., Gines, G.C., Dizon, M.A., Samson, M.I., and J.M. Alcantara. 1996. Nitrogen-use efficiency in tropical lowland rice systems: contributions from indigenous and applied nitrogen. Field Crops Res. 47:1-12.

Cassman, K.G., Peng, S., Olk, D.C., Ladha, J.K., Reichardt, W., Dobermann, A., and U. Singh. 1998. Opportunities for increased nitrogen-use efficiency from improved resource management in irrigated rice systems. Field Crops Res. 56:7-39.

Chuong, T., Plant, R.E., and B.A. Linquist. 2020. Fertilizer source and placement influence ammonia volatilization losses from water-seeded rice systems. Soil Sci. Soc. Am. J. 84:784-797.

CIMIS. 2020. California Irrigation Management Information System. Internet Resource. (http://www.cimis.water.ca.gov/WSNReportCriteria.aspx) (accessed 01 Sept. 2020).

Colaço, A.F. and R.G.V. Bramley. 2018. Do crop sensors promote improved nitrogen management in grain crops? Field Crops Res. 218:126-140.

Daughtry, C.S.T., Walthall, C.L., Kim, M. S., Brown de Colstoun, E., and J.E. McMurtrey III. 2000. Estimating corn leaf chlorophyll concentration from leaf and canopy reflectance. Remote Sens. Environ. 74:229-239.

Dobermann, A., Witt, C., Dawe, D., Abdulrachman, S., Gines, H.C., Nagarajan, R., Satawathananont, S., Son, T.T., Tan, P.S., Wang, G.H., and N.V. Chien. 2002. Site-specific nutrient management for intensive rice cropping systems in Asia. Field Crops Res. 74:37-66.

DeDatta, S.K. Principles and practices of rice production. 1981. John Wiley & Sons. Singapore.

Dunn, B.W., Dunn, T.S., and H.G. Beecher. 2014a. Nitrogen timing and rate effects on. Growth and grain yield of delayed permanent-water rice in south-eastern Australia. Crop Pasture Sci. 65: 878-887.

Dunn B.W., Dunn, T.S., and B.A. Orchard. 2016. Nitrogen rate and timing effects on growth and yield of drill-sown rice. 2016. Crop Pasture Sci. 67: 1149-1157.

Dunn, T., Dunn, B., and R. Whitworth. 2014b. Identifying panicle initiation in rice. NSW Department of Primary Industries.

Dzurella, K.N., Pettygrove, G.S., Fryjoff-Hung, A., Hollander, A., and T. Harter. 2015. Potential to assess nitrate leaching vulnerability of irrigated cropland. J. Soil Water Conserv. 70: 63-72.

Espe, M.B., Kirk, E., van Kessel, C., Horwath, W.H., and B.A. Linquist. 2015. Indigenous nitrogen supply of rice is predicted by soil organic carbon. Soil. Sci. Soc. Am. J. 79:569-576.

Espe, M.B., Yang, H., Cassman, K.G., Guilpart, N., Sharifi, H., and B.A. Linquist. 2016. Estimating yield potential in temperate high-yielding, direct-seeded US rice production systems. Field Crops Res. 193:123-132.

Foster, A., Atwell, S., and D. Dunn. 2017. Sensor-based nitrogen fertilization for midseason rice production in southeast Missouri. Crop Forage Turfgrass Manage. 3: 1-7.

Gnyp, M.L., Miao, Y., Yuan, F., Ustin, S.L., Yu, K., Yao, Y., Huang, S., and G. Bareth. 2014. Hyperspectral canopy sensing of paddy rice aboveground biomass at different growth stages. Field Crops Res. 155:42-55.

Hartley, C., and C. van Kessel. 2003. UC Davis rice fertility management survey. Univ. of California Coop. Ext., Rice Project.

Hill, J.E., Williams, J.F., Mutters, R.G., and C.A. Greer. 2006. The California rice cropping system: agronomic resource issues for long-term sustainability. Paddy Water Environ. 4: 13-19.

Hussain, F., Bronson, K.F., Yadvinder-Singh, Bijay-Singh, and S. Peng. 2000. Use of Chlorophyll Meter Sufficiency Indices for Nitrogen Management of Irrigated Rice in Asia. Agron. J. 92:875-879.

Ladha, J.K., Jat, M.L., Stirling, C.M., Chakraborty, D., Pradhan, P., Krupnik, T.J., Sapkota, T.B., Pathak, H., Rana, D.S., Tesfaye, K., and B. Gerard. 2020. Achieving the sustainable development goals in agriculture: The crucial role of nitrogen in cereal-based systems. Adv. Agron. 163:39-116.

LaHue, G.T., Chaney, R.T., Adviento-Borbe, M.A., and B.A. Linquist. 2016. Alternate wetting and drying in high yielding direct-seeded rice systems accomplishes multiple environmental and agronomic objectives. Agr. Ecosyst. Environ. 229:30-39.

Lenth, R. 2021. emmeans: Estimated marginal means, aka least-squares means. (https://CRAN.R-project.org/package=emmeans)

Linquist, B.A., Brouder, S.M., and J.E. Hill. 2006. Winter straw and water management effects on soil nitrogen dynamics in California rice systems. Agron. J. 98:1050-1059.

Linquist, B.A., Hill, J.E., Mutters, R.G., Greer, C.A., Hartley, C., Ruark, M., and C. van Kessel. 2009. Assessing the necessity of surface applied preplant nitrogen fertilizer in rice systems. Agron. J. 101:906-915.

Linquist, B.A. and P. Sengxua. 2003. Efficient and flexible management of nitrogen for rainfed lowland rice. Nutr. Cycl. Agroecosys. 67:139-146.

Lofton, J., Tubaña, B.S., Kanke, Y., Teboh, J., and H. Viator. 2012. Predicting sugarcane response to nitrogen using a canopy reflectance-based response index value. Agron. J. 104:106-113.

Lu, J., Miao, Y., Shi, W., Li, J., Hu, X., Chen, Z., Wang, X. and K. Kusnierek. 2020. Developing a proximal active canopy sensor-based precision nitrogen management strategy for high-yielding rice. Remote Sens. 12:1440.

Lu, J., Miao, Y., Shi, W., Li, J., and F. Yuan. 2017. Evaluating different approaches to non-destructive nitrogen status diagnosis of rice using portable rapidSCAN active canopy sensor. Sci. Rep. 7:14073.

Lukina, E.V., Freeman, K.W., Wynn, K.J., Thomason, W.E., Mullen, R.W., Stone, M.L., Solie, J.B., Klatt, A.R., Johnson, G.V., Elliott, R.L. and W.R. Raun. 2001. Nitrogen fertilization optimization algorithm based on in-season estimates of yield and plant nitrogen uptake. J. Plant Nutr. 24:885-898.

Mullen, R.W., Freeman, K.W., Raun, W.R., Johnson, G.V., Stone, M.L., and J.B. Solie. 2003. Identifying an in-season response index and the potential to increase wheat yield with nitrogen. Agron. J. 95:347-351.

Norman, R.J., Slaton, N.A., and T.L. Roberts. 2021. Soil fertility. In: J. Hardke, editor, Rice production handbook. Misc. Publ. 192. Arkansas Coop. Ext. Serv. Little Rock. 69–101.

Olk, D.C., Anders, M.M., Filley T.R., and C. Isbell. 2009a. Crop nitrogen uptake and soil phenols accumulation under continuous rice cropping in Arkansas. Soil Sci. Soc. Am. J. 73:952-960.

Olk, D.C., Brunetti, G., and N. Senesi. 1999. Organic matter in double-cropped lowland rice soils: Chemical and spectroscopic properties. Soil Sci. 164:633-649.

Olk, D.C., Brunetti, G., and N. Senesi, N., 2000. Decrease in humification of organic matter with intensified lowland rice cropping a wet chemical and spectroscopic investigation. Soil Sci. Soc. Am. J. 64:1337-1347.

Olk, D.C., Cassman, K.G., Mahieu, N., and E.W. Randall. 1998. Conserved chemical properties of young humic acid fractions in tropical lowland soil under intensive irrigated rice cropping. Eur. J. Soil Sci. 49:337–349.

Olk, D.C., Cassman, K.G., Randall, E.W., Kinchesh, P., Sanger, L.J., and J.M. Anderson. 1996. Changes in chemical properties of organic matter with intensified rice cropping in tropical lowland soil. Eur. J. Soil Sci. 47:293-303.

Olk, D.C., Jimenez, R.R., Moscoso, E., and P. Gapas. 2009b. Phenol accumulation in a young humic fraction following anerobic decomposition of rice crop residues. Soil Sci. Soc. Am. J. 73:943-951.

Olk, D.C., Samson M.I., and P. Gapas. 2007. Inhibition of nitrogen mineralization in young humic fractions by anaerobic decomposition of rice crop residues. Eur. J. Soil Sci. 58:270–281.

Peng, S., Buresh, R.J., Huang, J., Yang, J., Zou, Y., Zhong, X., Wang, G., and F. Zhang. 2006. Strategies for overcoming low agronomic nitrogen use efficiency in irrigated rice systems in China. Field Crops Res. 96:37-47.

Peng, S., Garcia, F.V., Laza, R.C., Sanico, A.L., Visperas, R.M., and K.G. Cassman. 1996. Increased N-use efficiency using a chlorophyll meter on high-yielding irrigated rice. Field Crops Res. 47:243-252.

Pinheiro, J., Bates, D., DebRoy, S., Sarkar, D., and R Core Team. 2021. nlme: Linear and Nonlinear Mixed Effects Models. (https://CRAN.R-project.org/package=nlme)

Pittelkow, C.M., Adviento-Borbe, M.A., van Kessel, C., Hill, J.E., and B.A. Linquist. 2014a. Optimizing rice yields while minimizing yield-scaled global warming potential. Glob Change Biol. 20:1382-1393.

Pittelkow, C.M., Assa, Y., Burger, M., Mutters, R.G., Greer, C.A., Espino, L.A., Hill, J.E., Horwath, W.R., van Kessel, C. and B.A. Linquist. 2014b. Nitrogen management and methane emissions in direct-seeded rice systems. Agron. J. 106:968-980.

R Core Team. 2021. R: A language and environment for statistical computing. R Foundation for Statistical Computing, Vienna, Austria. (https://www.R-project.org/)

Raun, W.R., Solie, J.B., Johnson, G.V., Stone, M.L., Mullen, R.W., Freeman, K.W., Thomason, W.E., and E.V. Lukina. 2002. Improving nitrogen use efficiency in cereal grain production with optical sensing and variable rate application. Agron. J. 94:815-820.

Raun, W.R., Solie, J.B., Stone, M.L., Martin, K.L., Freeman, K.W., Mullen, R.W., Zhang, H., Schepers, J.S. and G.V. Johnson. 2005. Optical sensor-based algorithm for crop nitrogen fertilization. Commun. Soil Sci. Plan. 36:2759-2781.

Rehman, T.R., Reis, A.F.B., Akbar, N., and B.A. Linquist. 2019. Use of Normalized Difference Vegetation Index to assess N status and predict grain yield in rice. Agron. J. 111:2889-2898.

Saberioon, M.M., Amin, M.S.M., Gholizadeh, A., and M.H. Ezri. 2014. A review of optical methods for assessing nitrogen contents during rice growth. Appl. Eng. Agric. 30:657-669.

Smith, J., Sutula, M., Bouma-Gregson, K., and M. Van Dyke. 2021. California Water Boards' Framework and Strategy for Freshwater Harmful Algal Bloom Monitoring: Executive Synthesis. Southern California Coastal Water Research Project Technical Report 1141.A

Sharp, Z. 2017. Principles of stable isotope geochemistry. 2nd edition. Univ. of New Mexico Press, Albuquerque.

Stevenson, F.J. 1994. Humus chemistry: Genesis, composition, reactions. 2nd ed. John Wiley & Sons, New York.

Thorn, K.A., and M.A. Mikita. 1992. Ammonia fixation by humic substances: A nitrogen-15 and carbon-13 NMR study. Sci. Total Environ. 113:67–87.

Thorn, K.A., W.S. Goldenberg, S.J. Younger, and E.J. Weber. 1996. Covalent binding of aniline to humic substances: Comparison of nucleophilic addition, enzyme-, and metal-catalyzed reactions by ^{15}N NMR. p. 299–326. In J.S. Gaffney et al. (ed.) Humic and fulvic acids: Isolation, structure, and environmental role. Am. Chem. Soc., Washington, DC.

Troldahl, D. 2018. Rice growing guide. New South Wales Govt. Dept. Primary Industries. 16-19.

Tubaña, B.S., Arnall, D.B., Walsh, O., Chung, B., Solie, J.B., Girma, K. and W.R. Raun. 2008. Adjusting midseason nitrogen rate using a sensor-based optimization algorithm to increase use efficiency in corn. J. Plant Nutr. 31:1393-1419.

Tubaña, B.S., Harrell, D.L., Walker, T., Teboh, J., Lofton, J. and Y. Kanke. 2012. In-season canopy reflectance-based estimation of rice yield response to nitrogen. Agron. J. 104:1604-1611.

Tucker, C.J. 1979. Red and photographic infrared linear combinations for monitoring vegetation. Remote Sens. Environ. 8:127-150.

Tucker, C.J., Vanpraet, C.L., Sharman, M.J., and G. van Ittersum. 1985. Satellite remote sensing of total herbaceous biomass production in the Sengalese Sahel 1980–1984. Remote Sens. Environ. 17:233–249.

Turner, F.T. and M.F. Jund. 1991. Chlorophyll meter to predict nitrogen topdress requirement for semidwarf rice. Agron. J., 83:926-928.

Univ. of California, Division of Agricultural and Natural Resources (UC-ANR). 2015. Sample costs to produce rice. Univ. of California, Davis, CA.

Univ. of California, Division of Agricultural and Natural Resources (UC-ANR). 2018. California rice production. UC-ANR Workshop Manual. Univ. of California, Davis, CA.

Univ. of California, Los Angeles (UCLA) Statistical Consulting Group. 2021. Decomposing, Probing, and Plotting Interactions in R. UCLA Institute for Digital Research and Education. Internet Resource. https://stats.idre.ucla.edu/r/seminars/interactions-r/#s4

United States Salinity Laboratory Staff. 1954. Diagnosis and improvement of saline and alkali soils. USDA Agric. Handb. 60. U.S. Gov. Print. Office, Washington, D.C.

USDA-NASS. 2021. California Historic Commodity Data, California Medium Grain Rice. Washington, D.C. http://www.nass.usda.gov/Statistics_by_State/California/Historical_Data/index.asp. Internet accessed August 2021.

Wickham, H. ggplot2: Elegant Graphics for Data Analysis. Springer-Verlag New York, 2016. https://ggplot2.tidyverse.org

Wickham, H., François, R., Henry, L., and K. Müller. 2021. dplyr: A Grammar of Data Manipulation. R package version 1.0.6. https://CRAN.R-project.org/package=dplyr

Williams, J.F. 2010. Rice nutrient management in California. UC ANR Publication 3516.

Xue, L., Li, G., Qin, X., Yang, L., and H. Zhang. 2014. Topdressing nitrogen recommendation for early rice with an active sensor in South China. Precis. Agric. 15:95-110.

Xue, L. and L. Yang. 2008. Recommendations for nitrogen fertiliser topdressing rates in rice using canopy reflectance spectra. Biosyst. Eng. 100:542-534.

Yao, Y., Miao, Y., Cao, Q., Wang, H., Gnyp, M.L., Bareth, G., Khosla, R., Yang, W., Liu, F., and C. Liu. 2014. In-season estimation of rice nitrogen status with an active crop canopy sensor. IEEE J-STARS. 7:4403-4413.

Yao, Y., Miao, Y., Huang, S., Gao, L., Ma, X., Zha, G., Jiang, R., Chen, X., Zhang, F., Yu, K., Gnyp, M.L., Bareth, G., Liu, C., Zhao, L., Yang, W., and H. Zhu. 2012. Active canopy sensor-based precision N management strategy for rice. Agron. Sustain. Dev. 32:925-933.

CONCLUSION

Prior to this work, few studies had explored the potential of remote sensing technology to inform sustainable N management in agricultural crops. This study demonstrated that remotely sensed vegetative indices can be used to accurately assess crop N status and predict the grain yield response to top-dress N fertilizer in direct seeded rice systems. The decision support tool presented here can help California rice farmers make precise mid-season N management decisions and improve the productivity and sustainability of California rice agroecosystems. Additionally, the findings of this study provide a strong framework for using remote sensing technology to improve N fertilizer management in similar rice systems worldwide. Future work should focus on further validating the application of the tool presented here through large scale field experiments throughout the Sacramento Valley rice growing region. Additionally, alternative vegetative indices should be examined to determine if indices that do not saturate provide the basis for a better tool.